Appendix IN-1-E. System E Performance for Cooking-Related Pollutants, June 12, 2014

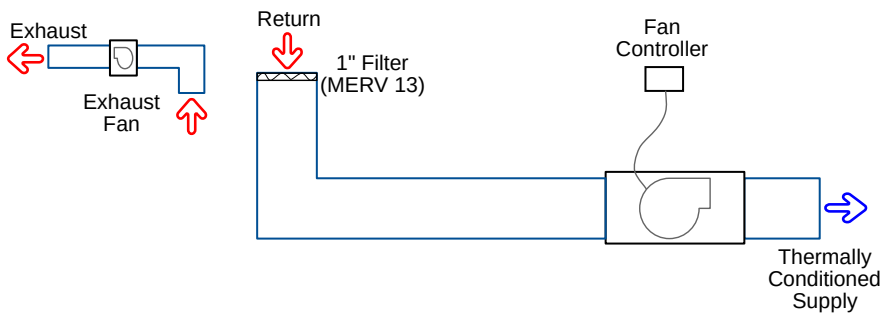

Notes about this monitoring period

We forgot to turn off the injectors and do a spike of SF6

Event Log
2014/06/12 09:36:21.7, The cooking burner was turned on

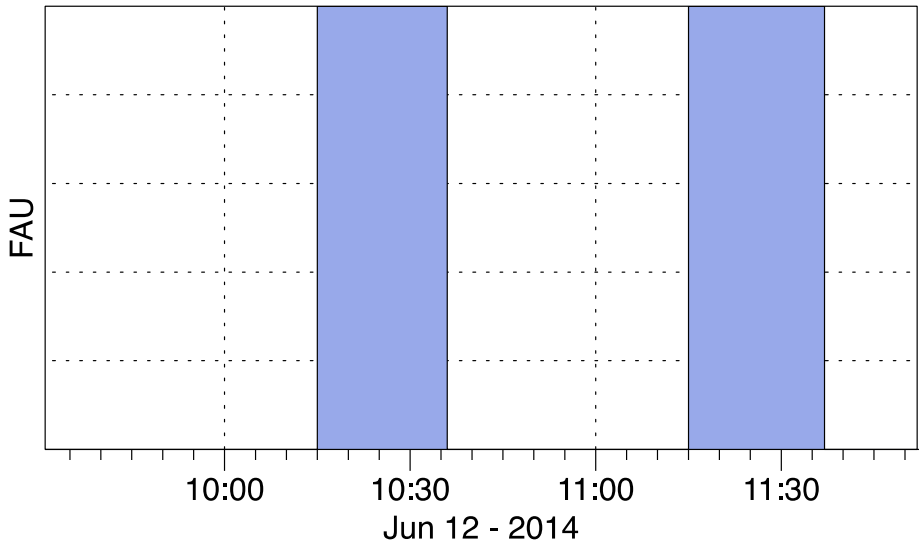

Figure IN-1-E-1. Operation of mechanical systems: fan on central forced air unit (FAU)

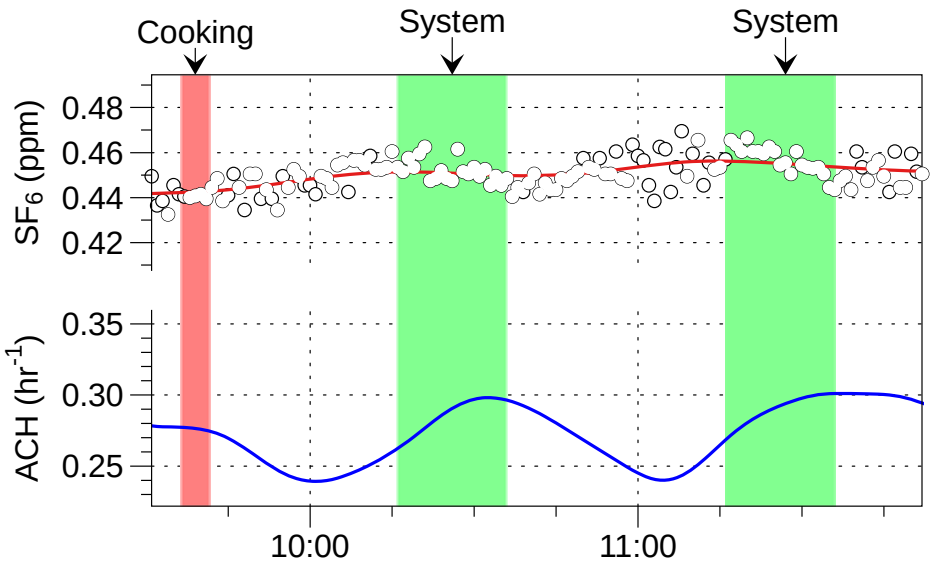

Figure IN-1-E-2. SF_6 during cooking experiment with System E on Jun 12, 2014. The top panel shows the concentration values, and the bottom panel shows the resulting ventilation rate. Ventilation decay rates determined for SF_6 are used to calculate first order removal rates of particle deposition and filtration.

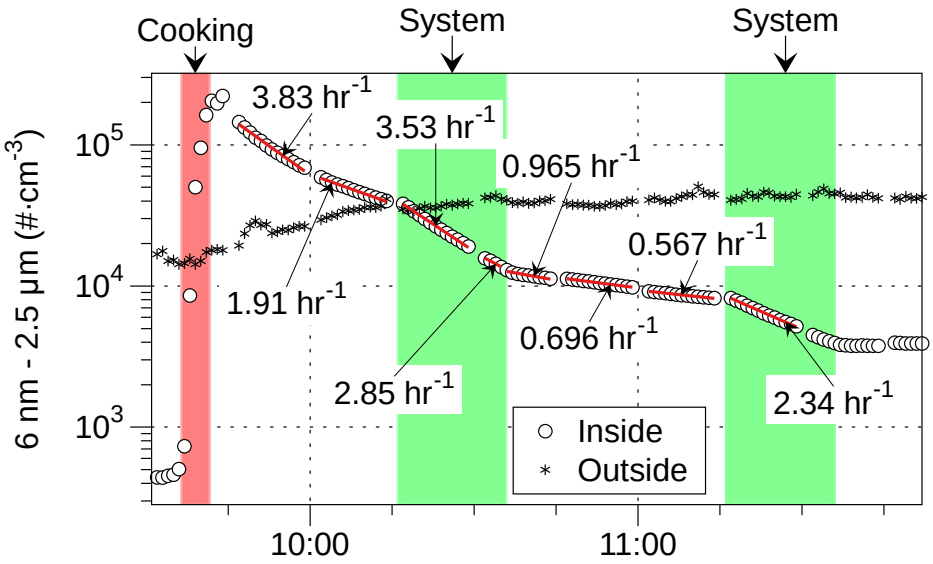

Figure IN-1-E-3. Number concentration of 6 nm to 2.5 µm diameter particles during cooking experiment with System E on Jun 12, 2014. Fitted decay rates during each period reflect sum of all particle transformation and removal mechanisms including growth, ventilation, deposition and filtration.

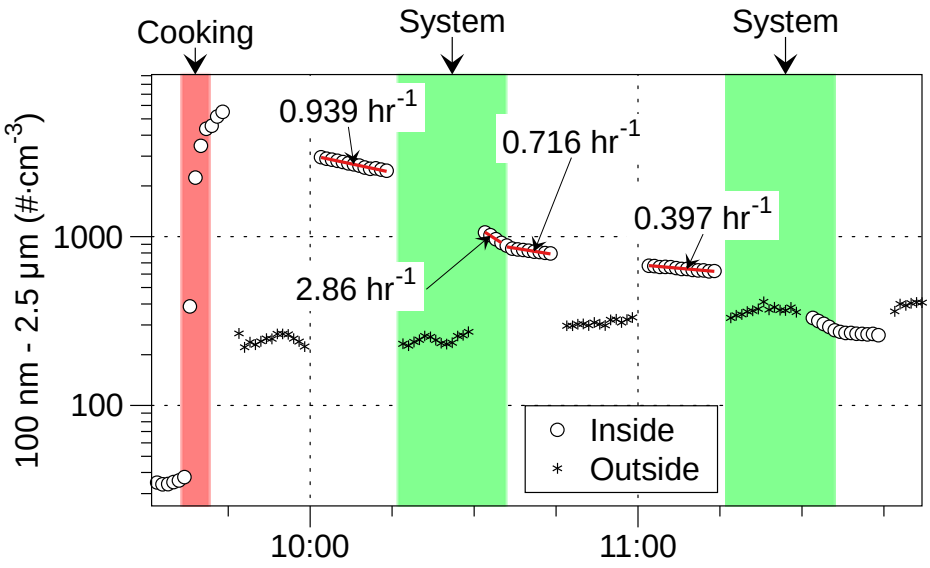

Figure IN-1-E-4. Number concentrations of 100 nm to 2.5 µm diameter particles during cooking experiment with System E on Jun 12, 2014. Data shown for only one of two CPC3781s. The other unit had a wick problem during this experiment. Fitted decay rates during each period reflect sum of all particle transformation and removal mechanisms including growth, ventilation, deposition and filtration.

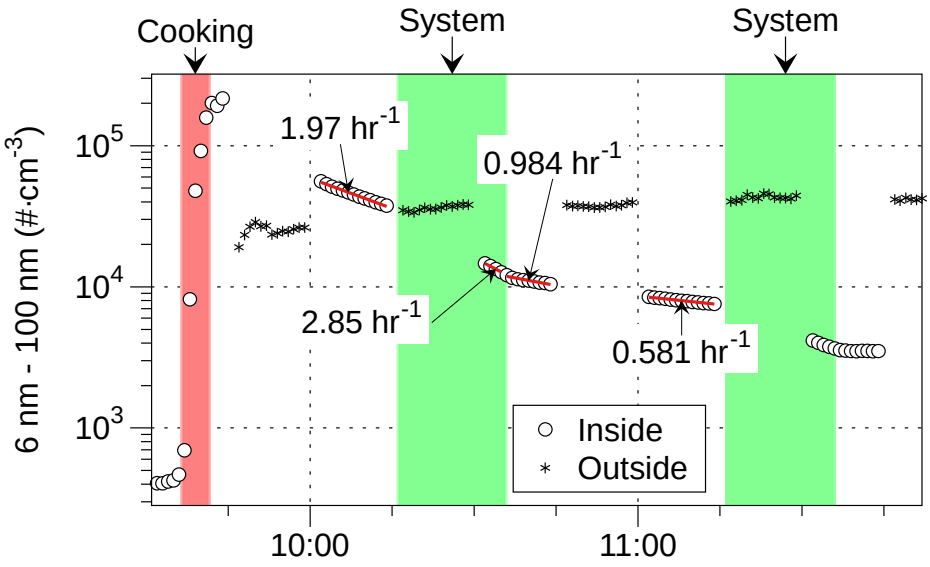

Figure IN-1-E-5. Number concentrations of 6–100 nm diameter particles during cooking experiment with System E on Jun 12, 2014. Data obtained by subtracting counts in range of 100 nm – 2.5 µm from counts in range of 6 nm – 2.5 µm. Fitted decay rates during each period reflect sum of all particle transformation and removal mechanisms including growth, ventilation, deposition and filtration.

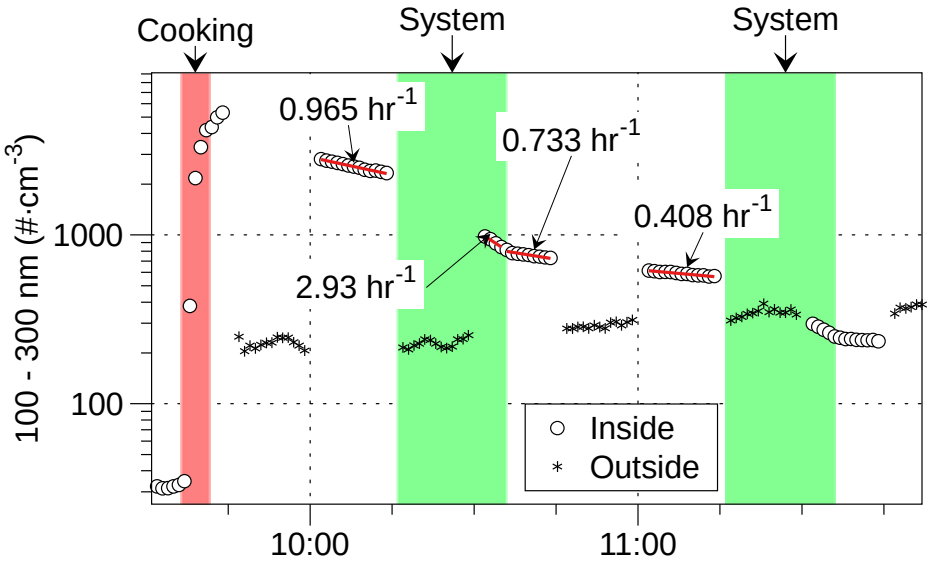

Figure IN-1-E-6. Number concentrations of 100-300 nm diameter particles during cooking experiment with System E on Jun 12, 2014. Data obtained by subtracting counts in range of 0.3–2.5 µm particles (MetOne 637) from the counts measured in the range of 100 nm–2.5 µm by the CPC3781 with size selective inlet. Fitted decay rates during each period reflect sum of all particle transformation and removal mechanisms including growth, ventilation, deposition and filtration.

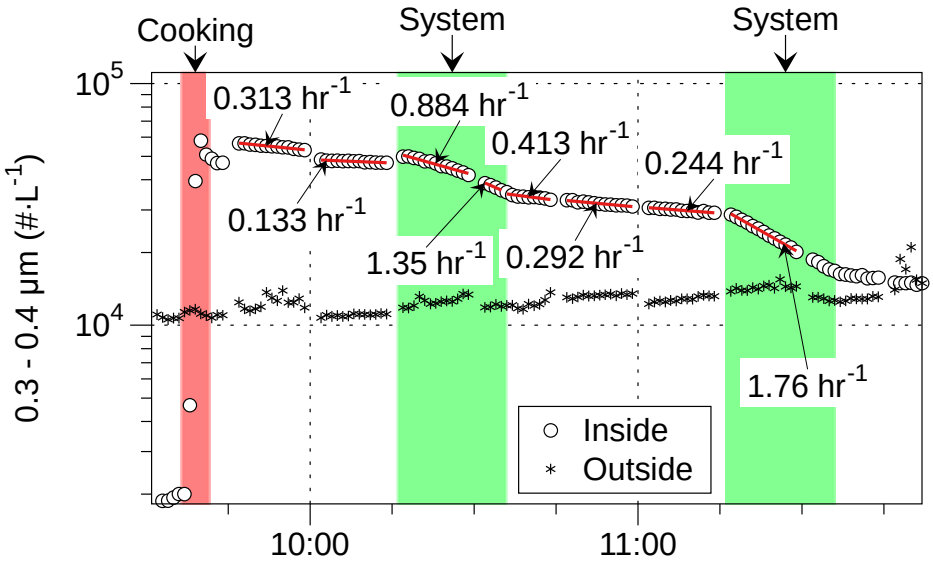

Figure IN-1-E-7. Number concentration of 0.3–0.4 µm diameter particles during cooking experiment with System E on Jun 12, 2014. Fitted decay rates during each period reflect sum of all particle transformation and removal mechanisms including growth, ventilation, deposition and filtration. Disconnected data during period just after cooking are from the two instruments switching between indoors and outdoors and may reflect small differences in the sampling efficiency at the lower cut point that is particularly sensitive to rapidly changing particle size distributions from the indoor source. Negative decay during this period indicates that the number of particles in this size bin is increasing.

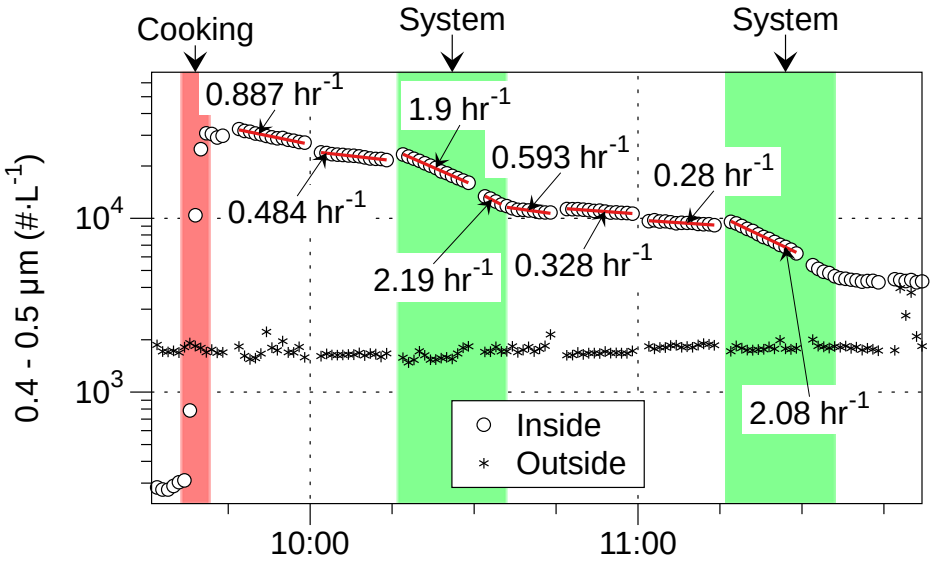

Figure IN-1-E-8. Number concentration of 0.4–0.5 µm diameter particles during cooking experiment with System E on Jun 12, 2014. Fitted decay rates during each period reflect sum of all particle transformation and removal mechanisms including growth, ventilation, deposition and filtration.

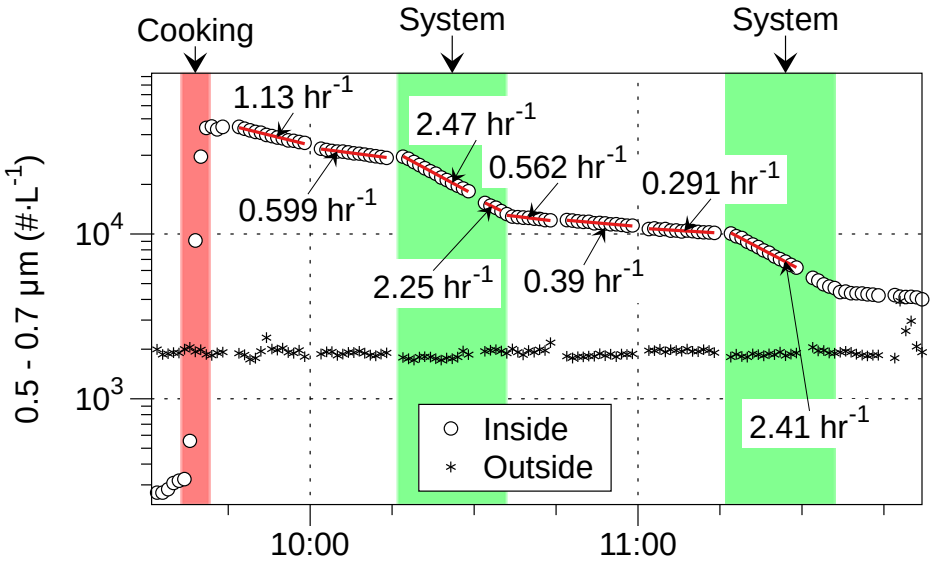

Figure IN-1-E-9. Number concentration of 0.5–0.7 µm diameter particles during cooking experiment with System E on Jun 12, 2014. Fitted decay rates during each period reflect sum of all particle transformation and removal mechanisms including growth, ventilation, deposition and filtration.

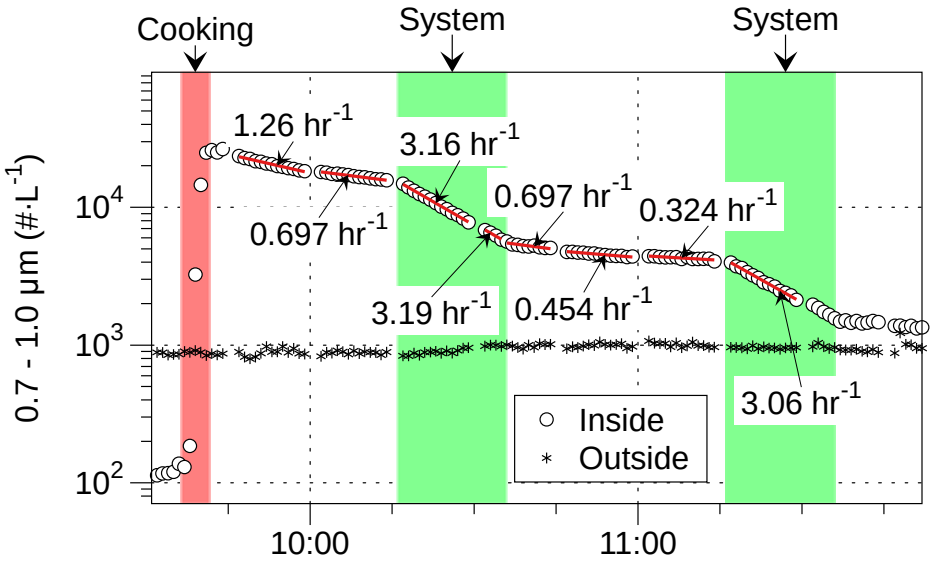

Figure IN-1-E-10. Number concentration of 0.7-1.0 µm diameter particles during cooking experiment with System E on Jun 12, 2014. Fitted decay rates during each period reflect sum of all particle transformation and removal mechanisms including growth, ventilation, deposition and filtration.

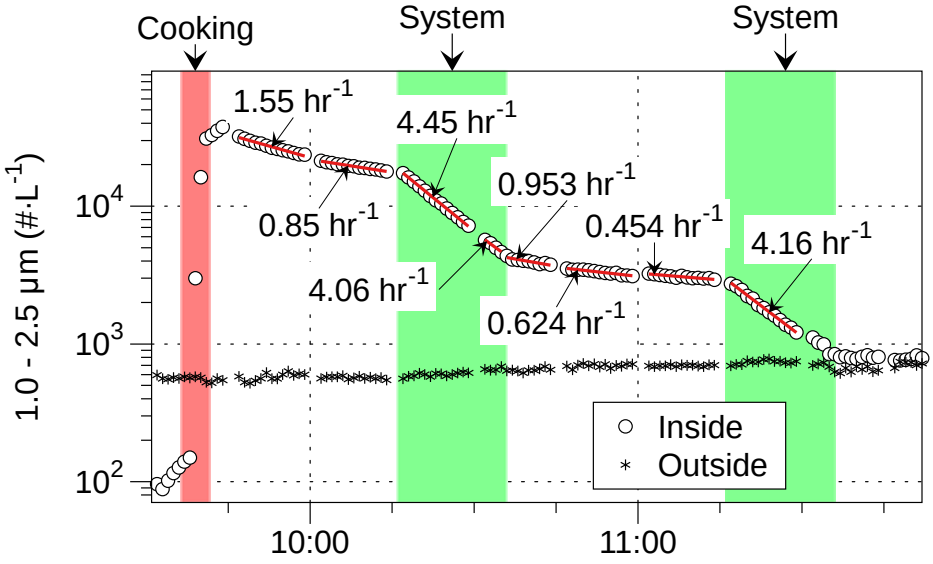

Figure IN-1-E-11. Number concentration of 1.0–2.5 µm diameter particles during cooking experiment with System E on Jun 12, 2014. Fitted decay rates during each period reflect sum of all particle transformation and removal mechanisms including growth, ventilation, deposition and filtration.

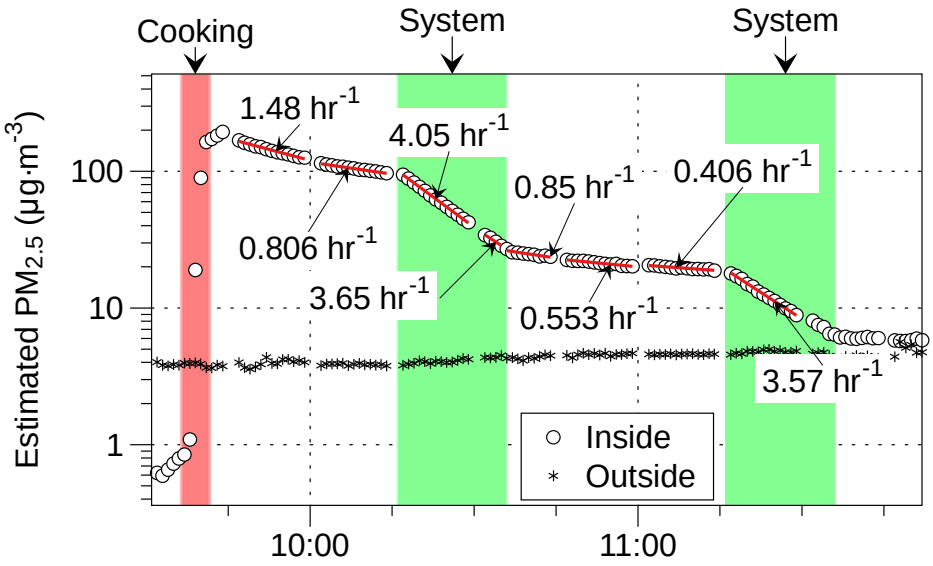

Figure IN-1-E-12. Estimated $PM_{2.5}$ concentration calculated from size-resolved particle number concentrations during cooking experiment with System E on Jun 12, 2014. Refer to Methods section of main report for details on this calculation. Fitted decay rates during each period reflect sum of all particle transformation and removal mechanisms including growth, ventilation, deposition and filtration.

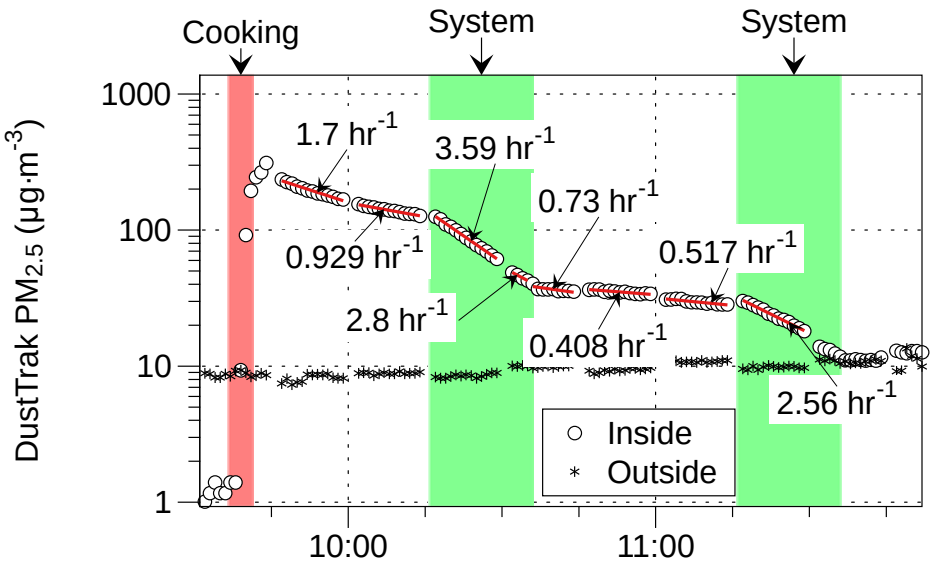

Figure IN-1-E-13. $PM_{2.5}$ concentrations measured by TSI DustTrak II 8530 during cooking experiment with System E on Jun 12, 2014. Fitted decay rates during each period reflect sum of all particle transformation and removal mechanisms including growth, ventilation, deposition and filtration.

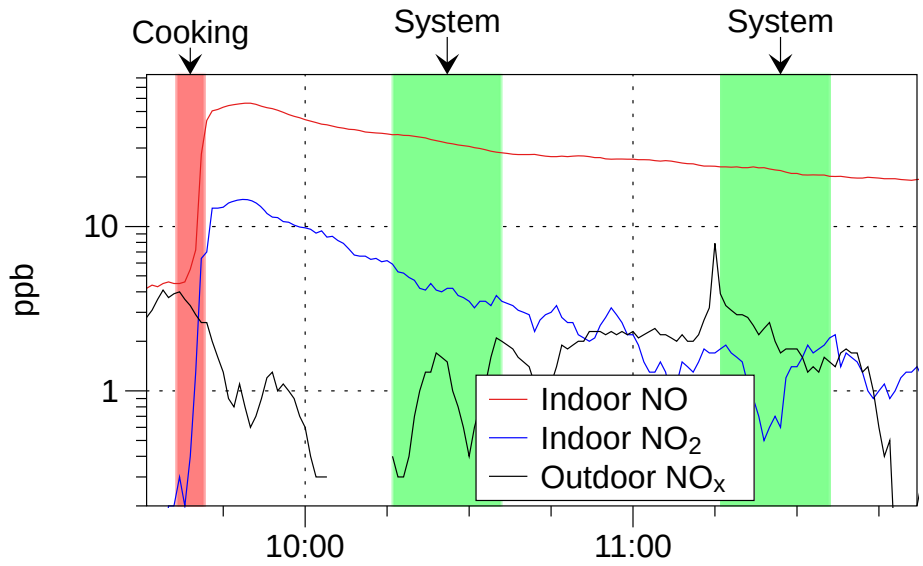

Figure IN-1-E-14. Concentration of NO and NO_2 during cooking experiment with System E on Jun 12, 2014.

Appendix IN-2-A. System A Performance for Cooking-Related Pollutants, June 18, 2014

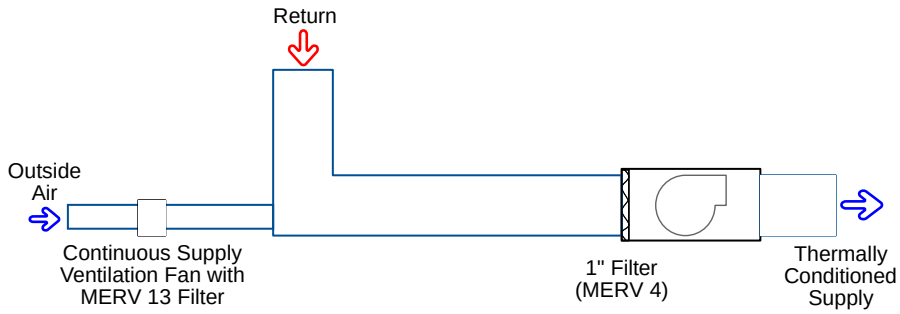

Notes about this monitoring period

6/18/14 7:31:15 - Burner on (a bit smoky, regular cook time)
6/18/14 8:32:53 - FAU on
6/18/14 9:09:04 - FAU off
6/18/14 9:29:59 - HEPAs on

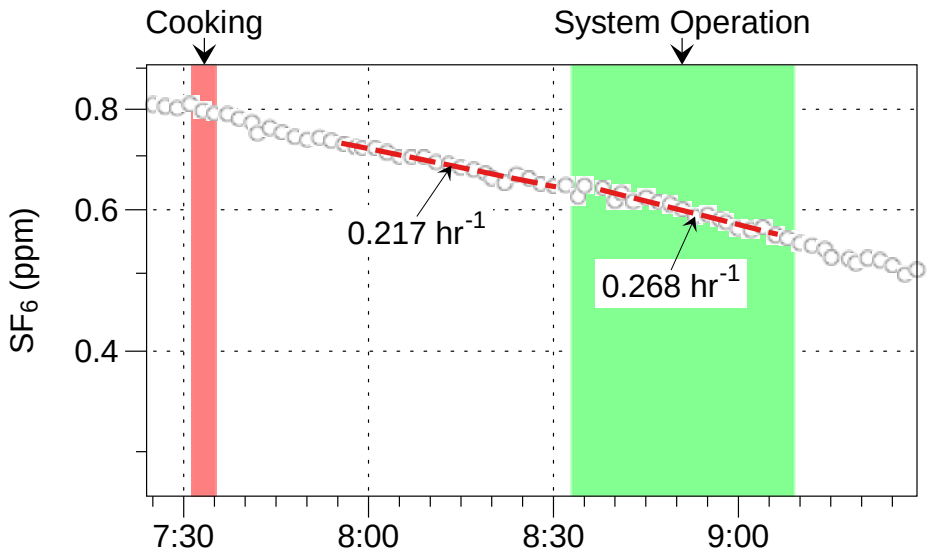

Figure IN-2-A-1. SF_6 during cooking experiment with System A on Jun 18, 2014. Injection occurred prior to the display interval. During each interval, a red line shows a best-fit, first-order decay rate that indicates the air exchange rate. Stir-frying of green beans occurred during the first shaded interval. This system was not on a fan controller, but the FAU fan was manually turned on ~8:33. Ventilation decay rates determined for SF_6 are used to calculate first order removal rates of particle deposition and filtration.

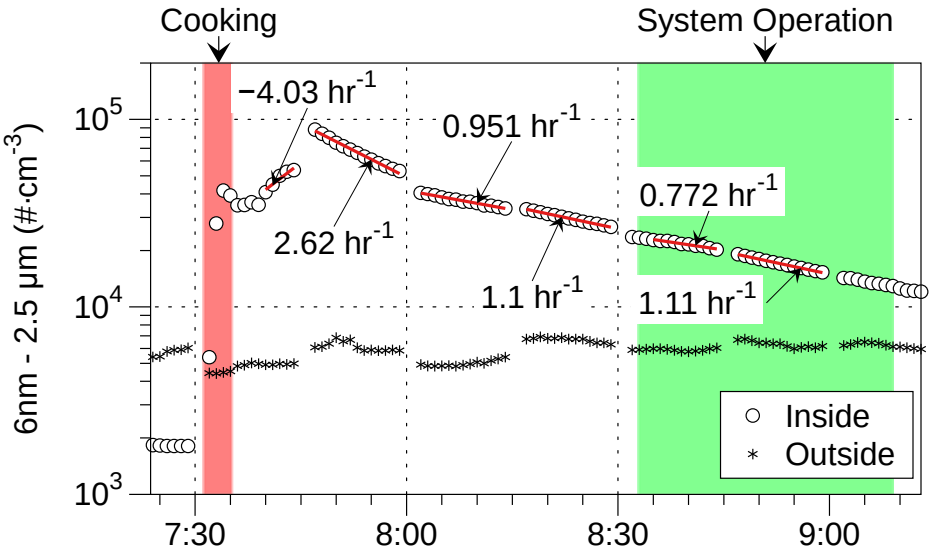

Figure IN-2-A-2. Number concentration of 6 nm to 2.5 µm diameter particles during cooking experiment with System A on Jun 18, 2014. Fitted decay rates during each period reflect sum of all particle transformation and removal mechanisms including growth, ventilation, deposition and filtration.

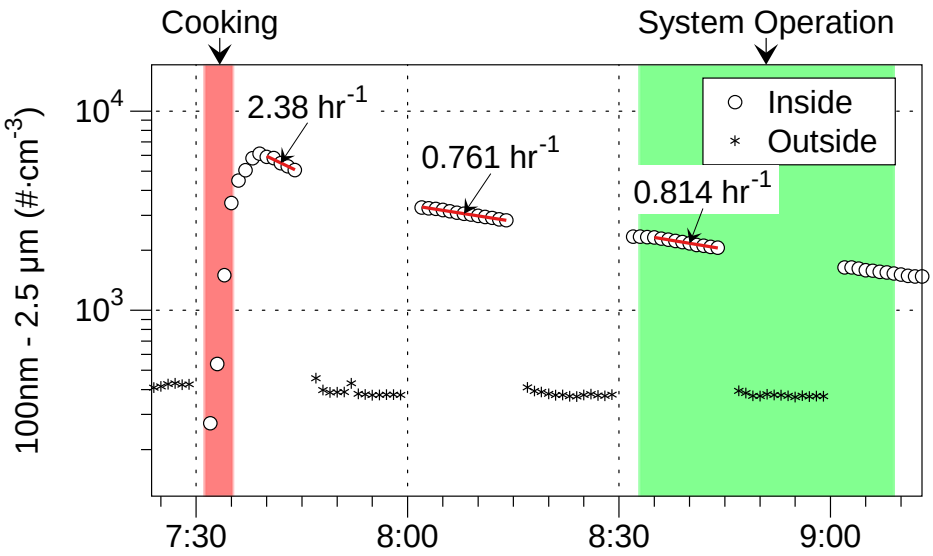

Figure IN-2-A-3. Number concentrations of 100 nm to 2.5 µm diameter particles during cooking experiment with System A on Jun 18, 2014. Data shown for only one of two CPC3781s. The other unit had a wick problem during this experiment. Fitted decay rates during each period reflect sum of all particle transformation and removal mechanisms including growth, ventilation, deposition and filtration.

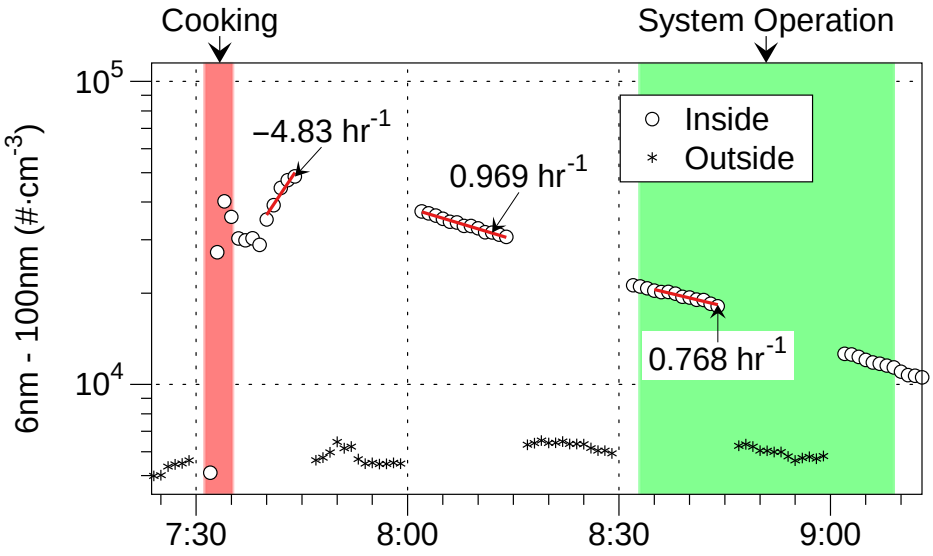

Figure IN-2-A-4. Number concentrations of 6–100 nm diameter particles during cooking experiment with System A on Jun 18, 2014. Data obtained by subtracting counts in range of 100 nm – 2.5 µm from counts in range of 6 nm – 2.5 µm. Fitted decay rates during each period reflect sum of all particle transformation and removal mechanisms including growth, ventilation, deposition and filtration.

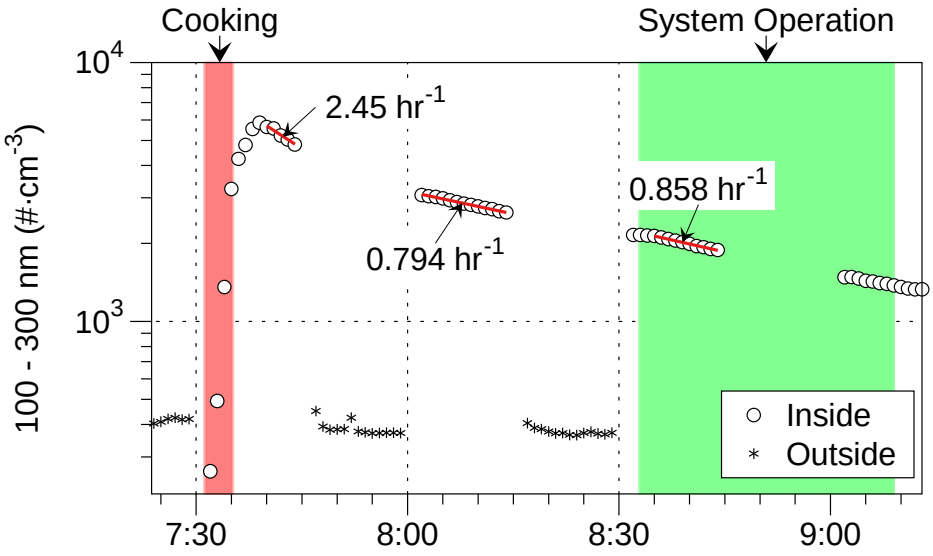

Figure IN-2-A-5. Number concentrations of 100-300 nm diameter particles during cooking experiment with System A on Jun 18, 2014. Data obtained by subtracting counts in range of 0.3–2.5 μm particles (MetOne 637) from the counts measured in the range of 100 nm–2.5 μm by the CPC3781 with size selective inlet. Fitted decay rates during each period reflect sum of all particle transformation and removal mechanisms including growth, ventilation, deposition and filtration.

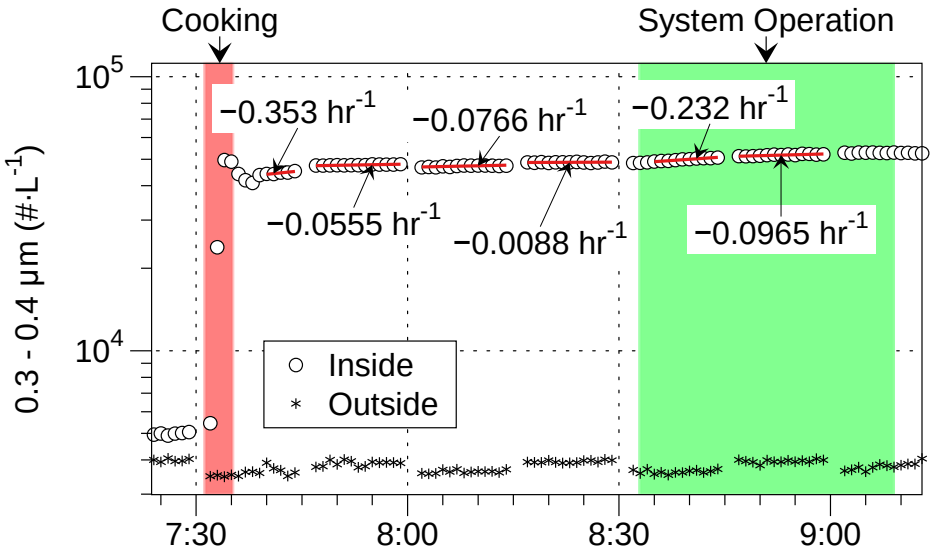

Figure IN-2-A-6. Number concentration of 0.3–0.4 μm diameter particles during cooking experiment with System A on Jun 18, 2014. Fitted decay rates during each period reflect sum of all particle transformation and removal mechanisms including growth, ventilation, deposition and filtration. Disconnected data during period just after cooking are from the two instruments switching between indoors and outdoors and may reflect small differences in the sampling efficiency at the lower cut point that is particularly sensitive to rapidly changing particle size distributions from the indoor source. Negative decay during this period indicates that the number of particles in this size bin is increasing.

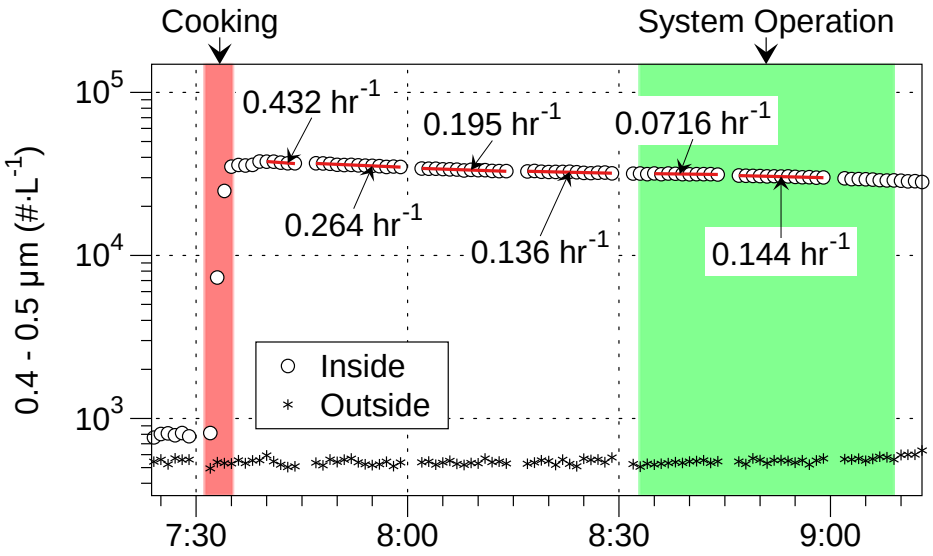

Figure IN-2-A-7. Number concentration of 0.4–0.5 µm diameter particles during cooking experiment with System A on Jun 18, 2014. Fitted decay rates during each period reflect sum of all particle transformation and removal mechanisms including growth, ventilation, deposition and filtration.

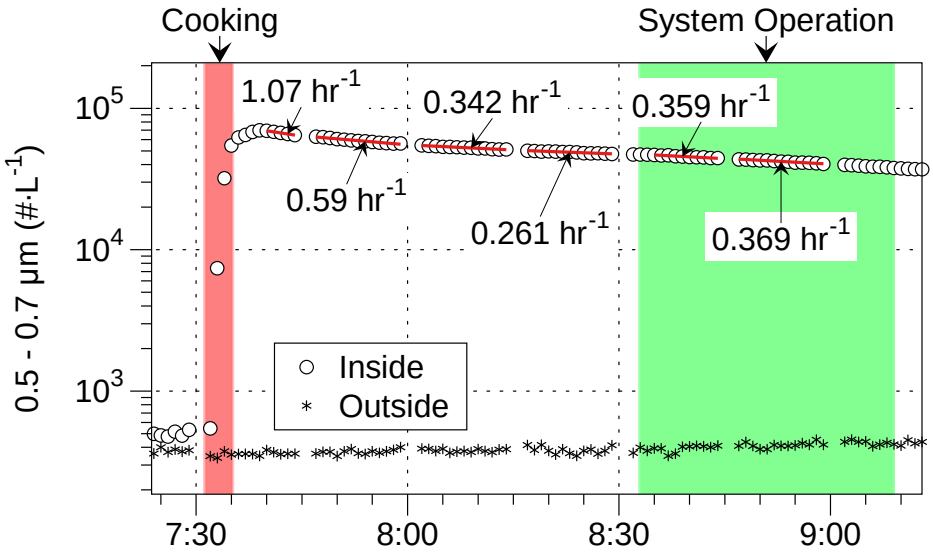

Figure IN-2-A-8. Number concentration of 0.5–0.7 µm diameter particles during cooking experiment with System A on Jun 18, 2014. Fitted decay rates during each period reflect sum of all particle transformation and removal mechanisms including growth, ventilation, deposition and filtration.

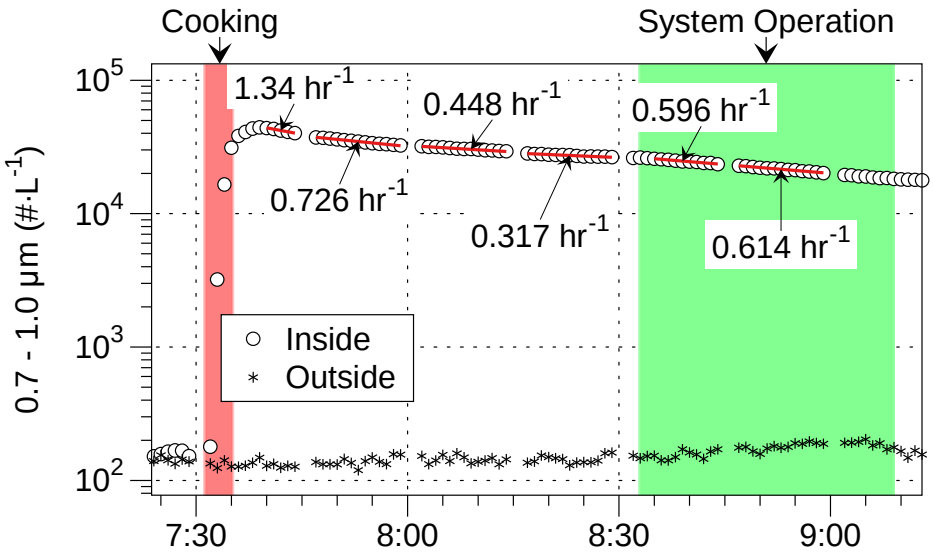

Figure IN-2-A-9. Number concentration of 0.7-1.0 µm diameter particles during cooking experiment with System A on Jun 18, 2014. Fitted decay rates during each period reflect sum of all particle transformation and removal mechanisms including growth, ventilation, deposition and filtration.

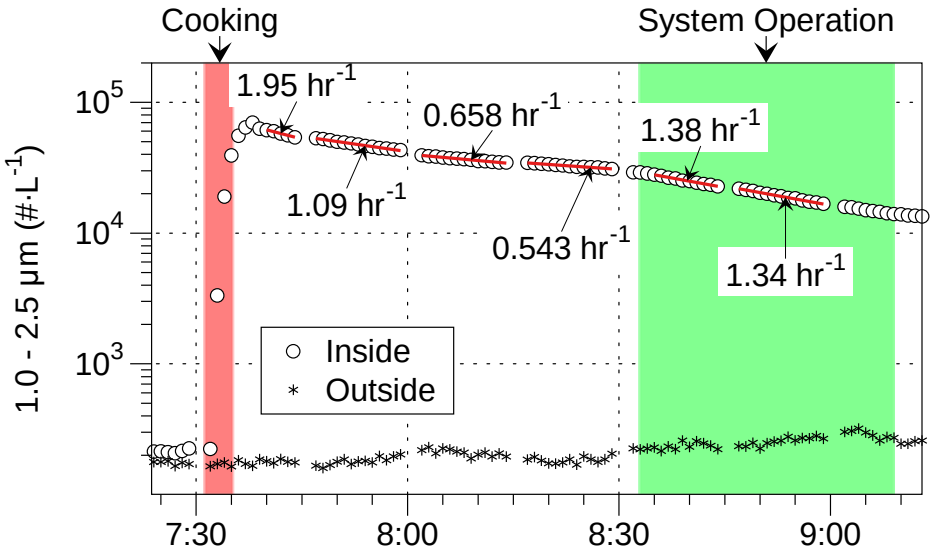

Figure IN-2-A-10. Number concentration of 1.0–2.5 µm diameter particles during cooking experiment with System A on Jun 18, 2014. Fitted decay rates during each period reflect sum of all particle transformation and removal mechanisms including growth, ventilation, deposition and filtration.

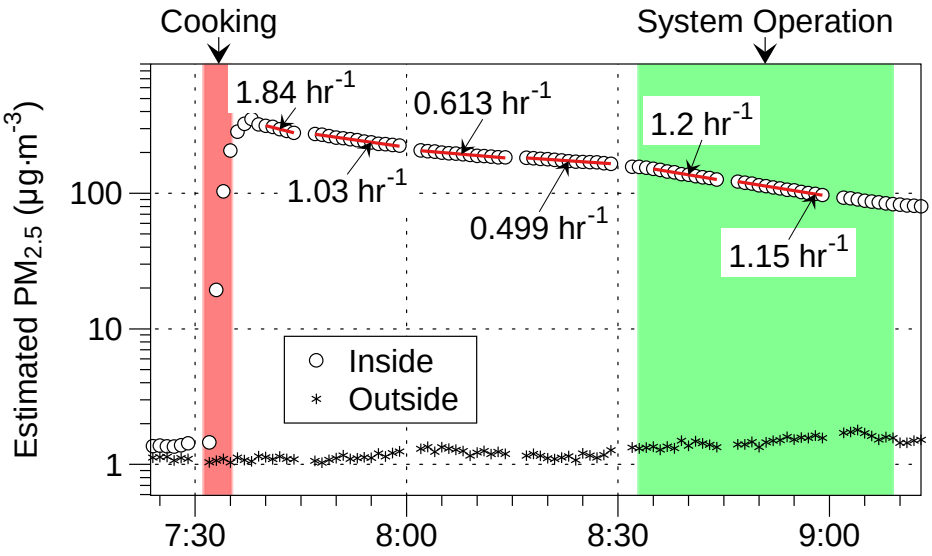

Figure IN-2-A-11. Estimated $PM_{2.5}$ concentration calculated from size-resolved particle number concentrations during cooking experiment with System A on Jun 18, 2014. Refer to Methods section of main report for details on this calculation. Fitted decay rates during each period reflect sum of all particle transformation and removal mechanisms including growth, ventilation, deposition and filtration.

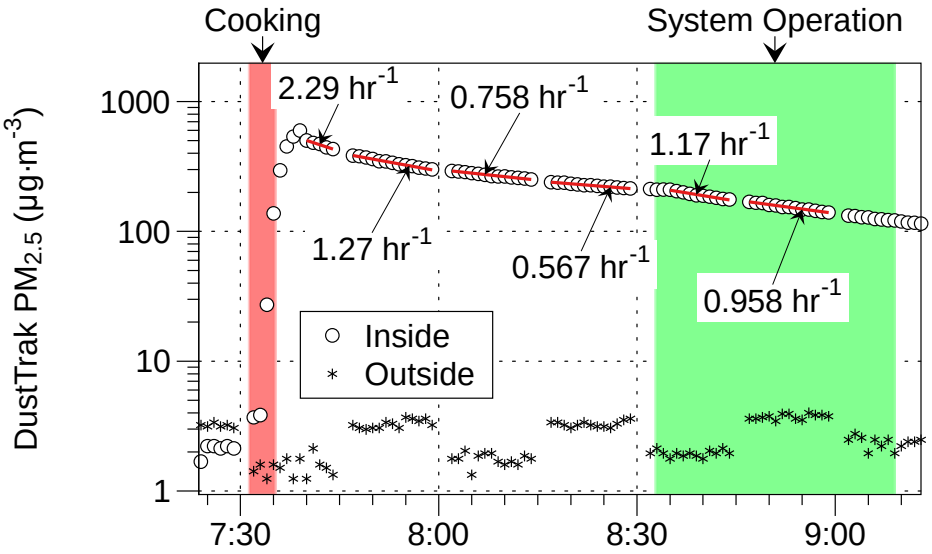

Figure IN-2-A-12. $PM_{2.5}$ concentrations measured by TSI DustTrak II 8530 during cooking experiment with System A on Jun 18, 2014. Fitted decay rates during each period reflect sum of all particle transformation and removal mechanisms including growth, ventilation, deposition and filtration.

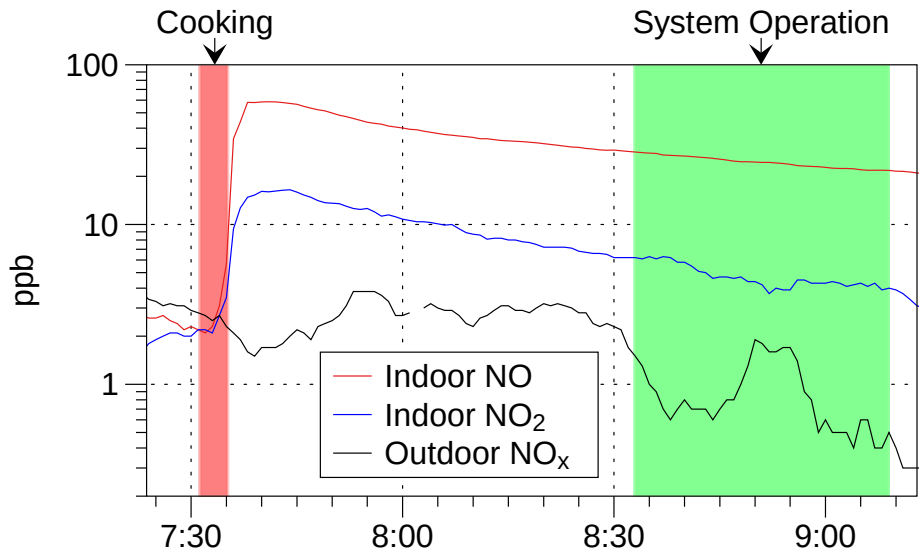

Figure IN-2-A-13. Concentration of NO and NO_2 during cooking experiment with System A on Jun 18, 2014.

Appendix IN-3-F. System F Performance for Cooking-Related Pollutants, June 23, 2014

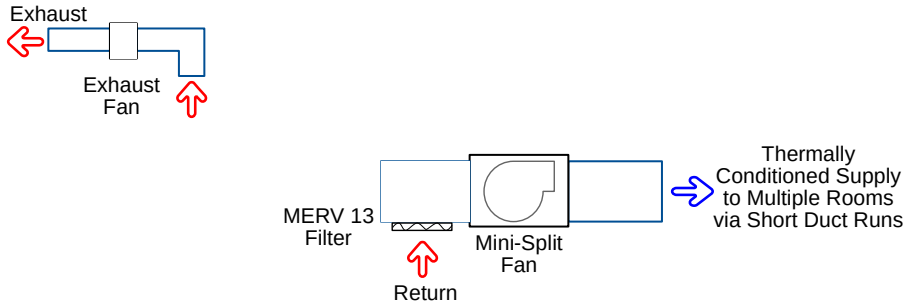

Notes about this monitoring period

2014/06/23 13:36:18.5,Turned off the SF6 injectors and did a spiked 60 ml SF6 release
2014/06/23 13:47:19.4,On with the burner
2014/06/23 13:52:21.8,Off with the burner

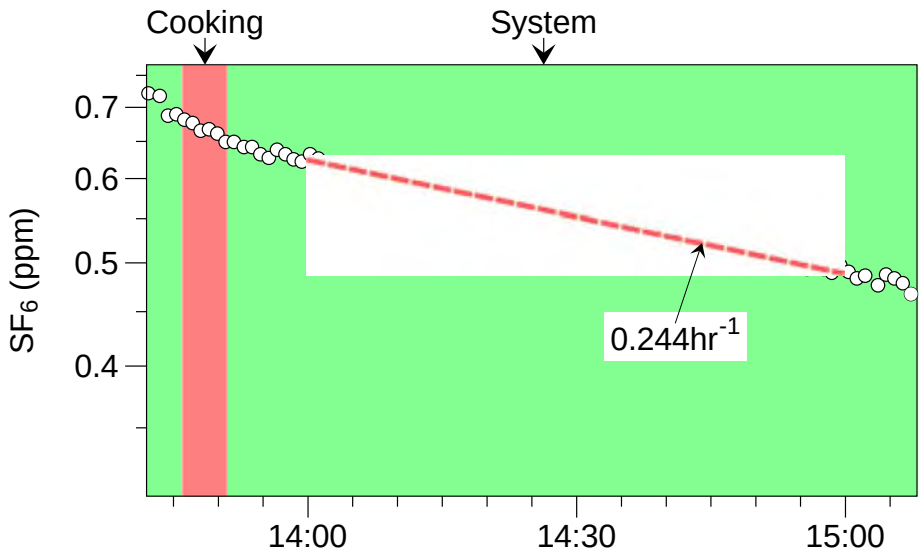

Figure IN-3-F-1. SF_6 during cooking experiment with System F on Jun 23, 2014. Injection occurred prior to the display interval. During each interval, a red line shows a best-fit, first-order decay rate that indicates the air exchange rate. Stir-frying of green beans occurred during the brown-colored interval. This system was on for the entire period. Ventilation decay rates determined for SF_6 are used to calculate first order removal rates of particle deposition and filtration.

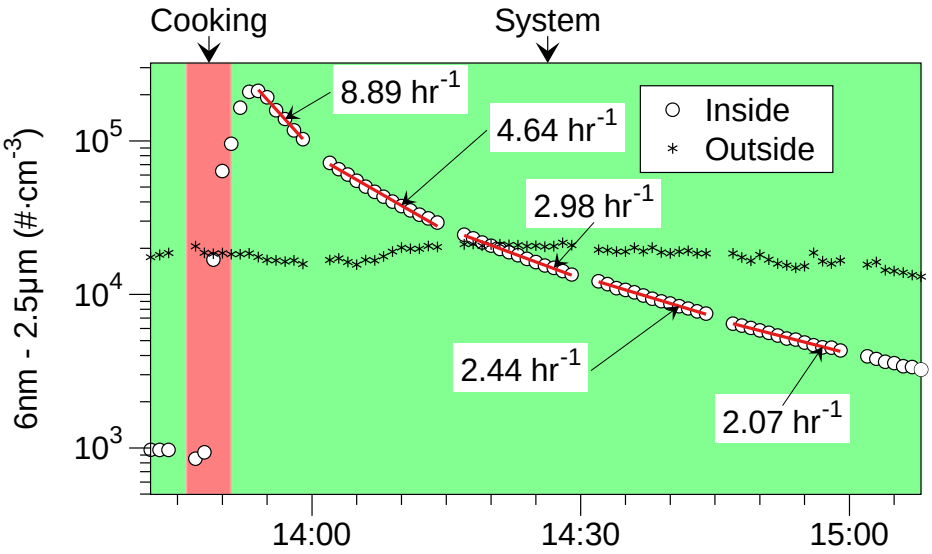

Figure IN-3-F-2. Number concentration of 6 nm to 2.5 µm diameter particles during cooking experiment with System F on Jun 23, 2014. Fitted decay rates during each period reflect sum of all particle transformation and removal mechanisms including growth, ventilation, deposition and filtration.

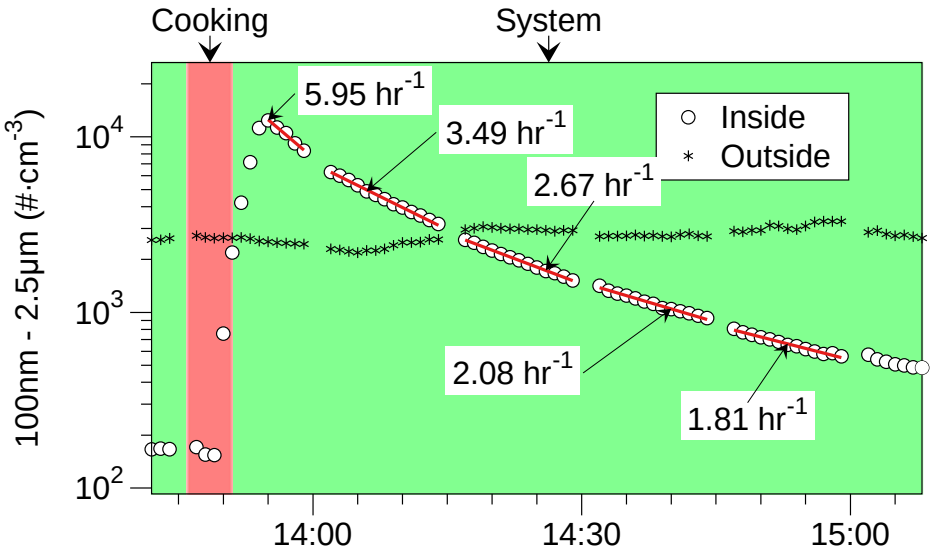

Figure IN-3-F-3. Number concentrations of 100 nm to 2.5 µm diameter particles during cooking experiment with System F on Jun 23, 2014. Fitted decay rates during each period reflect sum of all particle transformation and removal mechanisms including growth, ventilation, deposition and filtration.

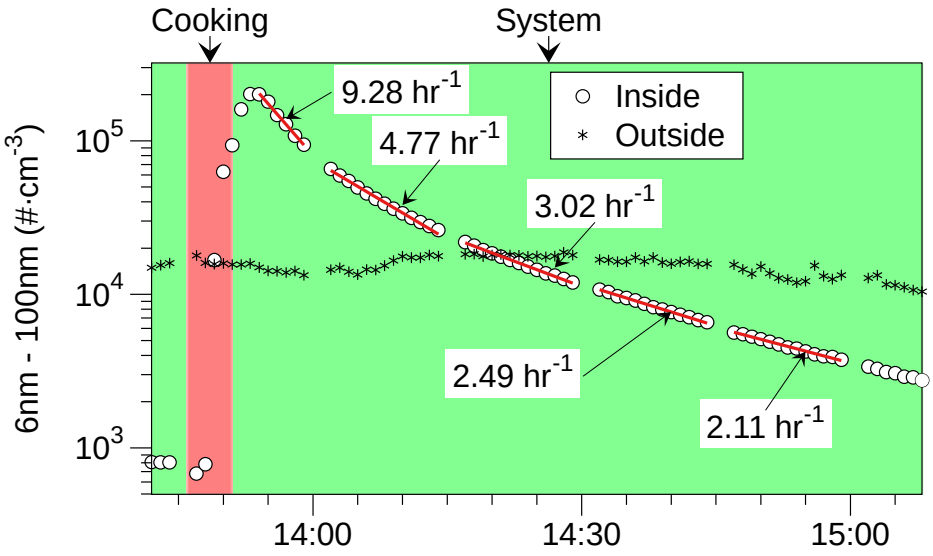

Figure IN-3-F-4. Number concentrations of 6–100 nm diameter particles during cooking experiment with System F on Jun 23, 2014. Data obtained by subtracting counts in range of 100 nm – 2.5 µm from counts in range of 6 nm – 2.5 µm. Fitted decay rates during each period reflect sum of all particle transformation and removal mechanisms including growth, ventilation, deposition and filtration.

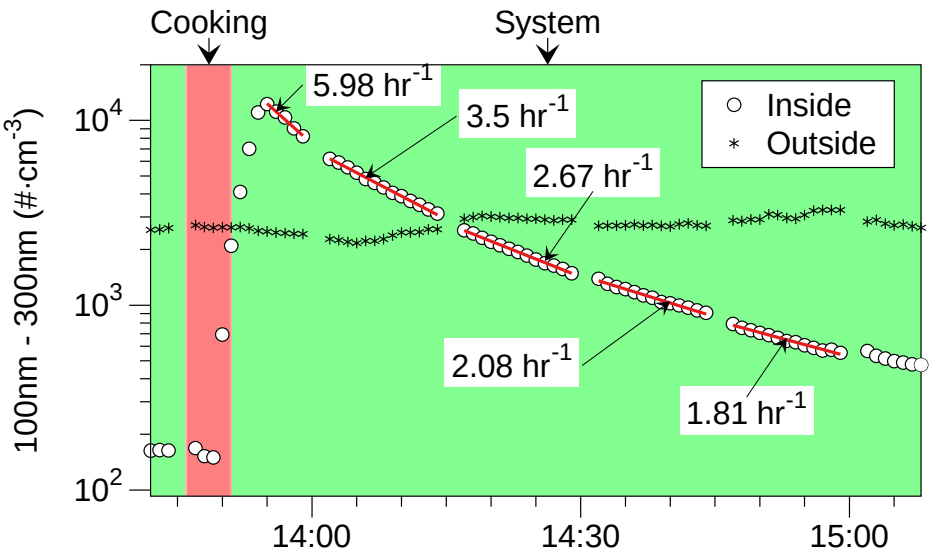

Figure IN-3-F-5. Number concentrations of 100-300 nm diameter particles during cooking experiment with System F on Jun 23, 2014. Data obtained by subtracting counts in range of 0.3–2.5 µm particles (MetOne 637) from the counts measured in the range of 100 nm–2.5 µm by the CPC3781 with size selective inlet. Fitted decay rates during each period reflect sum of all particle transformation and removal mechanisms including growth, ventilation, deposition and filtration.

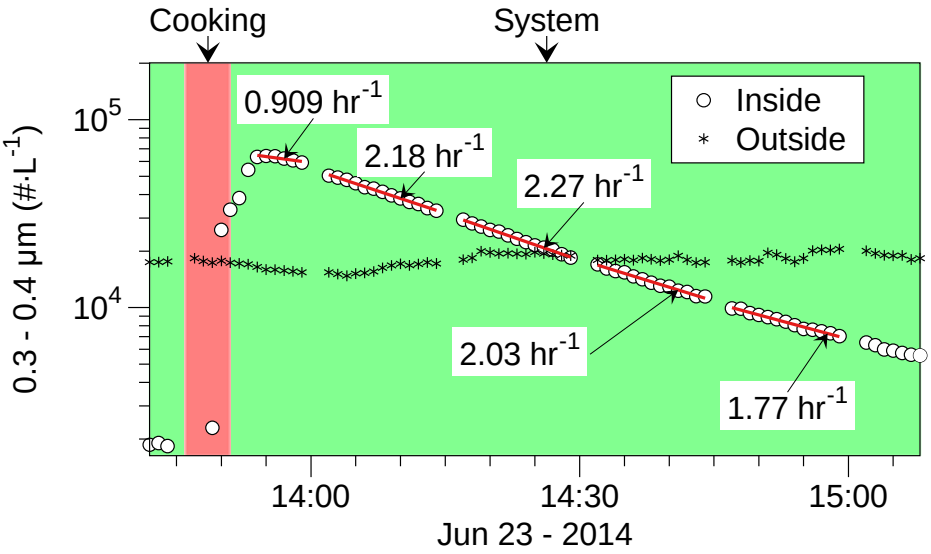

Figure IN-3-F-6. Number concentration of 0.3–0.4 µm diameter particles during cooking experiment with System F on Jun 23, 2014. Fitted decay rates during each period reflect sum of all particle transformation and removal mechanisms including growth, ventilation, deposition and filtration. Disconnected data during period just after cooking are from the two instruments switching between indoors and outdoors and may reflect small differences in the sampling efficiency at the lower cut point that is particularly sensitive to rapidly changing particle size distributions from the indoor source. Negative decay during this period indicates that the number of particles in this size bin is increasing.

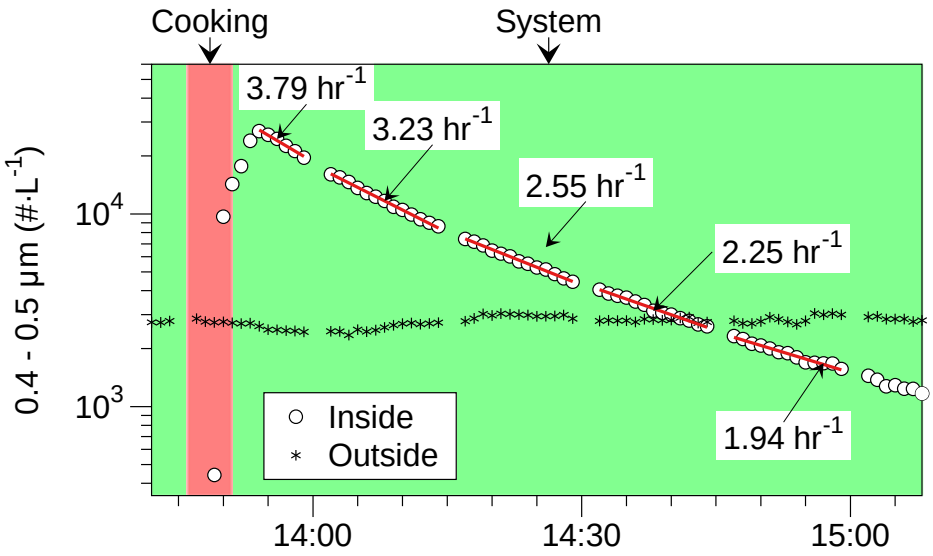

Figure IN-3-F-7. Number concentration of 0.4–0.5 µm diameter particles during cooking experiment with System F on Jun 23, 2014. Fitted decay rates during each period reflect sum of all particle transformation and removal mechanisms including growth, ventilation, deposition and filtration.

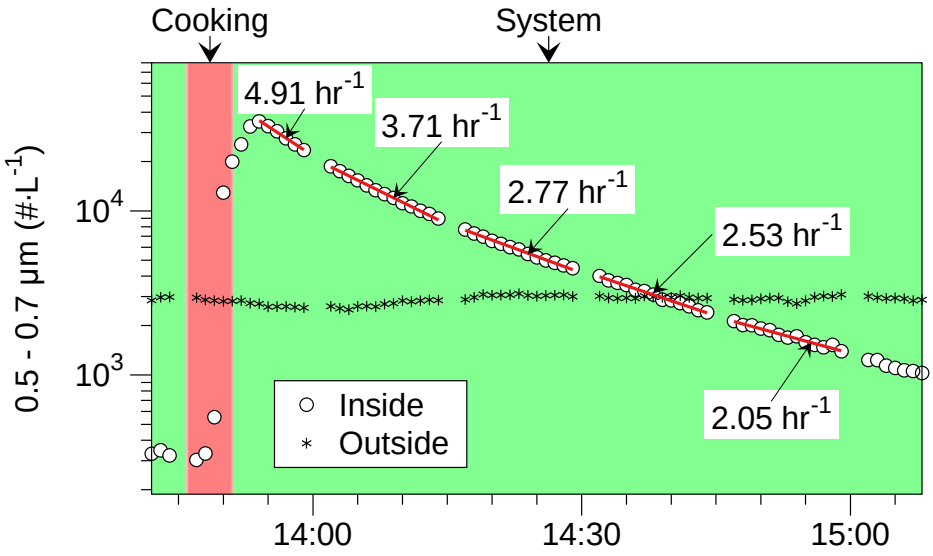

Figure IN-3-F-8. Number concentration of 0.5–0.7 µm diameter particles during cooking experiment with System F on Jun 23, 2014. Fitted decay rates during each period reflect sum of all particle transformation and removal mechanisms including growth, ventilation, deposition and filtration.

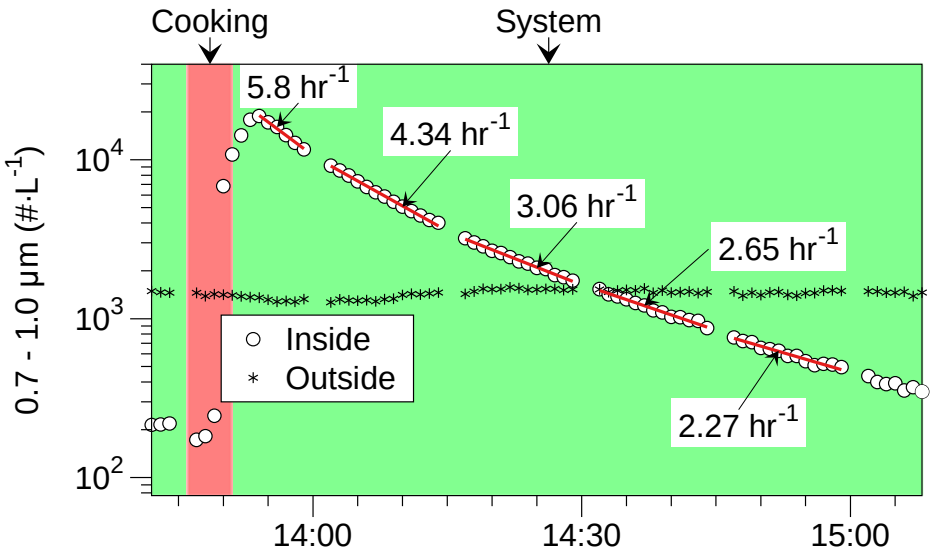

Figure IN-3-F-9. Number concentration of 0.7–1.0 µm diameter particles during cooking experiment with System F on Jun 23, 2014. Fitted decay rates during each period reflect sum of all particle transformation and removal mechanisms including growth, ventilation, deposition and filtration.

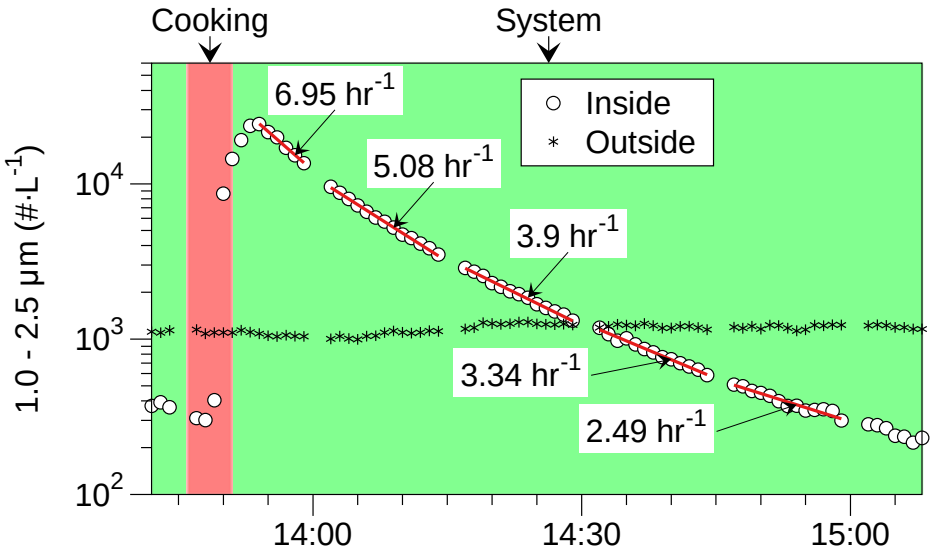

Figure IN-3-F-10. Number concentration of 1.0–2.5 µm diameter particles during cooking experiment with System F on Jun 23, 2014. Fitted decay rates during each period reflect sum of all particle transformation and removal mechanisms including growth, ventilation, deposition and filtration.

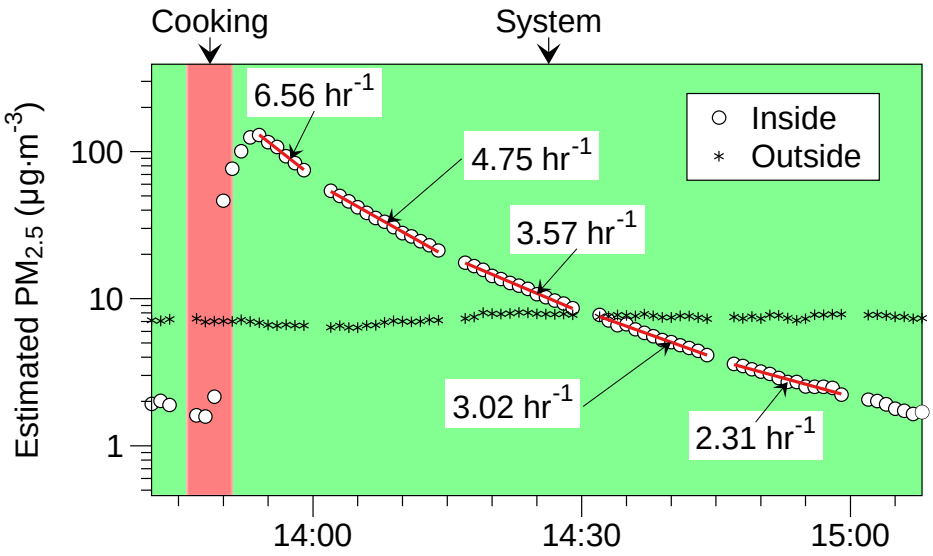

Figure IN-3-F-11. Estimated $PM_{2.5}$ concentration calculated from size-resolved particle number concentrations during cooking experiment with System F on Jun 23, 2014. Refer to Methods section of main report for details on this calculation. Fitted decay rates during each period reflect sum of all particle transformation and removal mechanisms including growth, ventilation, deposition and filtration.

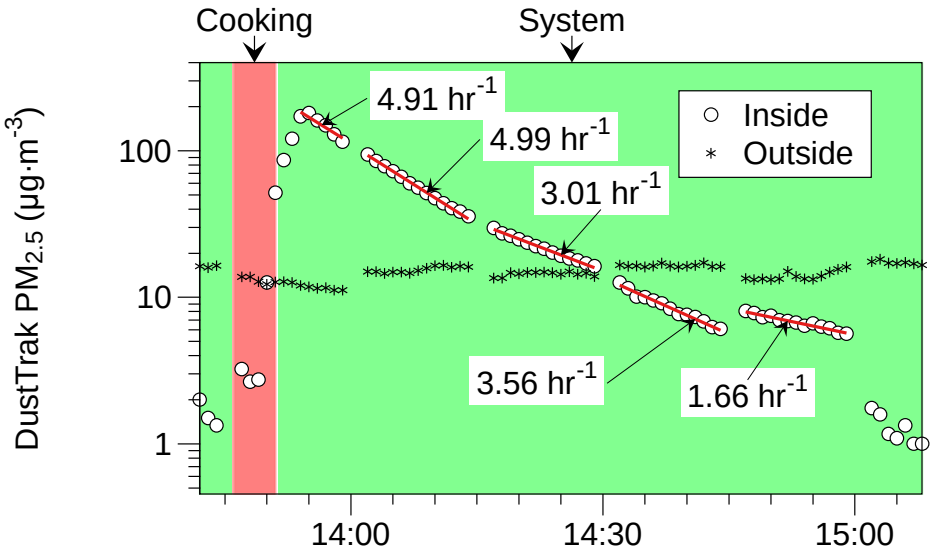

Figure IN-3-F-12. $PM_{2.5}$ concentrations measured by TSI DustTrak II 8530 during cooking experiment with System F on Jun 23, 2014. Fitted decay rates during each period reflect sum of all particle transformation and removal mechanisms including growth, ventilation, deposition and filtration.

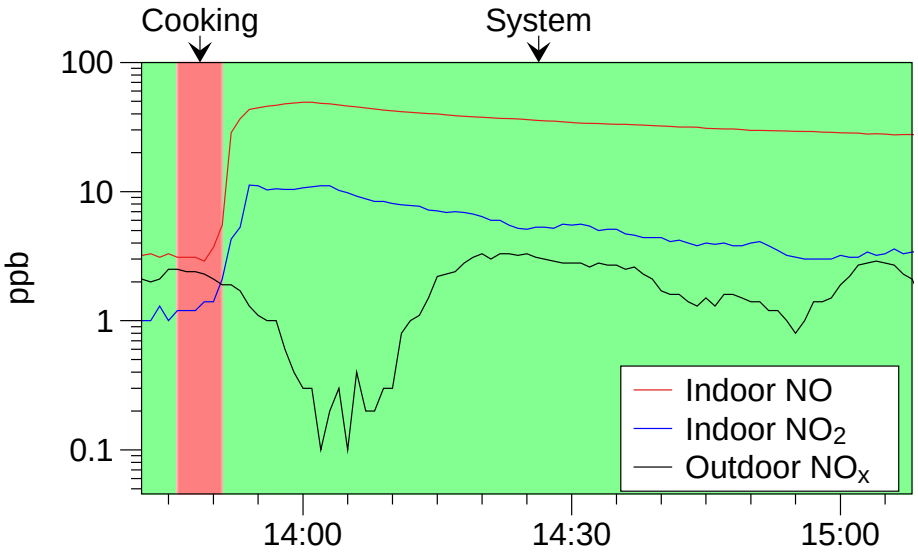

Figure IN-3-F-13. Concentration of NO and NO_2 during cooking experiment with System F on Jun 23, 2014.

Appendix IN-4-G. System G Performance for Cooking-Related Pollutants, July 2, 2014

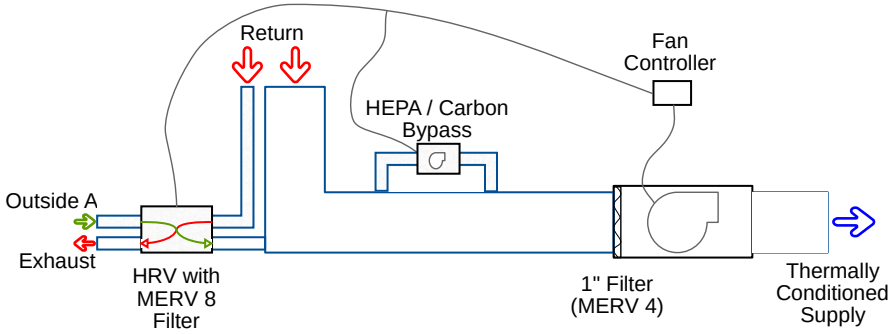

Notes about this monitoring period

2014/07/02 08:48:25.3,Walked into the house
2014/07/02 09:24:41.8,Burner on
2014/07/02 09:29:41.5,Burner off

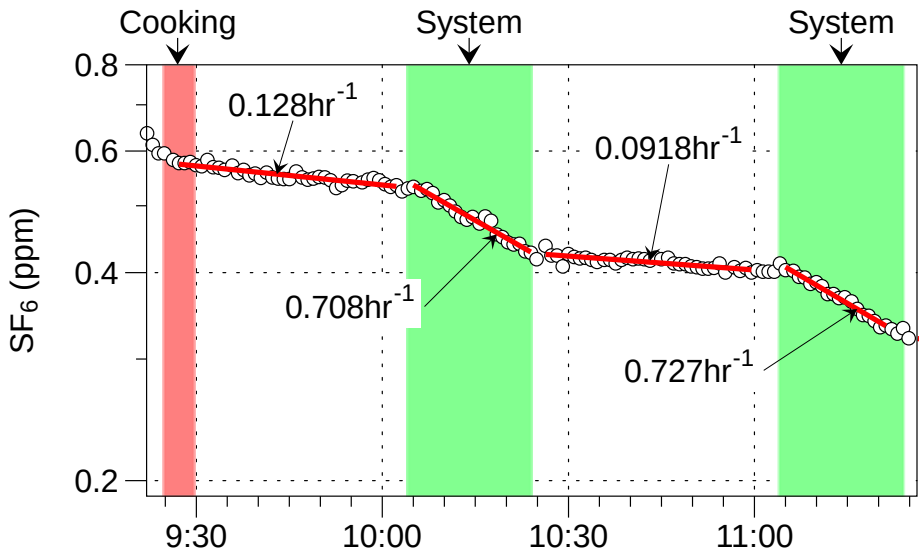

Figure IN-4-G-1. SF_6 during cooking experiment with System G on Jul 2, 2014. Injection occurred prior to the display interval. During each interval, a red line shows a best-fit, first-order decay rate that indicates the air exchange rate. Stir-frying of green beans occurred during the first shaded interval. A timer operated the central air handler for 20 min of each hour. Faster decay occurred during system operation because of intermittent ventilation supply connected to the air handler. Ventilation decay rates determined for SF_6 are used to calculate first order removal rates of particle deposition and filtration.

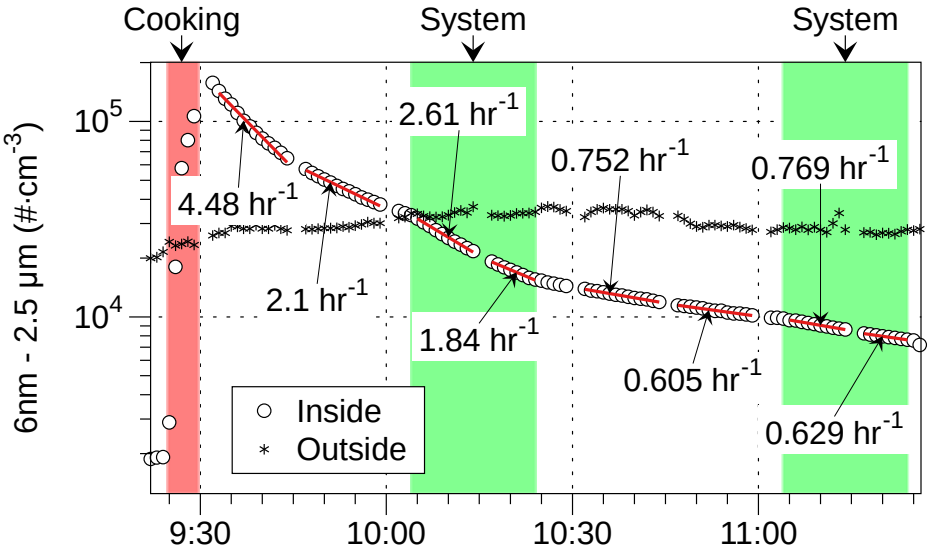

Figure IN-4-G-2. Number concentration of 6 nm to 2.5 µm diameter particles during cooking experiment with System G on Jul 2, 2014. Fitted decay rates during each period reflect sum of all particle transformation and removal mechanisms including growth, ventilation, deposition and filtration.

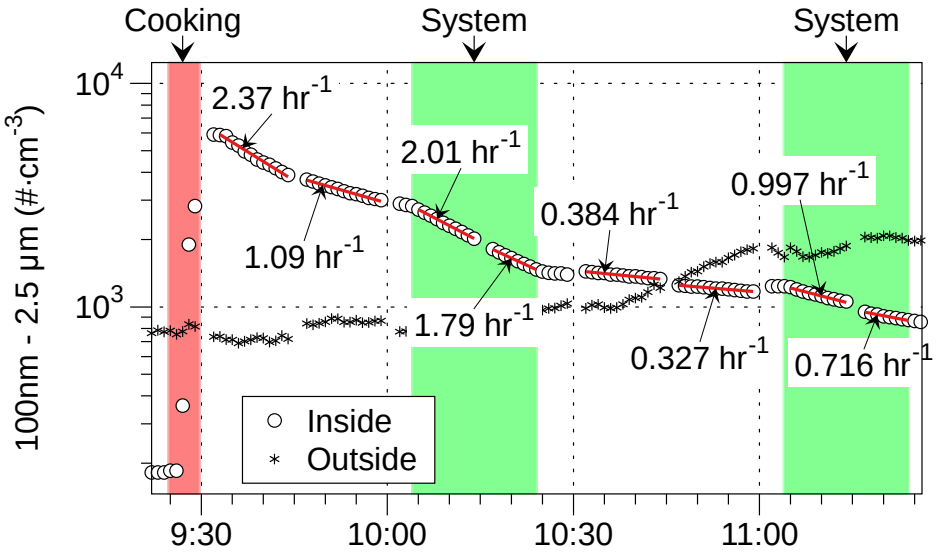

Figure IN-4-G-3. Number concentrations of 100 nm to 2.5 µm diameter particles during cooking experiment with System G on Jul 2, 2014. Fitted decay rates during each period reflect sum of all particle transformation and removal mechanisms including growth, ventilation, deposition and filtration.

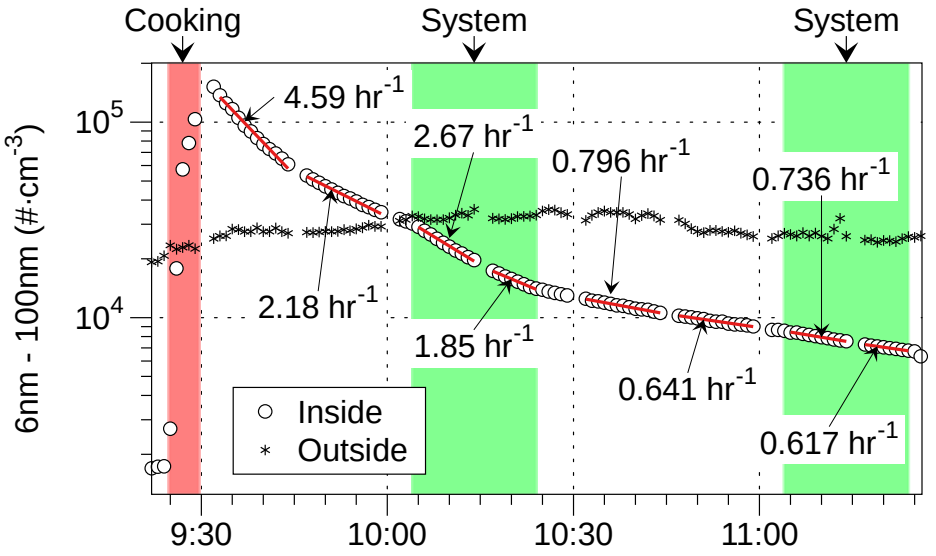

Figure IN-4-G-4. Number concentrations of 6–100 nm diameter particles during cooking experiment with System G on Jul 2, 2014. Data obtained by subtracting counts in range of 100 nm – 2.5 µm from counts in range of 6 nm – 2.5 µm. Fitted decay rates during each period reflect sum of all particle transformation and removal mechanisms including growth, ventilation, deposition and filtration.

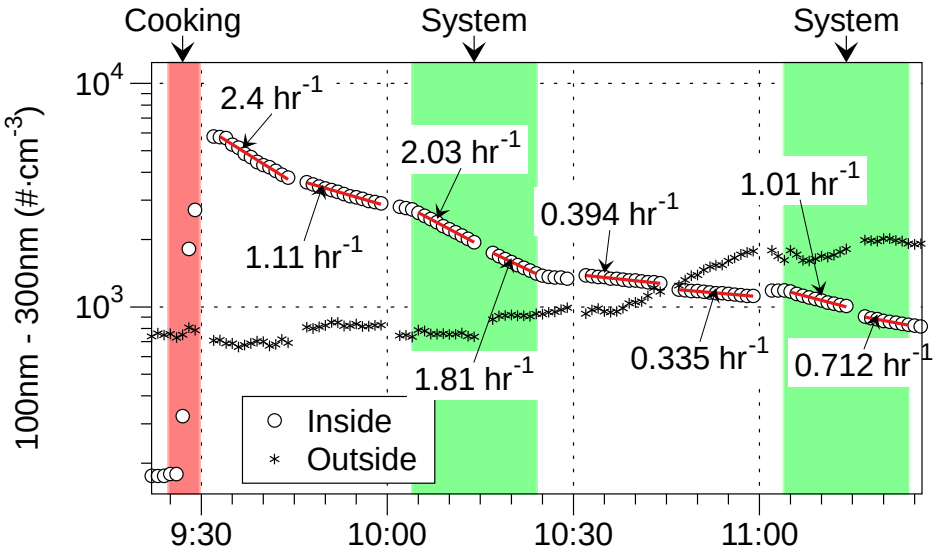

Figure IN-4-G-5. Number concentrations of 100-300 nm diameter particles during cooking experiment with System G on Jul 2, 2014. Data obtained by subtracting counts in range of 0.3–2.5 µm particles (MetOne 637) from the counts measured in the range of 100 nm–2.5 µm by the CPC3781 with size selective inlet. Fitted decay rates during each period reflect sum of all particle transformation and removal mechanisms including growth, ventilation, deposition and filtration.

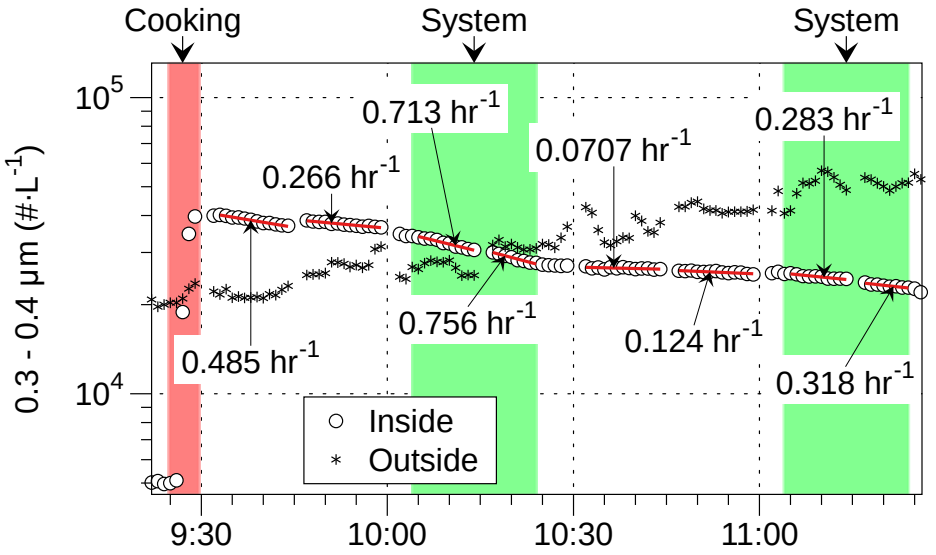

Figure IN-4-G-6. Number concentration of 0.3–0.4 µm diameter particles during cooking experiment with System G on Jul 2, 2014. Fitted decay rates during each period reflect sum of all particle transformation and removal mechanisms including growth, ventilation, deposition and filtration. Disconnected data during period just after cooking are from the two instruments switching between indoors and outdoors and may reflect small differences in the sampling efficiency at the lower cut point that is particularly sensitive to rapidly changing particle size distributions from the indoor source. Negative decay during this period indicates that the number of particles in this size bin is increasing.

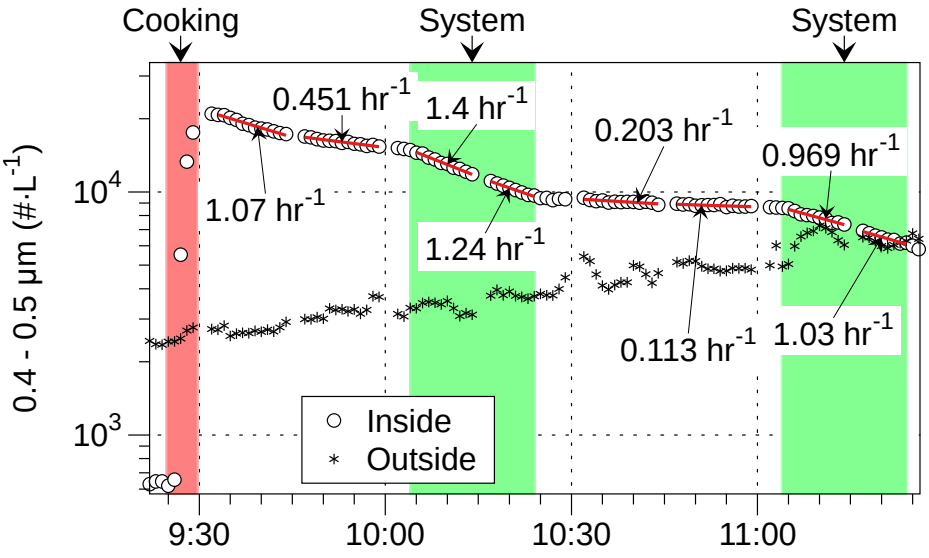

Figure IN-4-G-7. Number concentration of 0.4–0.5 µm diameter particles during cooking experiment with System G on Jul 2, 2014. Fitted decay rates during each period reflect sum of all particle transformation and removal mechanisms including growth, ventilation, deposition and filtration.

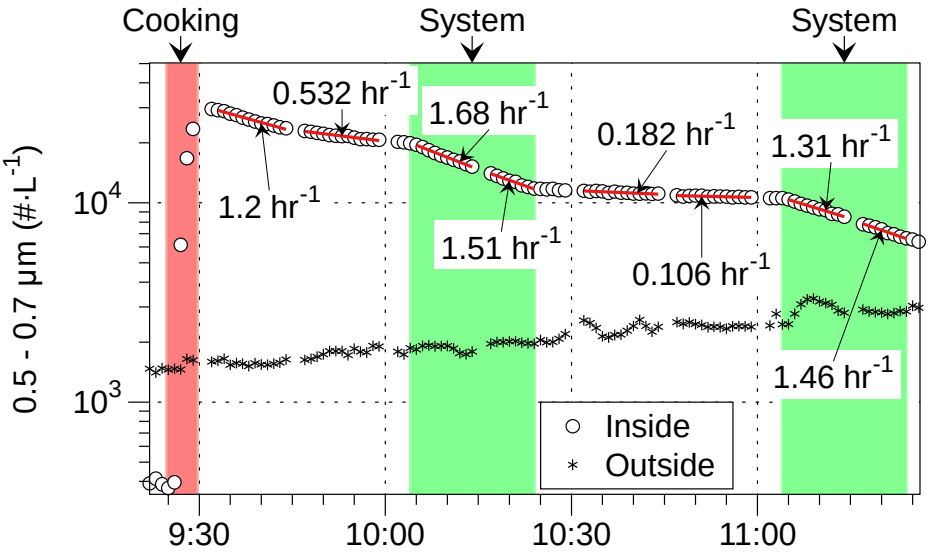

Figure IN-4-G-8. Number concentration of 0.5–0.7 µm diameter particles during cooking experiment with System G on Jul 2, 2014. Fitted decay rates during each period reflect sum of all particle transformation and removal mechanisms including growth, ventilation, deposition and filtration.

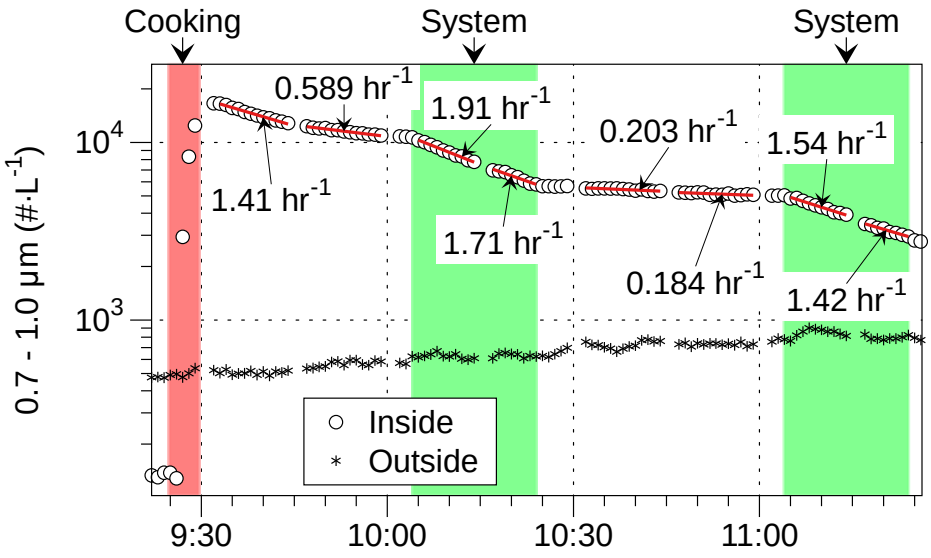

Figure IN-4-G-9. Number concentration of 0.7-1.0 µm diameter particles during cooking experiment with System G on Jul 2, 2014. Fitted decay rates during each period reflect sum of all particle transformation and removal mechanisms including growth, ventilation, deposition and filtration.

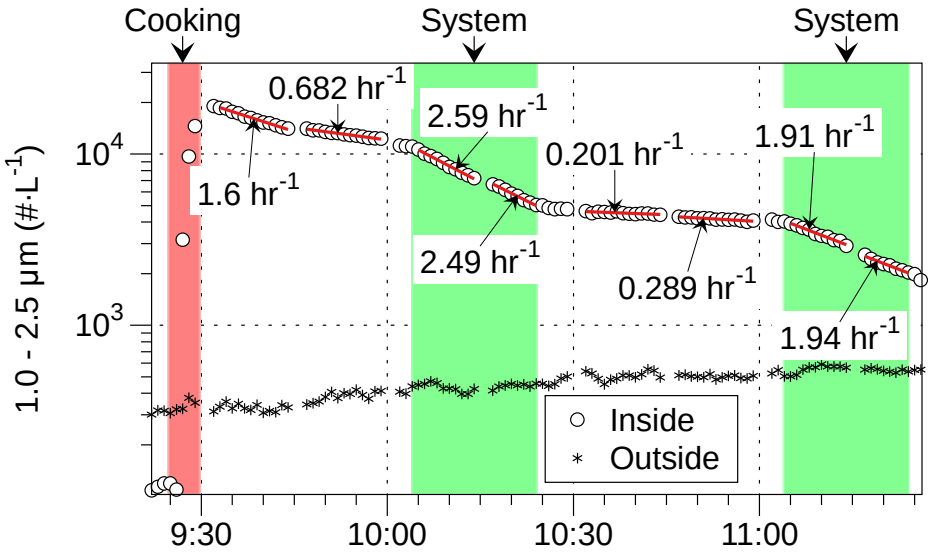

Figure IN-4-G-10. Number concentration of 1.0–2.5 µm diameter particles during cooking experiment with System G on Jul 2, 2014. Fitted decay rates during each period reflect sum of all particle transformation and removal mechanisms including growth, ventilation, deposition and filtration.

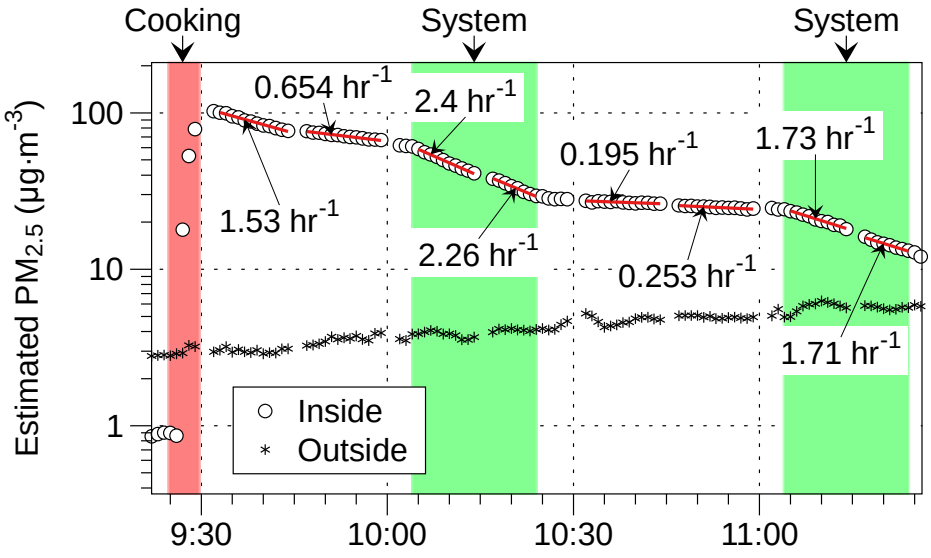

Figure IN-4-G-11. Estimated $PM_{2.5}$ concentration calculated from size-resolved particle number concentrations during cooking experiment with System G on Jul 2, 2014. Refer to Methods section of main report for details on this calculation. Fitted decay rates during each period reflect sum of all particle transformation and removal mechanisms including growth, ventilation, deposition and filtration.

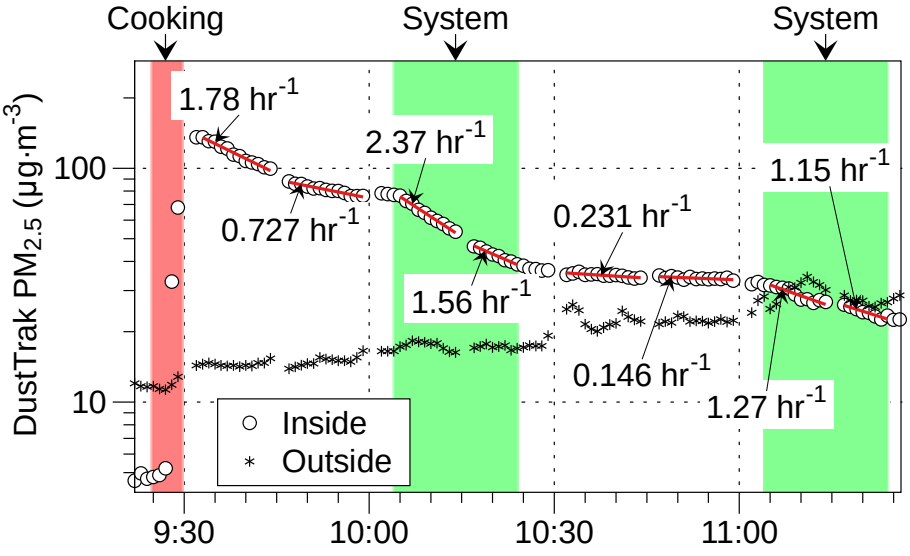

Figure IN-4-G-12. $PM_{2.5}$ concentrations measured by TSI DustTrak II 8530 during cooking experiment with System G on Jul 2, 2014. Fitted decay rates during each period reflect sum of all particle transformation and removal mechanisms including growth, ventilation, deposition and filtration.

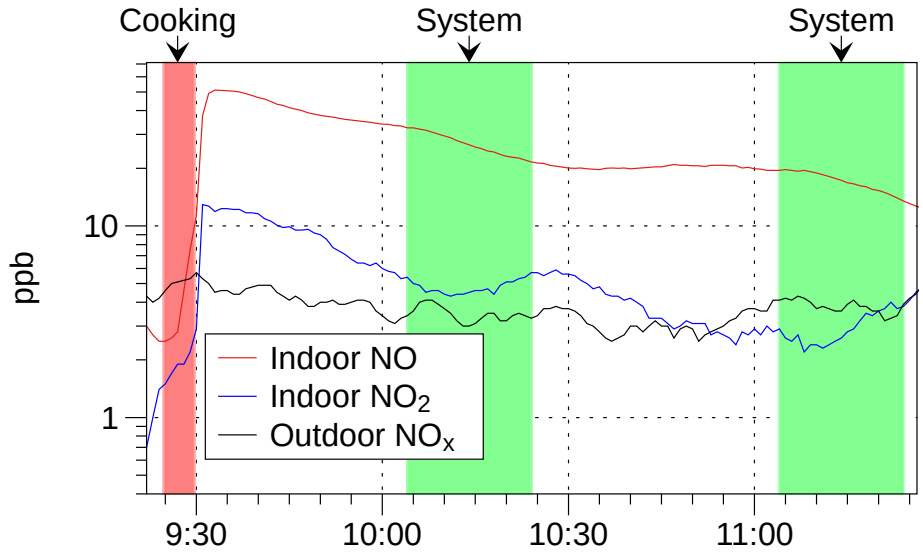

Figure IN-4-G-13. Concentration of NO and NO_2 during cooking experiment with System G on Jul 2, 2014.

Appendix IN-5-R. Reference System Performance for Cooking-Related Pollutants, July 9, 2014

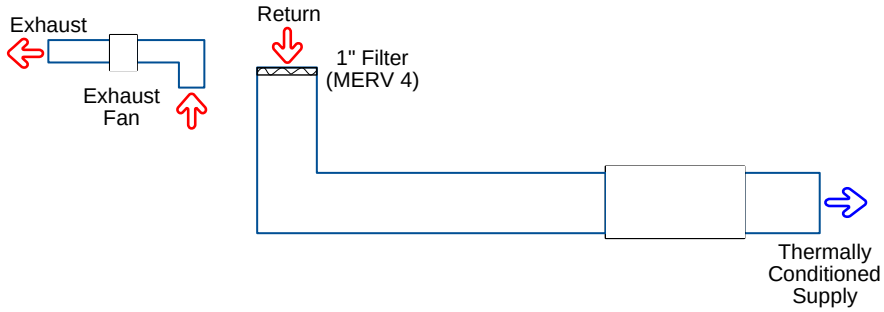

Notes about this monitoring period

We forgot to disconnect the injectors and do spike a release of SF_6, ACH values are calculated over an averaging period using the constant injection technique.

2014/07/09 09:57:49.5, Burner On
2014/07/09 10:02:50.2, Burner Off

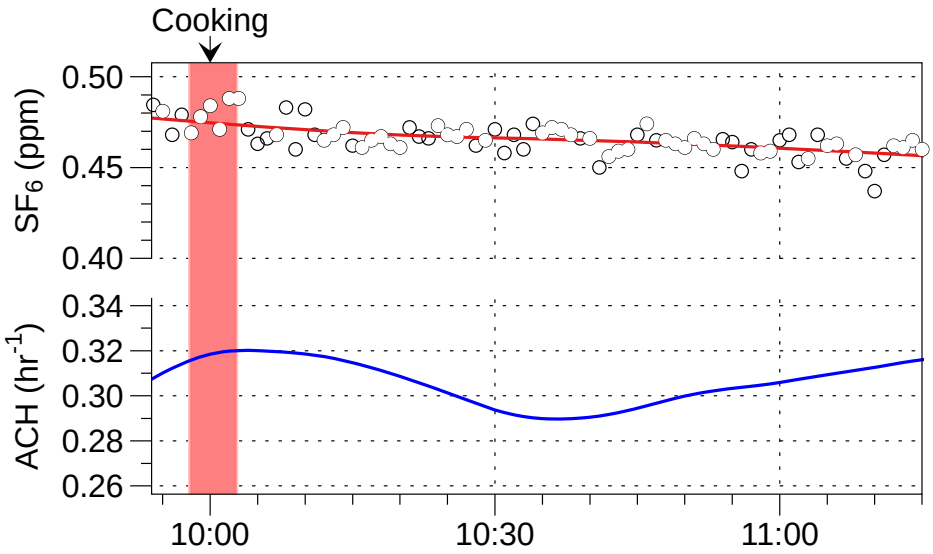

Figure IN-5-R-1. SF_6 during cooking experiment with Reference System on Jul 9, 2014. The top panel shows the concentration values, and the bottom panel shows the resulting ventilation rate. Ventilation decay rates determined for SF_6 are used to calculate first order removal rates of particle deposition and filtration.

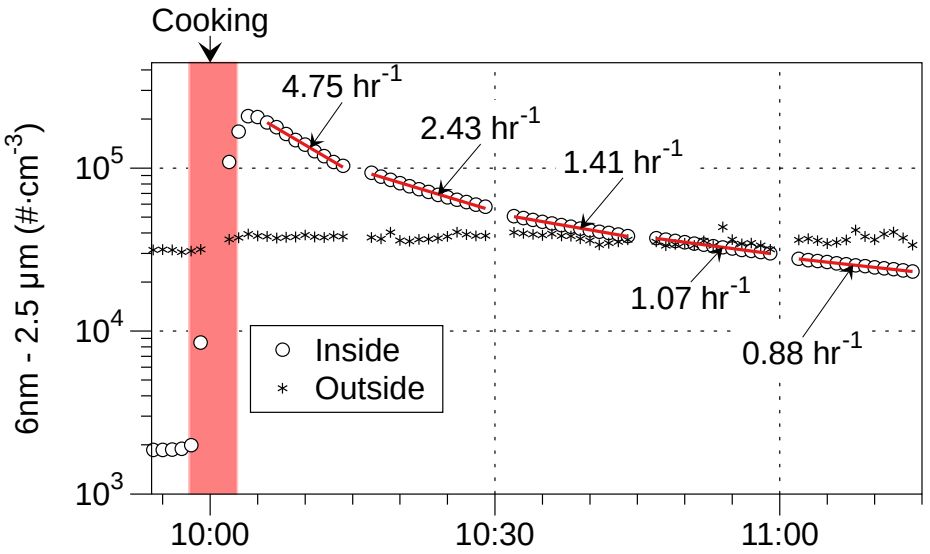

Figure IN-5-R-2. Number concentration of 6 nm to 2.5 µm diameter particles during cooking experiment with Reference System on Jul 9, 2014. Fitted decay rates during each period reflect sum of all particle transformation and removal mechanisms including growth, ventilation, deposition and filtration.

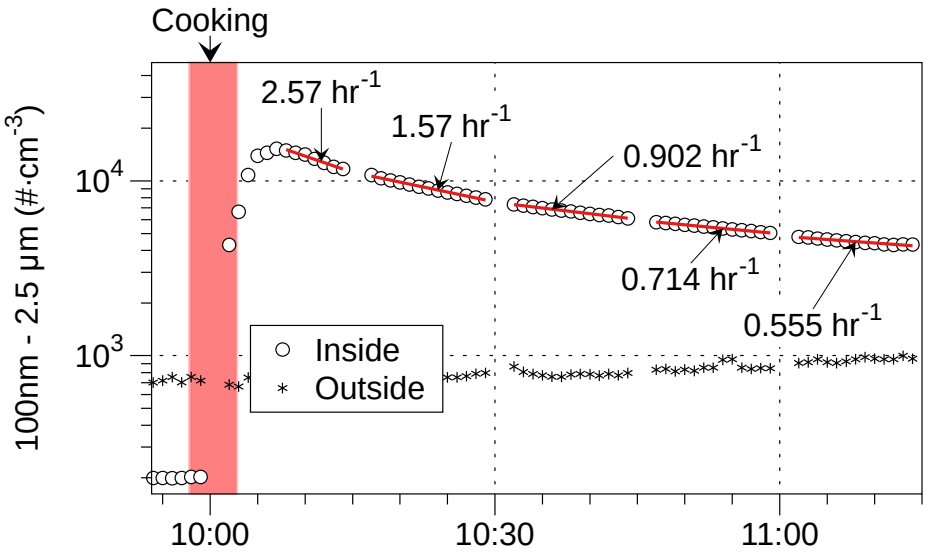

Figure IN-5-R-3. Number concentrations of 100 nm to 2.5 µm diameter particles during cooking experiment with Reference System on Jul 9, 2014. Fitted decay rates during each period reflect sum of all particle transformation and removal mechanisms including growth, ventilation, deposition and filtration.

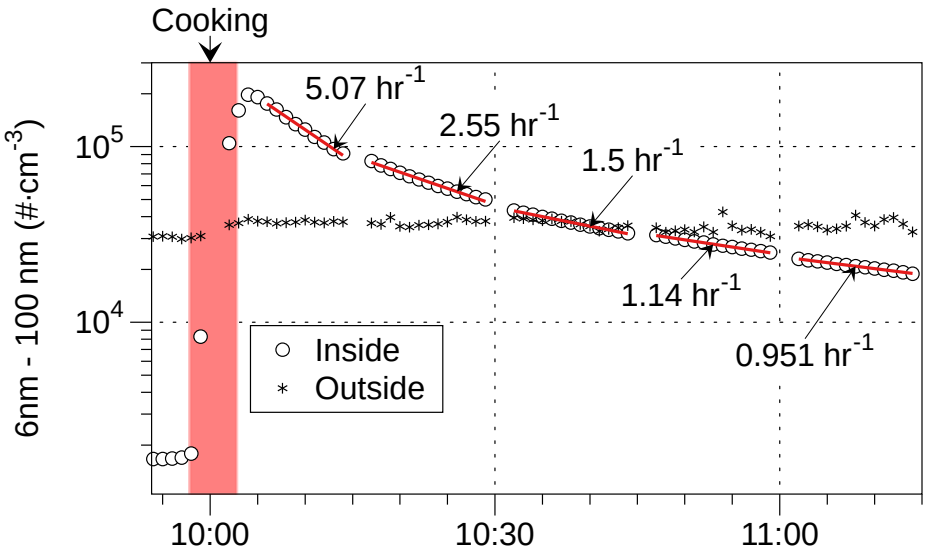

Figure IN-5-R-4. Number concentrations of 6–100 nm diameter particles during cooking experiment with Reference System on Jul 9, 2014. Data obtained by subtracting counts in range of 100 nm – 2.5 µm from counts in range of 6 nm – 2.5 µm. Fitted decay rates during each period reflect sum of all particle transformation and removal mechanisms including growth, ventilation, deposition and filtration.

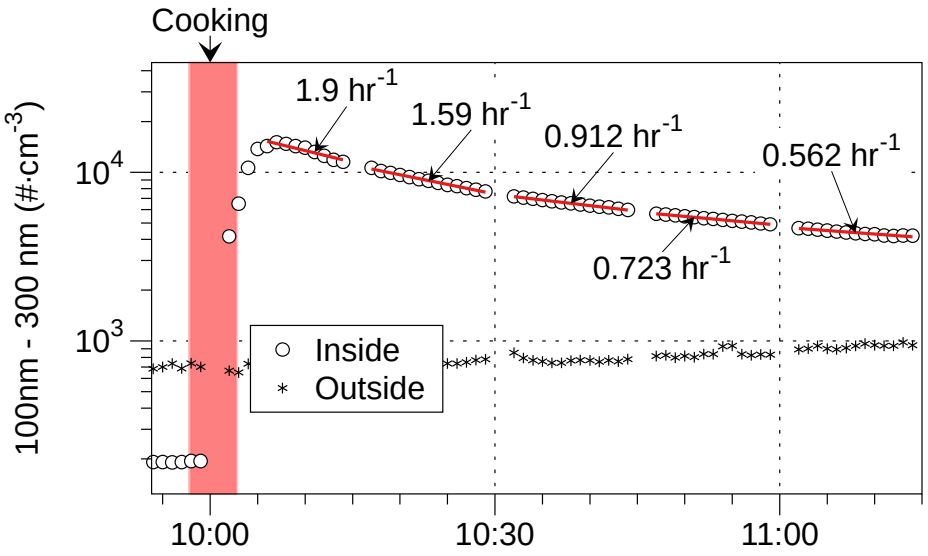

Figure IN-5-R-5. Number concentrations of 100-300 nm diameter particles during cooking experiment with Reference System on Jul 9, 2014. Data obtained by subtracting counts in range of 0.3–2.5 μm particles (MetOne 637) from the counts measured in the range of 100 nm–2.5 μm by the CPC3781 with size selective inlet. Fitted decay rates during each period reflect sum of all particle transformation and removal mechanisms including growth, ventilation, deposition and filtration.

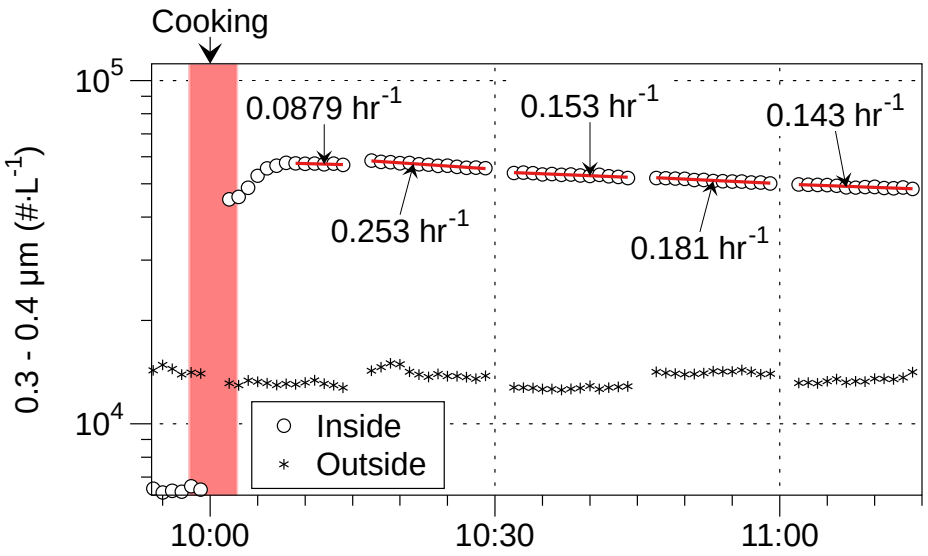

Figure IN-5-R-6. Number concentration of 0.3–0.4 μm diameter particles during cooking experiment with Reference System on Jul 9, 2014. Fitted decay rates during each period reflect sum of all particle transformation and removal mechanisms including growth, ventilation, deposition and filtration. Disconnected data during period just after cooking are from the two instruments switching between indoors and outdoors and may reflect small differences in the sampling efficiency at the lower cut point that is particularly sensitive to rapidly changing particle size distributions from the indoor source. Negative decay during this period indicates that the number of particles in this size bin is increasing.

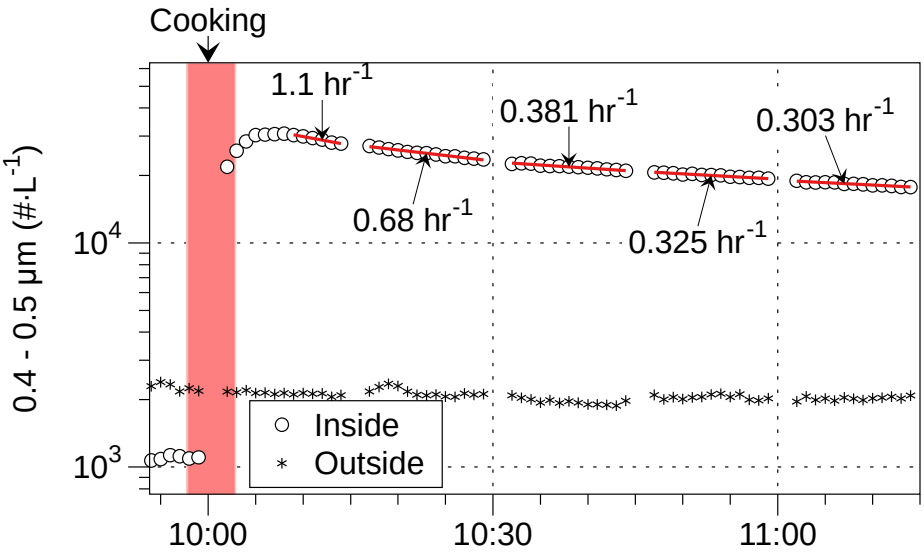

Figure IN-5-R-7. Number concentration of 0.4–0.5 µm diameter particles during cooking experiment with Reference System on Jul 9, 2014. Fitted decay rates during each period reflect sum of all particle transformation and removal mechanisms including growth, ventilation, deposition and filtration.

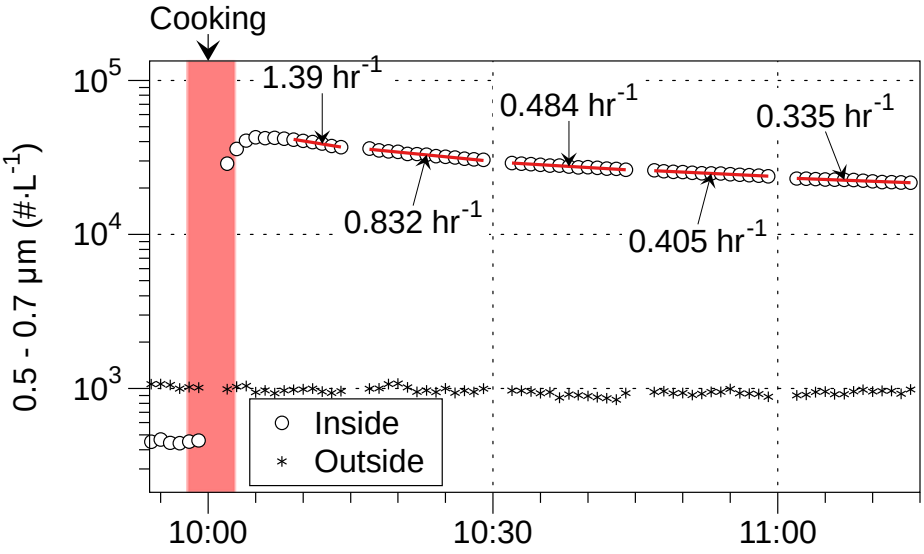

Figure IN-5-R-8. Number concentration of 0.5–0.7 µm diameter particles during cooking experiment with Reference System on Jul 9, 2014. Fitted decay rates during each period reflect sum of all particle transformation and removal mechanisms including growth, ventilation, deposition and filtration.

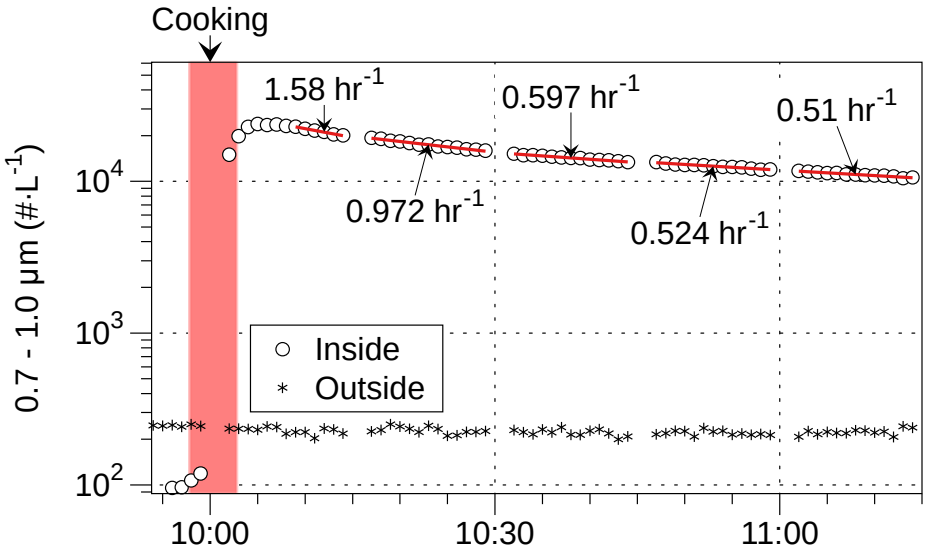

Figure IN-5-R-9. Number concentration of 0.7-1.0 µm diameter particles during cooking experiment with Reference System on Jul 9, 2014. Fitted decay rates during each period reflect sum of all particle transformation and removal mechanisms including growth, ventilation, deposition and filtration.

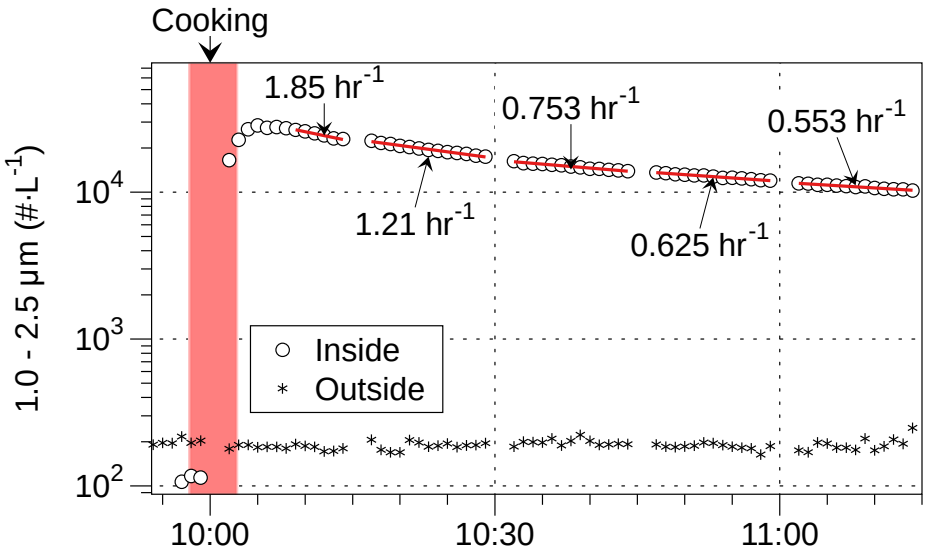

Figure IN-5-R-10. Number concentration of 1.0–2.5 µm diameter particles during cooking experiment with Reference System on Jul 9, 2014. Fitted decay rates during each period reflect sum of all particle transformation and removal mechanisms including growth, ventilation, deposition and filtration.

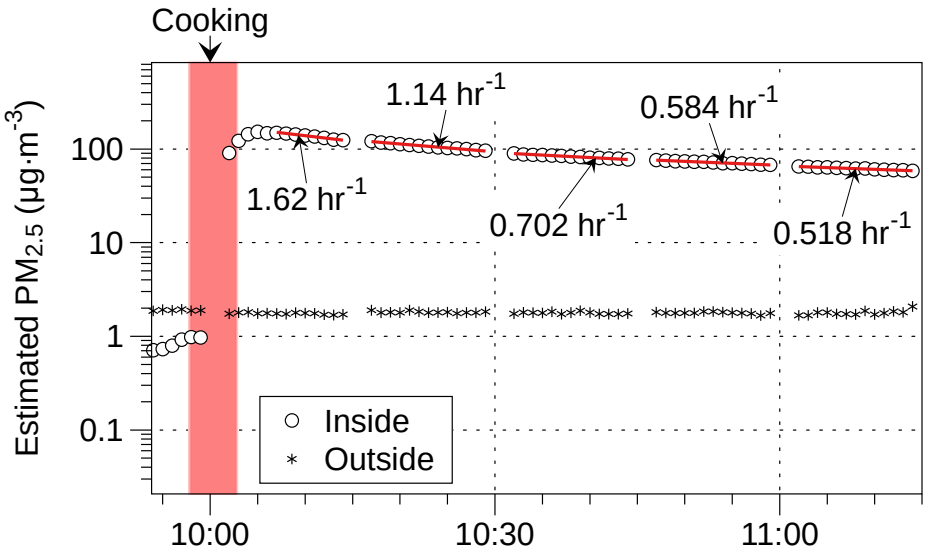

Figure IN-5-R-11. Estimated $PM_{2.5}$ concentration calculated from size-resolved particle number concentrations during cooking experiment with Reference System on Jul 9, 2014. Refer to Methods section of main report for details on this calculation. Fitted decay rates during each period reflect sum of all particle transformation and removal mechanisms including growth, ventilation, deposition and filtration.

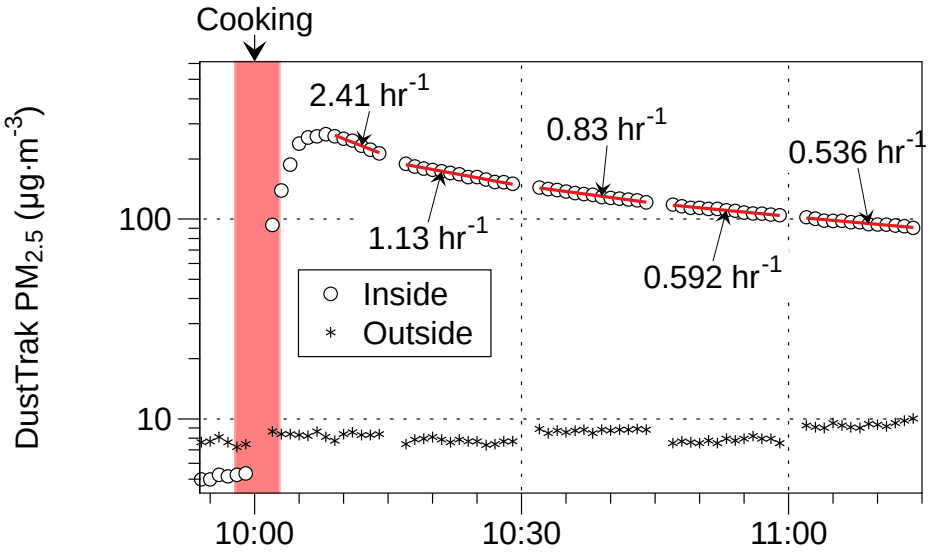

Figure IN-5-R-12. $PM_{2.5}$ concentrations measured by TSI DustTrak II 8530 during cooking experiment with Reference System on Jul 9, 2014. Fitted decay rates during each period reflect sum of all particle transformation and removal mechanisms including growth, ventilation, deposition and filtration.

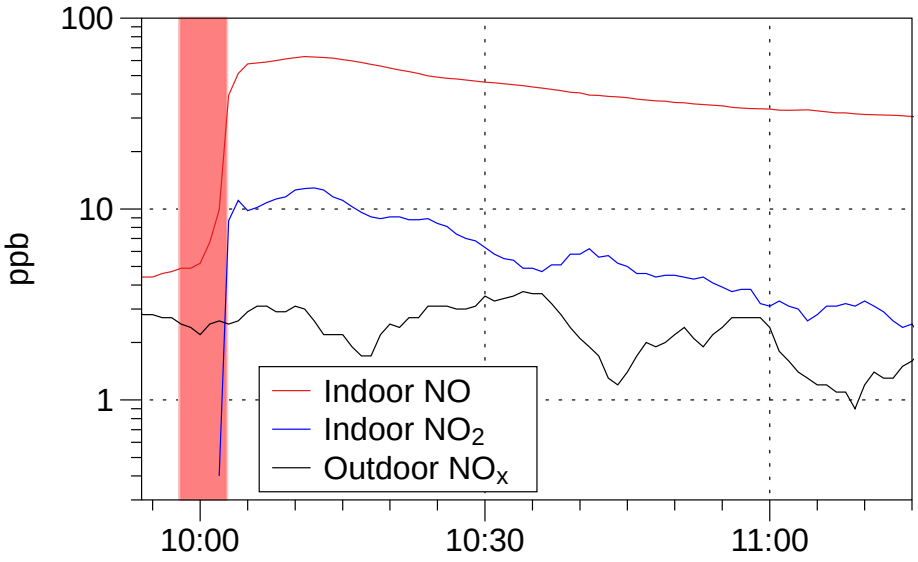

Figure IN-5-R-13. Concentration of NO and NO_2 during cooking experiment with Reference System on Jul 9, 2014. Fitted decay rates during each period reflect sum of all generation and removal mechanisms.

Appendix IN-6-D. System D Performance for Cooking-Related Pollutants, July 16, 2014

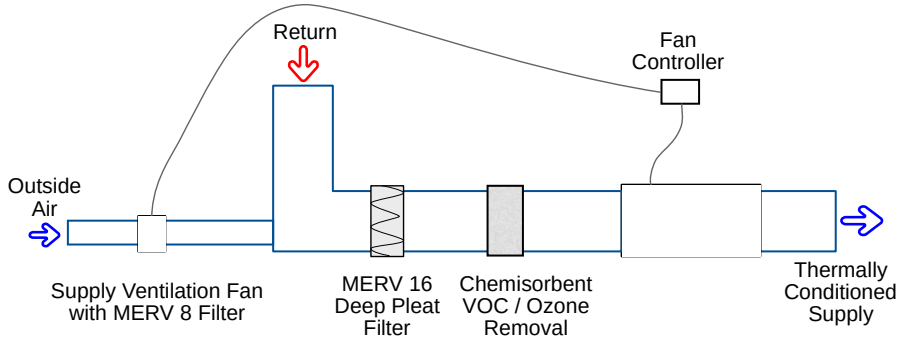

Notes about this monitoring period

2014/07/16 08:54:52.6, SF_6 Injection ~70ml
2014/07/16 09:01:54.5, Burner on
2014/07/16 09:06:54.4, Burner Off

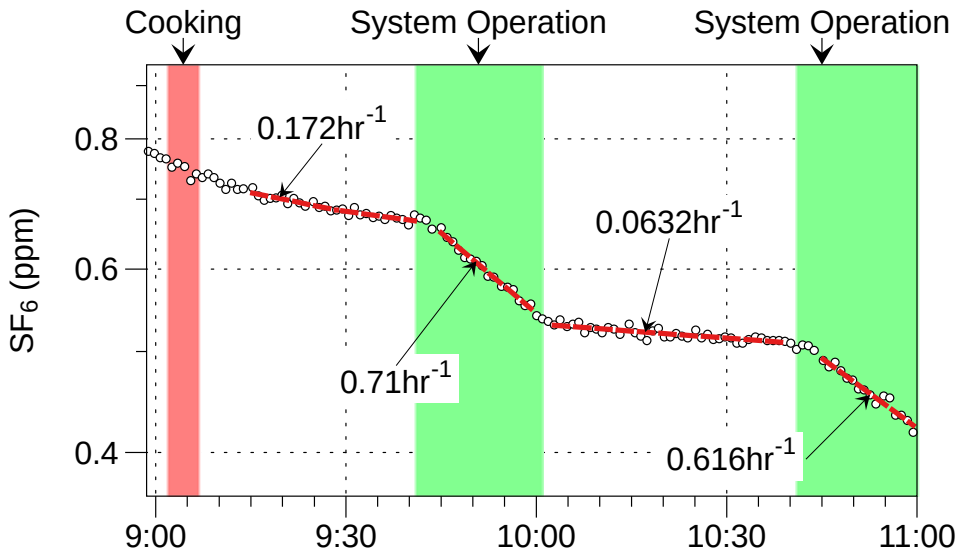

Figure IN-6-D-1. SF_6 during cooking experiment with System D on Jul 16, 2014. Injection occurred prior to the display interval. During each interval, a red line shows a best-fit, first-order decay rate that indicates the air exchange rate. Stir-frying of green beans occurred during the first shaded interval. A timer operated the central air handler for 20 min of each hour. Faster decay occurred during system operation because of intermittent ventilation supply connected to the air handler. Ventilation decay rates determined for SF_6 are used to calculate first order removal rates of particle deposition and filtration.

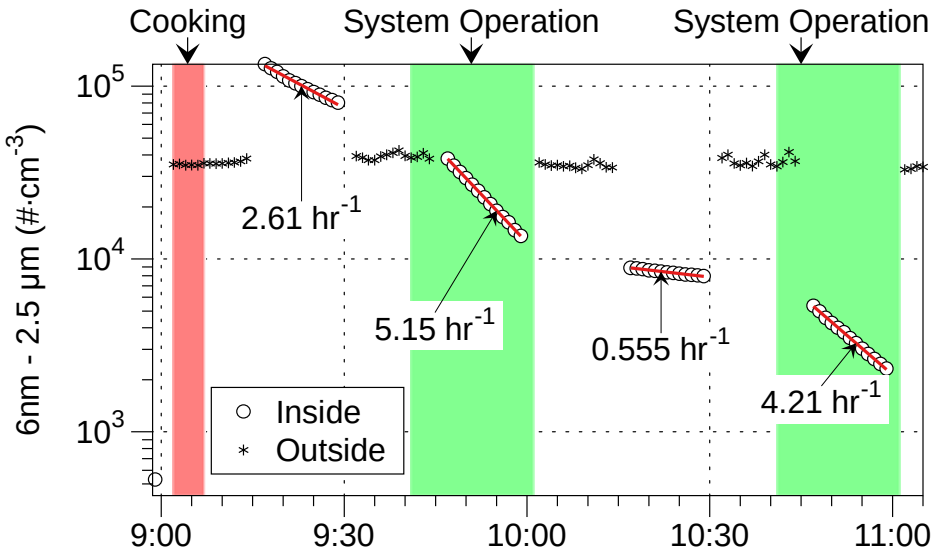

Figure IN-6-D-2. Number concentration of 6 nm to 2.5 µm diameter particles during cooking experiment with System D on Jul 16, 2014. Data shown for only one of two CPC3787s. The other unit had a wick problem during this experiment. Fitted decay rates during each period reflect sum of all particle transformation and removal mechanisms including growth, ventilation, deposition and filtration.

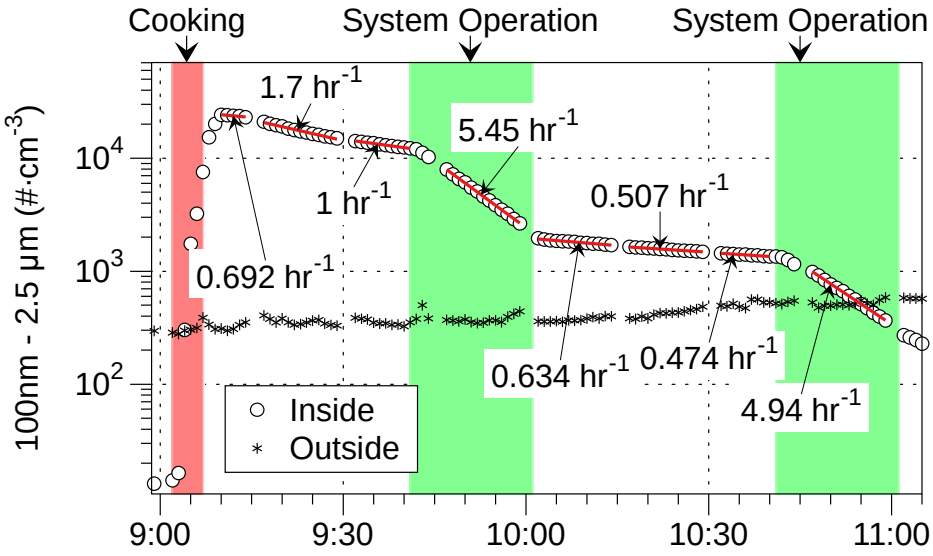

Figure IN-6-D-3. Number concentrations of 100 nm to 2.5 µm diameter particles during cooking experiment with System D on Jul 16, 2014. Fitted decay rates during each period reflect sum of all particle transformation and removal mechanisms including growth, ventilation, deposition and filtration.

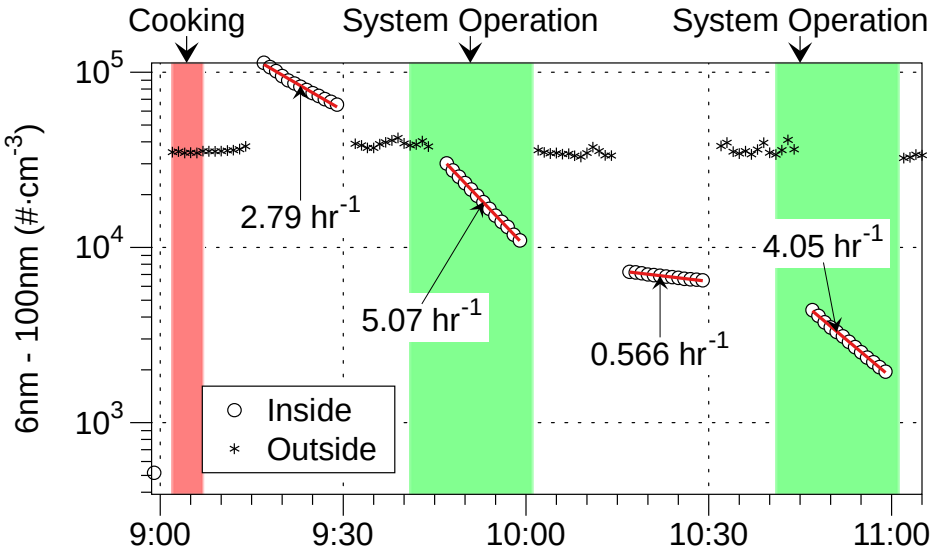

Figure IN-6-D-4. Number concentrations of 6–100 nm diameter particles during cooking experiment with System D on Jul 16, 2014. Data obtained by subtracting counts in range of 100 nm – 2.5 µm from counts in range of 6 nm – 2.5 µm. Fitted decay rates during each period reflect sum of all particle transformation and removal mechanisms including growth, ventilation, deposition and filtration.

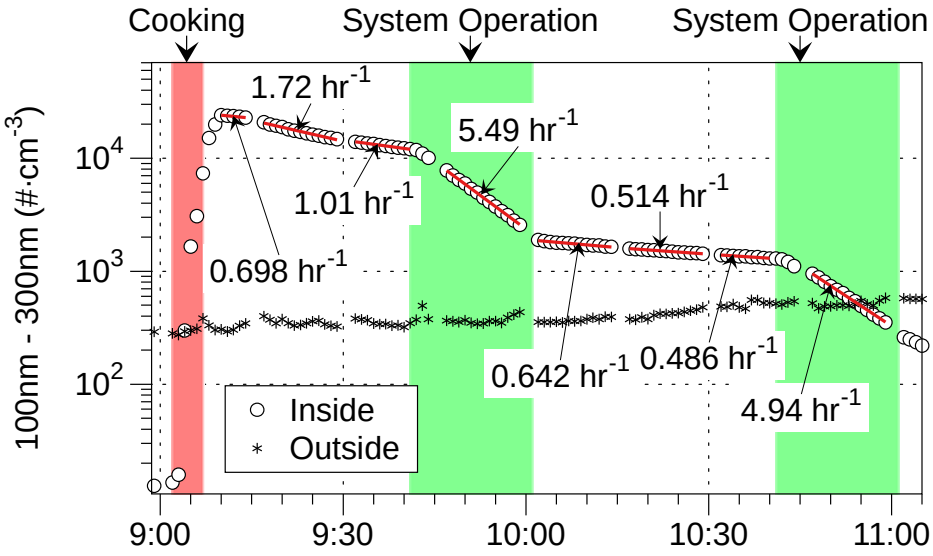

Figure IN-6-D-5. Number concentrations of 100-300 nm diameter particles during cooking experiment with System D on Jul 16, 2014. Data obtained by subtracting counts in range of 0.3–2.5 μm particles (MetOne 637) from the counts measured in the range of 100 nm–2.5 μm by the CPC3781 with size selective inlet. Fitted decay rates during each period reflect sum of all particle transformation and removal mechanisms including growth, ventilation, deposition and filtration.

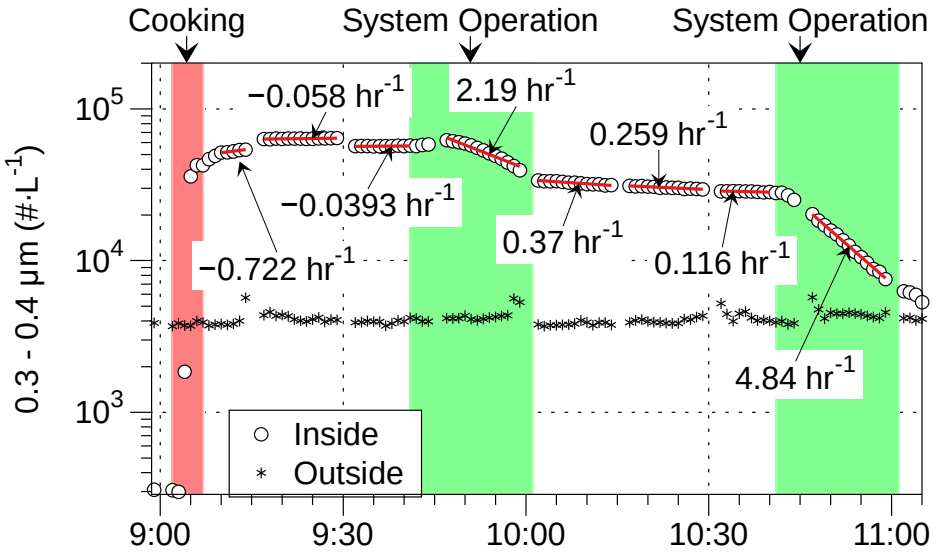

Figure IN-6-D-6. Number concentration of 0.3–0.4 μm diameter particles during cooking experiment with System D on Jul 16, 2014. Fitted decay rates during each period reflect sum of all particle transformation and removal mechanisms including growth, ventilation, deposition and filtration. Disconnected data during period just after cooking are from the two instruments switching between indoors and outdoors and may reflect small differences in the sampling efficiency at the lower cut point that is particularly sensitive to rapidly changing particle size distributions from the indoor source. Negative decay during this period indicates that the number of particles in this size bin is increasing.

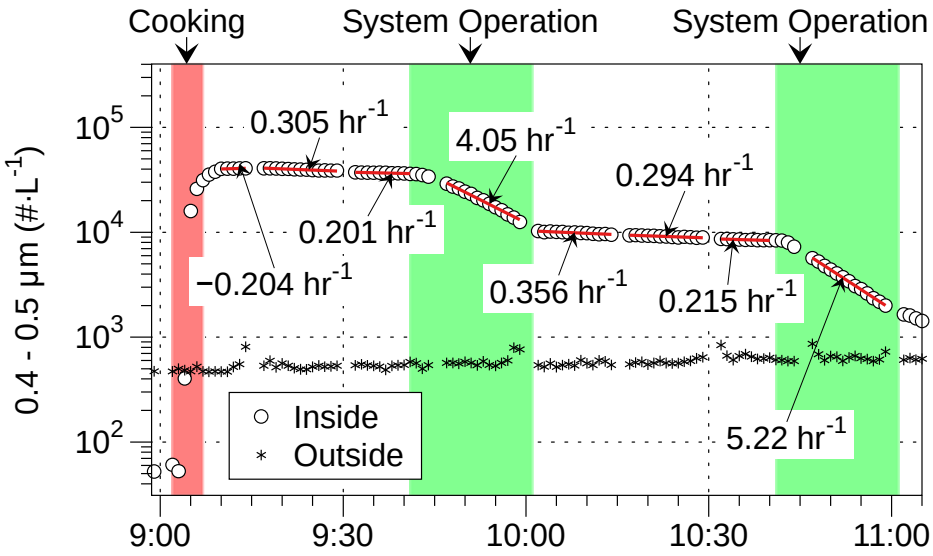

Figure IN-6-D-7. Number concentration of 0.4–0.5 µm diameter particles during cooking experiment with System D on Jul 16, 2014. Fitted decay rates during each period reflect sum of all particle transformation and removal mechanisms including growth, ventilation, deposition and filtration.

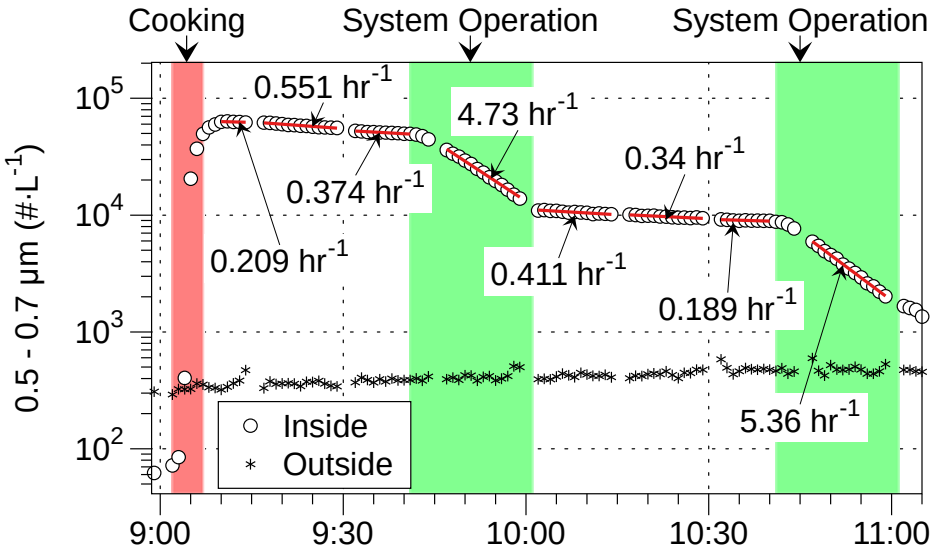

Figure IN-6-D-8. Number concentration of 0.5–0.7 µm diameter particles during cooking experiment with System D on Jul 16, 2014. Fitted decay rates during each period reflect sum of all particle transformation and removal mechanisms including growth, ventilation, deposition and filtration.

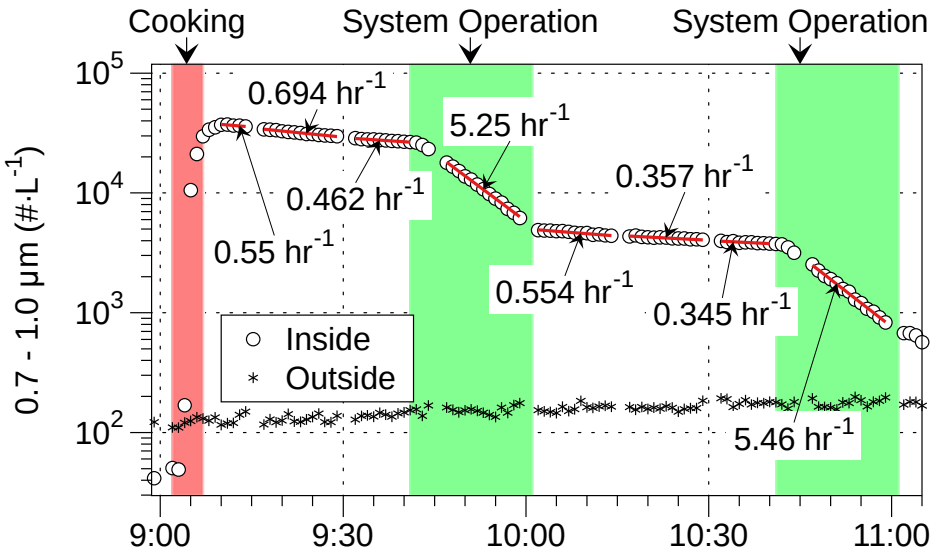

Figure IN-6-D-9. Number concentration of 0.7-1.0 µm diameter particles during cooking experiment with System D on Jul 16, 2014. Fitted decay rates during each period reflect sum of all particle transformation and removal mechanisms including growth, ventilation, deposition and filtration.

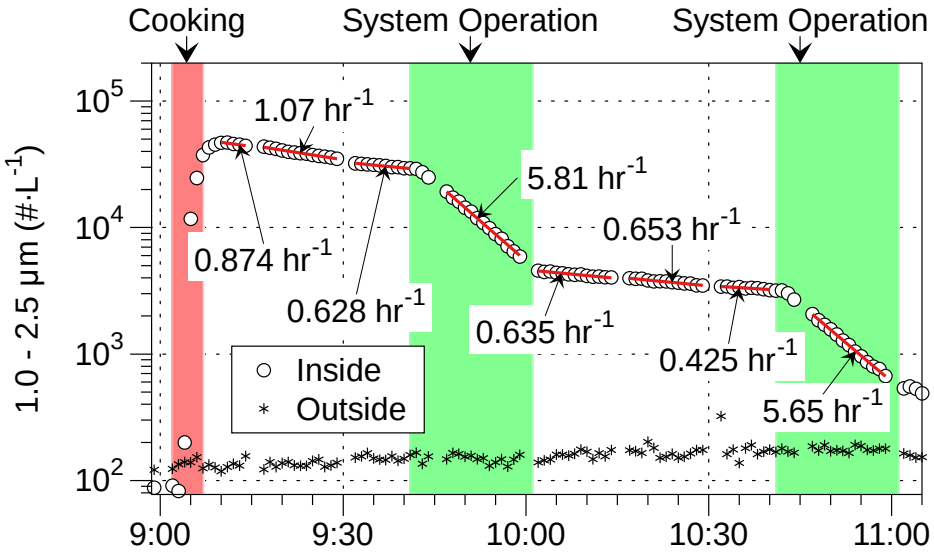

Figure IN-6-D-10. Number concentration of 1.0–2.5 µm diameter particles during cooking experiment with System D on Jul 16, 2014. Fitted decay rates during each period reflect sum of all particle transformation and removal mechanisms including growth, ventilation, deposition and filtration.

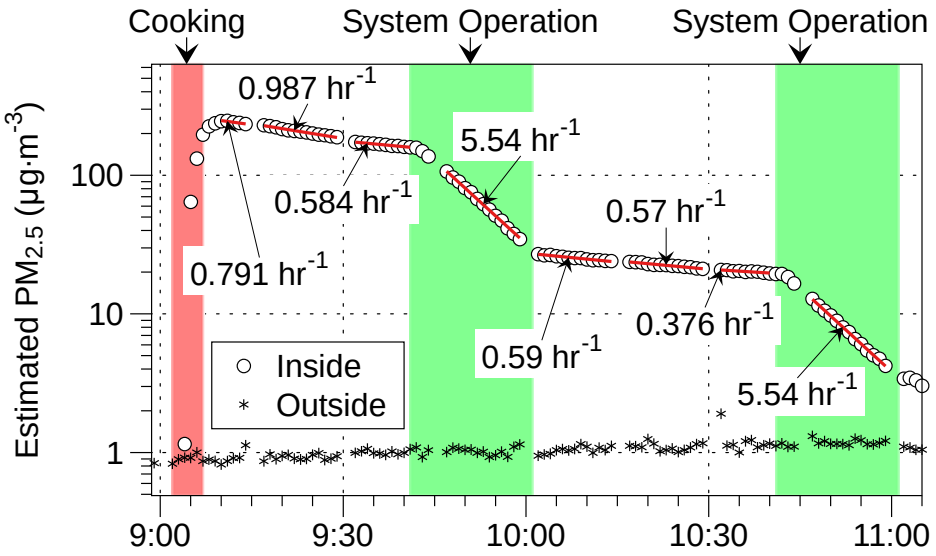

Figure IN-6-D-11. Estimated $PM_{2.5}$ concentration calculated from size-resolved particle number concentrations during cooking experiment with System D on Jul 16, 2014. Refer to Methods section of main report for details on this calculation. Fitted decay rates during each period reflect sum of all particle transformation and removal mechanisms including growth, ventilation, deposition and filtration.

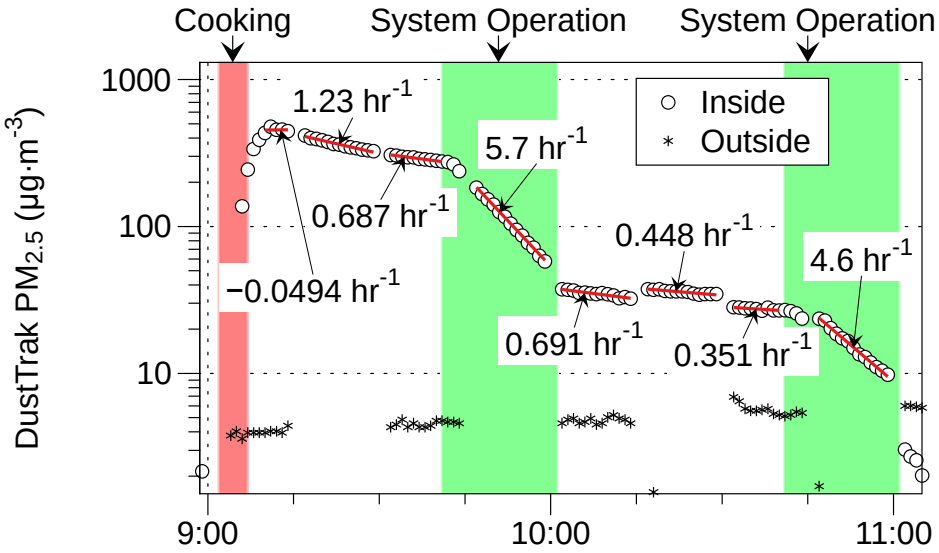

Figure IN-6-D-12. $PM_{2.5}$ concentrations measured by TSI DustTrak II 8530 during cooking experiment with System D on Jul 16, 2014. Fitted decay rates during each period reflect sum of all particle transformation and removal mechanisms including growth, ventilation, deposition and filtration.

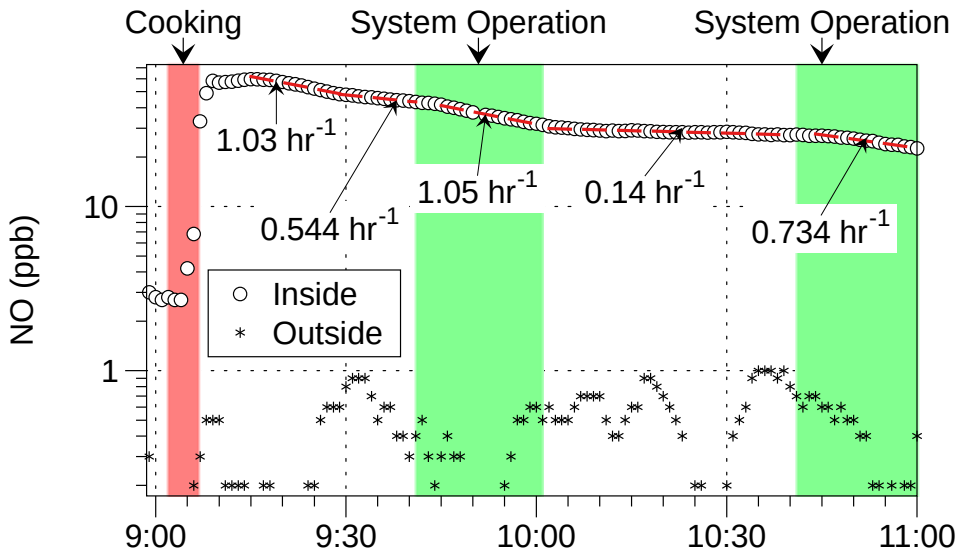

Figure IN-6-D-13. Concentration of NO during cooking experiment with System D on Jul 16, 2014. Fitted decay rates during each period reflect sum of all generation and removal mechanisms.

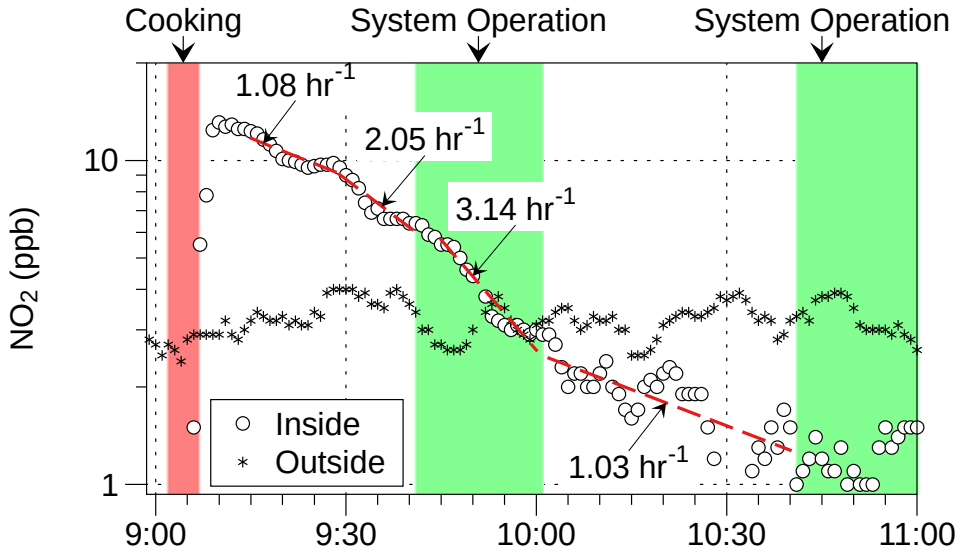

Figure IN-6-D-14. Concentration of NO_2 during cooking experiment with System D on Jul 16, 2014. Fitted decay rates during each period reflect sum of all generation and removal mechanisms.

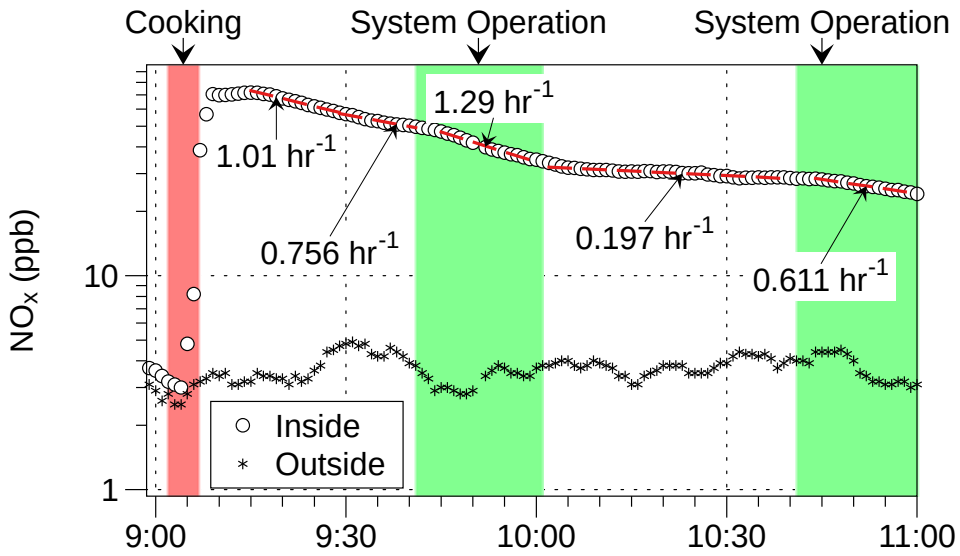

Figure IN-6-D-15. Concentration of total NO_X during cooking experiment with System D on Jul 16, 2014. Fitted decay rates during each period reflect sum of all generation and removal mechanisms.

Appendix IN-7-R. Reference System Performance for Cooking-Related Pollutants, July 23, 2014

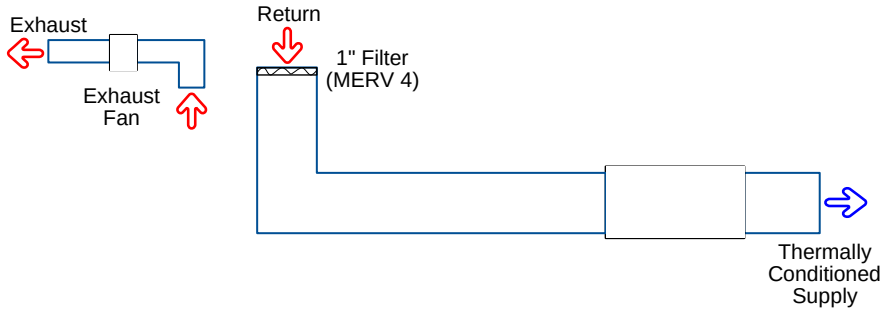

Notes about this monitoring period

2014/07/23 08:34:01.9,Turned off the SF_6 injectors and did a spiked release
2014/07/23 08:44:36.5, Turned on the cooking burner
2014/07/23 08:49:44.0,Burner off
2014/07/23 09:55:36.8,Forced the FAU on
2014/07/23 10:16:55.1, Turned the FAU back off

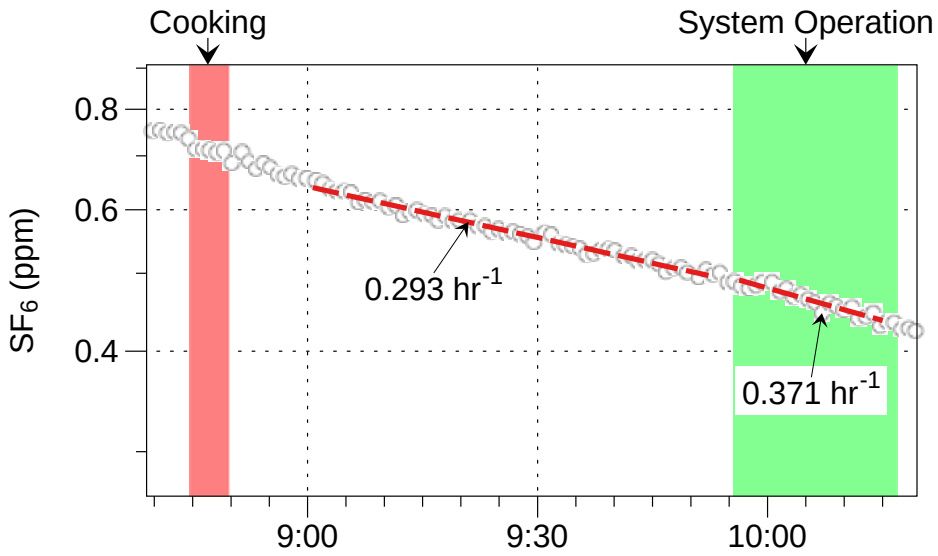

Figure IN-7-R-1. SF_6 during cooking experiment with Reference System on Jul 23, 2014. Injection occurred prior to the display interval. During each interval, a red line shows a best-fit, first-order decay rate that indicates the air exchange rate. Stir-frying of green beans occurred during the first shaded interval. This system was not on a fan controller, but the FAU fan was manually turned on ~9:56. Ventilation decay rates determined for SF_6 are used to calculate first order removal rates of particle deposition and filtration.

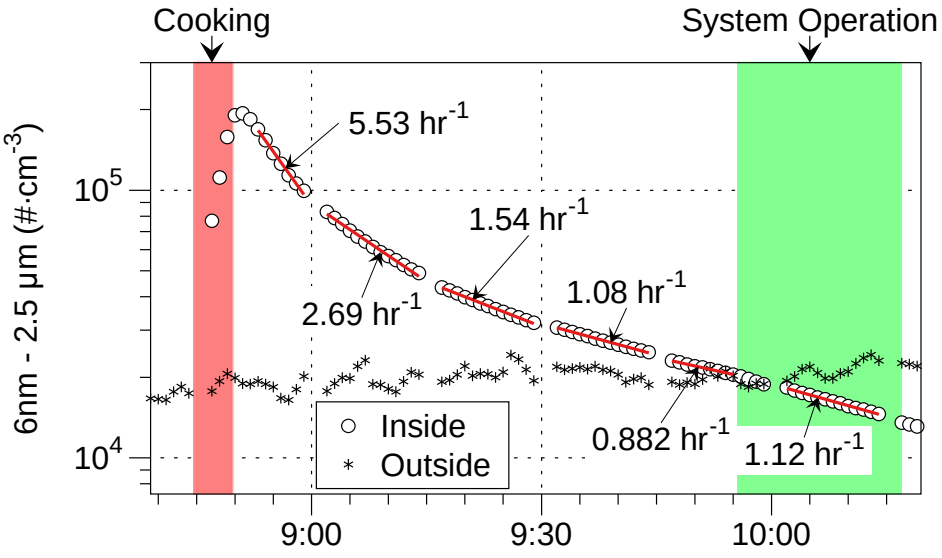

Figure IN-7-R-2. Number concentration of 6 nm to 2.5 µm diameter particles during cooking experiment with Reference System on Jul 23, 2014. Fitted decay rates during each period reflect sum of all particle transformation and removal mechanisms including growth, ventilation, deposition and filtration.

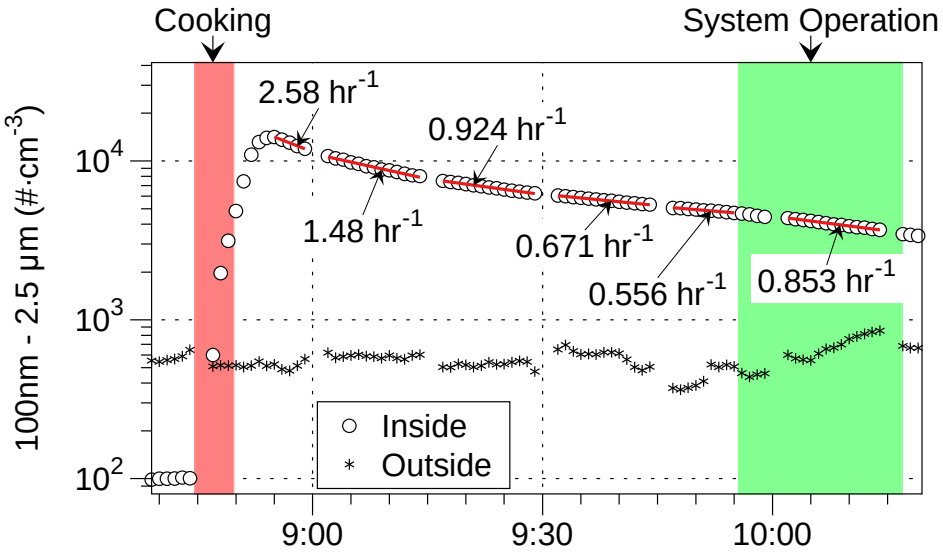

Figure IN-7-R-3. Number concentrations of 100 nm to 2.5 µm diameter particles during cooking experiment with Reference System on Jul 23, 2014. Fitted decay rates during each period reflect sum of all particle transformation and removal mechanisms including growth, ventilation, deposition and filtration.

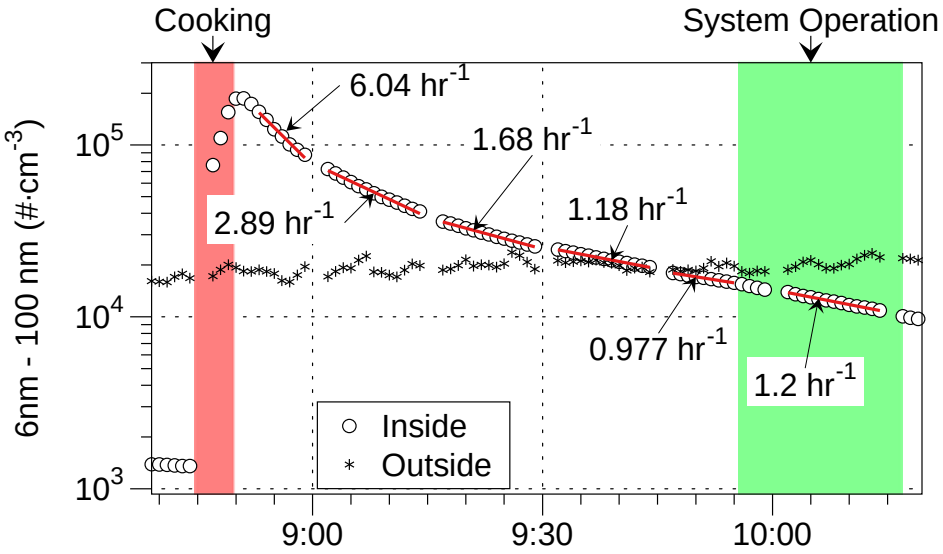

Figure IN-7-R-4. Number concentrations of 6–100 nm diameter particles during cooking experiment with Reference System on Jul 23, 2014. Data obtained by subtracting counts in range of 100 nm – 2.5 µm from counts in range of 6 nm – 2.5 µm. Fitted decay rates during each period reflect sum of all particle transformation and removal mechanisms including growth, ventilation, deposition and filtration.

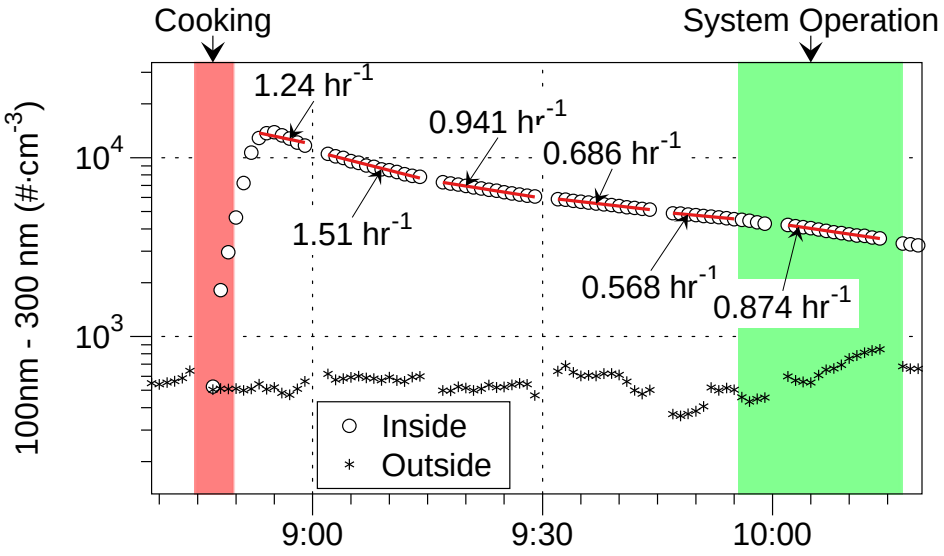

Figure IN-7-R-5. Number concentrations of 100-300 nm diameter particles during cooking experiment with Reference System on Jul 23, 2014. Data obtained by subtracting counts in range of 0.3–2.5 µm particles (MetOne 637) from the counts measured in the range of 100 nm–2.5 µm by the CPC3781 with size selective inlet. Fitted decay rates during each period reflect sum of all particle transformation and removal mechanisms including growth, ventilation, deposition and filtration.

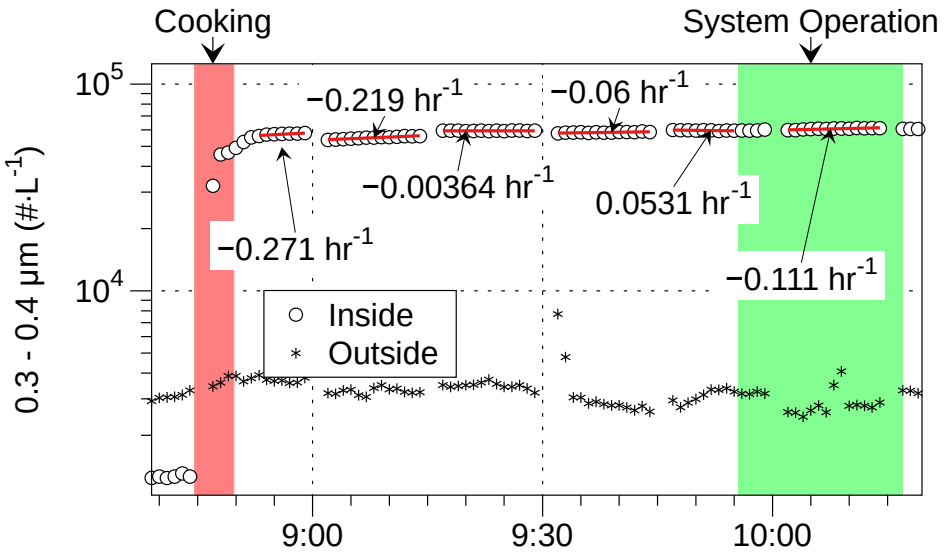

Figure IN-7-R-6. Number concentration of 0.3–0.4 µm diameter particles during cooking experiment with Reference System on Jul 23, 2014. Fitted decay rates during each period reflect sum of all particle transformation and removal mechanisms including growth, ventilation, deposition and filtration. Disconnected data during period just after cooking are from the two instruments switching between indoors and outdoors and may reflect small differences in the sampling efficiency at the lower cut point that is particularly sensitive to rapidly changing particle size distributions from the indoor source. Negative decay during this period indicates that the number of particles in this size bin is increasing.

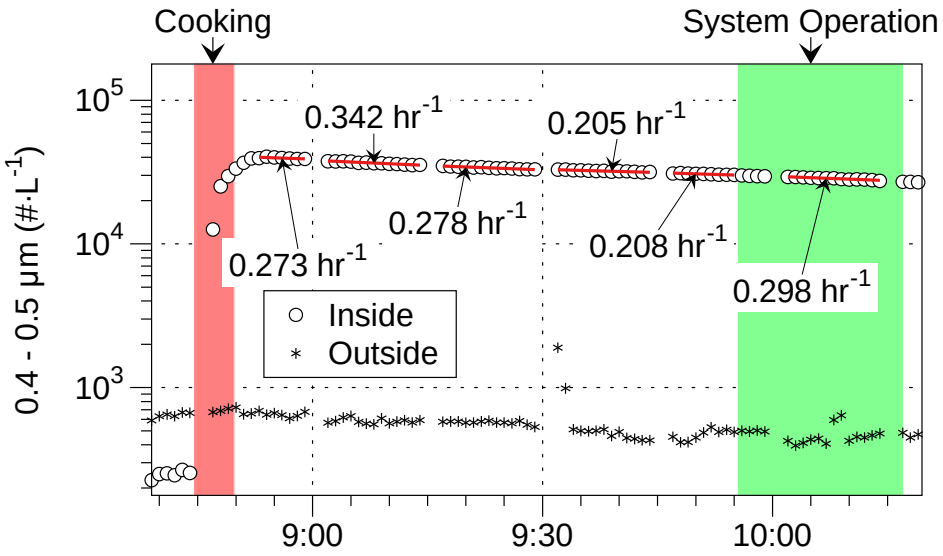

Figure IN-7-R-7. Number concentration of 0.4–0.5 µm diameter particles during cooking experiment with Reference System on Jul 23, 2014. Fitted decay rates during each period reflect sum of all particle transformation and removal mechanisms including growth, ventilation, deposition and filtration.

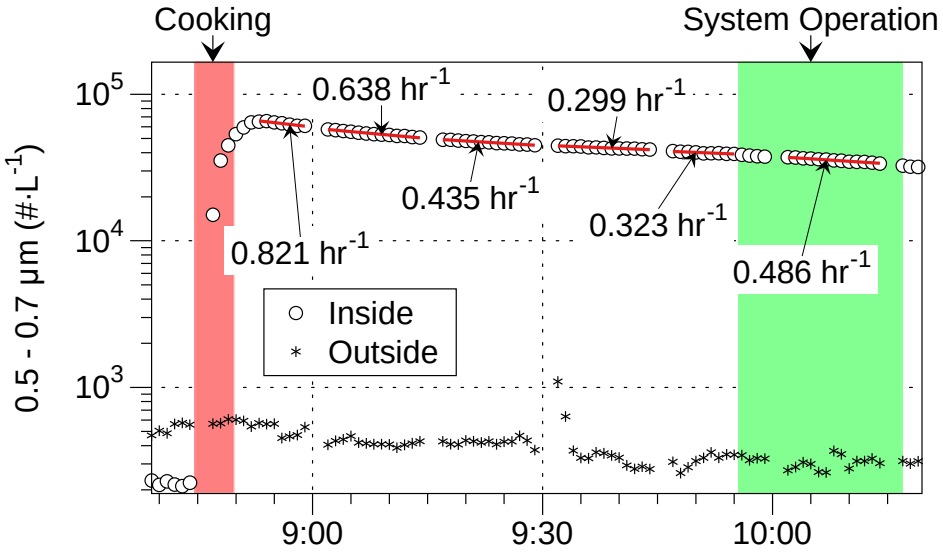

Figure IN-7-R-8. Number concentration of 0.5–0.7 µm diameter particles during cooking experiment with Reference System on Jul 23, 2014. Fitted decay rates during each period reflect sum of all particle transformation and removal mechanisms including growth, ventilation, deposition and filtration.

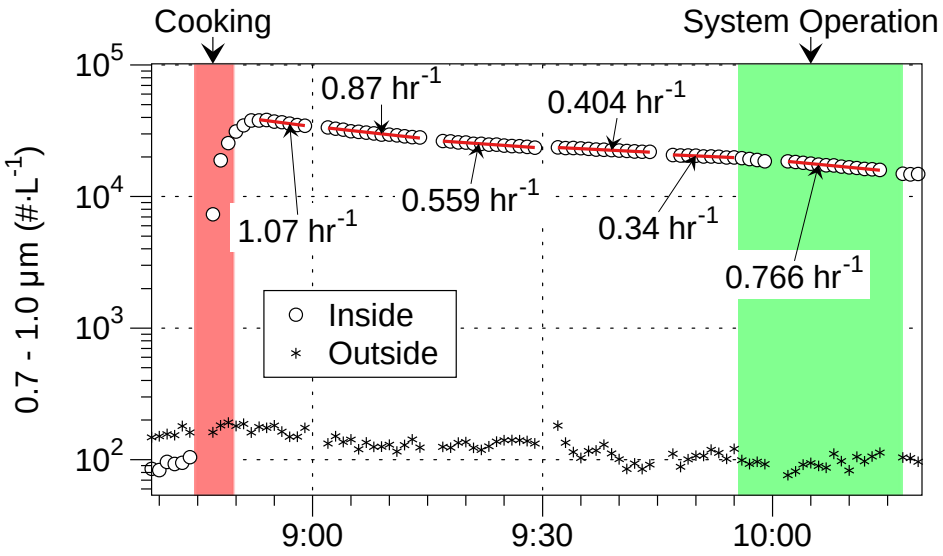

Figure IN-7-R-9. Number concentration of 0.7-1.0 µm diameter particles during cooking experiment with Reference System on Jul 23, 2014. Fitted decay rates during each period reflect sum of all particle transformation and removal mechanisms including growth, ventilation, deposition and filtration.

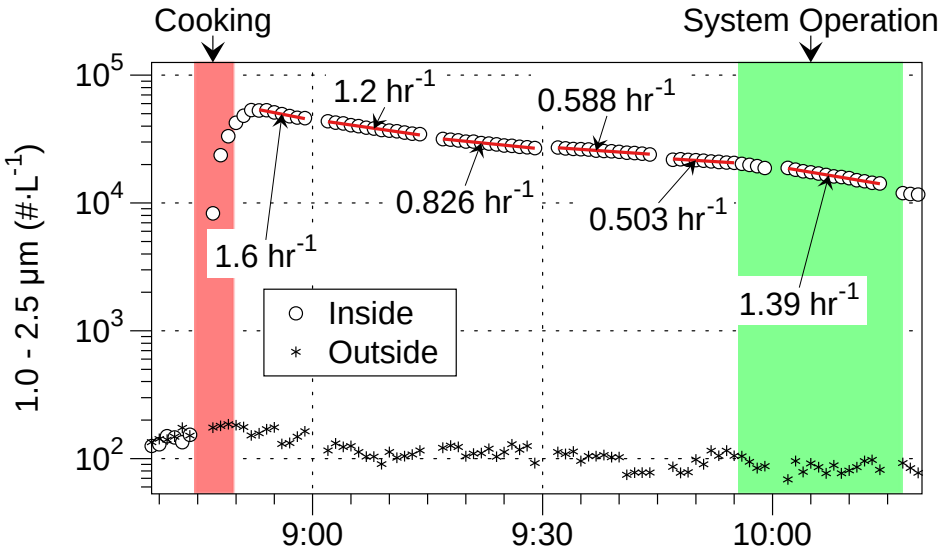

Figure IN-7-R-10. Number concentration of 1.0–2.5 µm diameter particles during cooking experiment with Reference System on Jul 23, 2014. Fitted decay rates during each period reflect sum of all particle transformation and removal mechanisms including growth, ventilation, deposition and filtration.

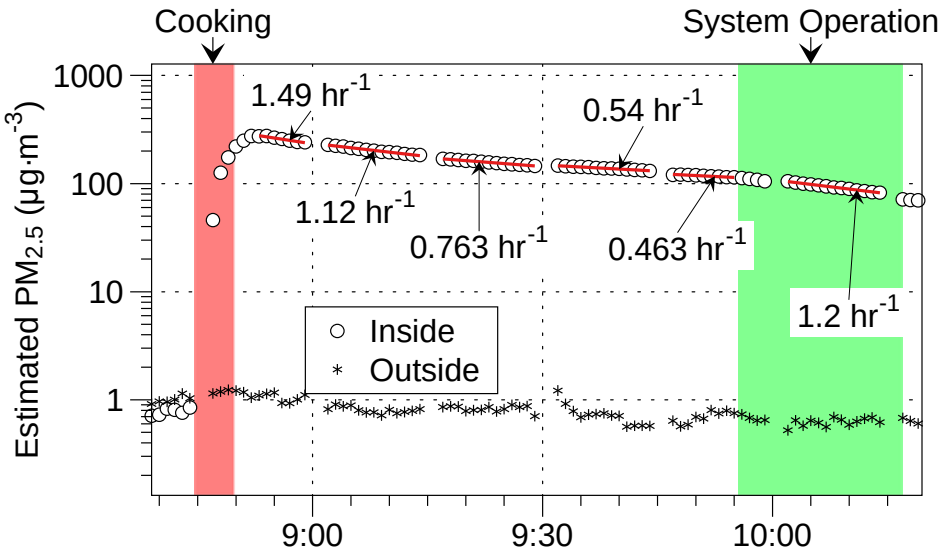

Figure IN-7-R-11. Estimated $PM_{2.5}$ concentration calculated from size-resolved particle number concentrations during cooking experiment with Reference System on Jul 23, 2014. Refer to Methods section of main report for details on this calculation. Fitted decay rates during each period reflect sum of all particle transformation and removal mechanisms including growth, ventilation, deposition and filtration.

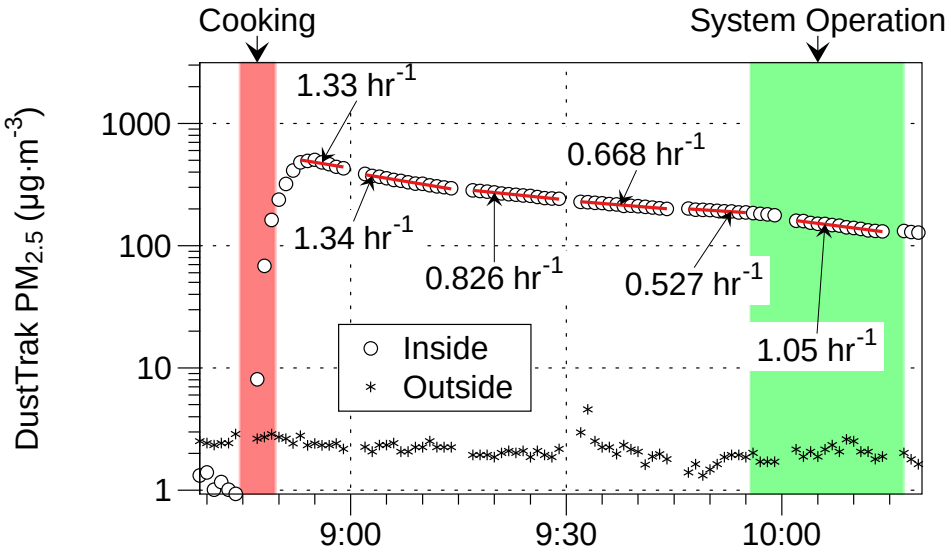

Figure IN-7-R-12. $PM_{2.5}$ concentrations measured by TSI DustTrak II 8530 during cooking experiment with Reference System on Jul 23, 2014. Fitted decay rates during each period reflect sum of all particle transformation and removal mechanisms including growth, ventilation, deposition and filtration.

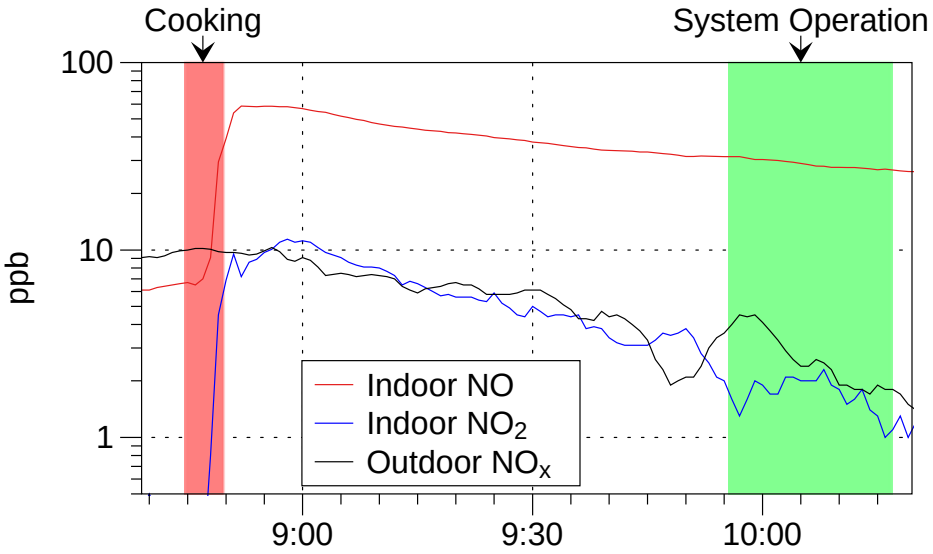

Figure IN-7-R-13. Concentration of NO and NO_2 during cooking experiment with Reference System on Jul 23, 2014.

Appendix IN-8-C. System C Performance for Cooking-Related Pollutants, July 30, 2014

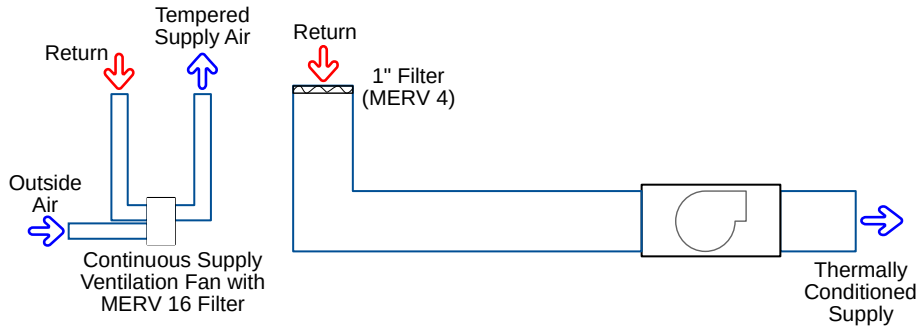

Notes about this monitoring period

2014/07/30 11:37, On with the burner
2014/07/30 11:42, Off with burner

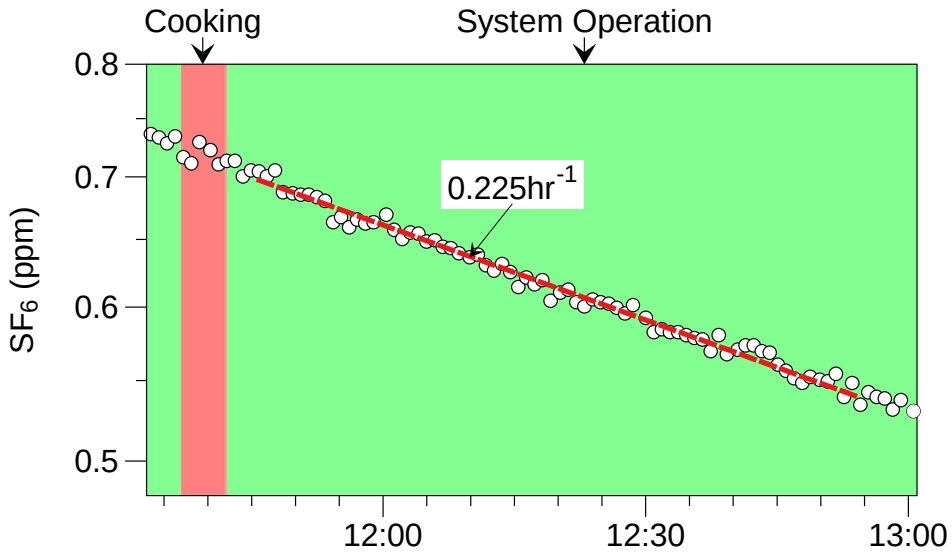

Figure IN-8-C-1. SF_6 during cooking experiment with System C on Jul 30, 2014. Injection occurred prior to the display interval. During each interval, a red line shows a best-fit, first-order decay rate that indicates the air exchange rate. Stir-frying of green beans occurred during the brown-colored interval. This system was on for the entire period. Ventilation decay rates determined for SF_6 are used to calculate first order removal rates of particle deposition and filtration.

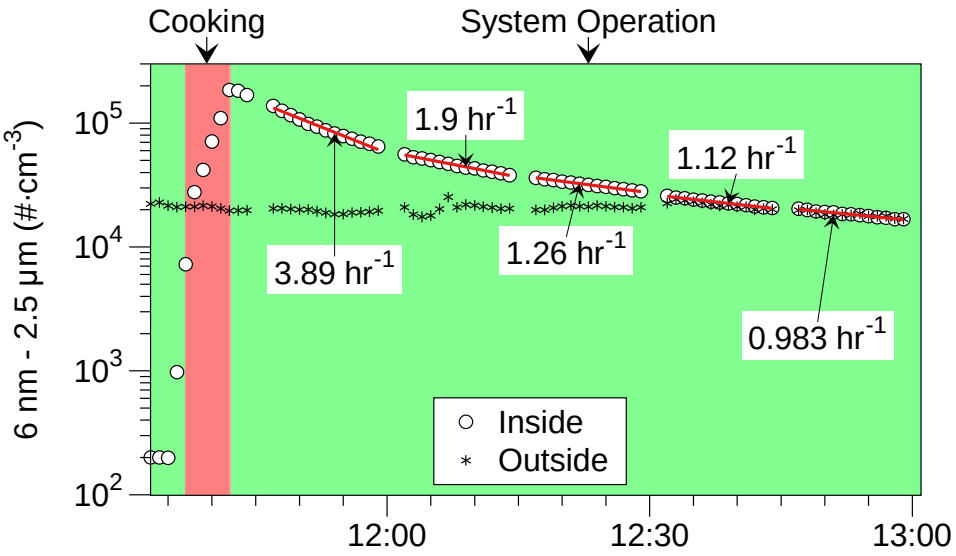

Figure IN-8-C-2. Number concentration of 6 nm to 2.5 µm diameter particles during cooking experiment with System C on Jul 30, 2014. Fitted decay rates during each period reflect sum of all particle transformation and removal mechanisms including growth, ventilation, deposition and filtration.

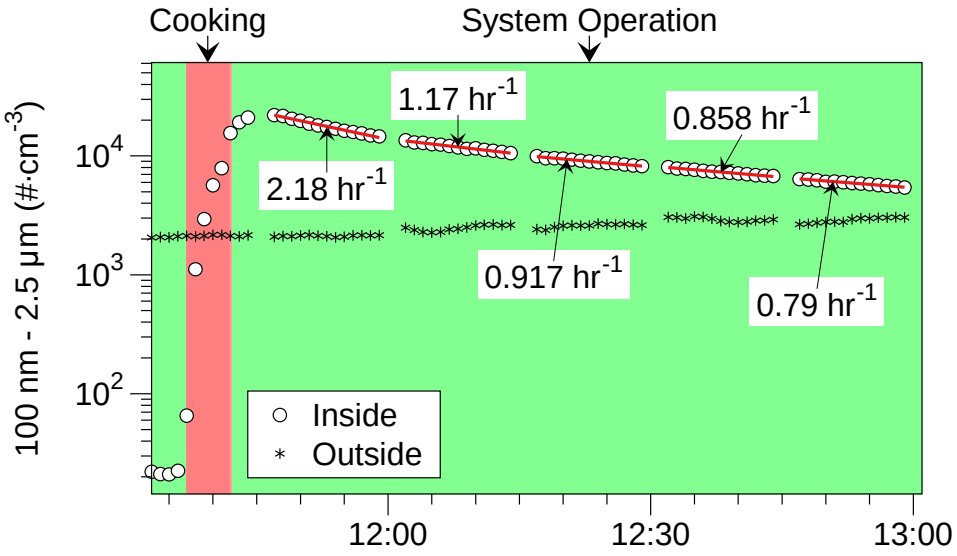

Figure IN-8-C-3. Number concentrations of 100 nm to 2.5 µm diameter particles during cooking experiment with System C on Jul 30, 2014. Fitted decay rates during each period reflect sum of all particle transformation and removal mechanisms including growth, ventilation, deposition and filtration.

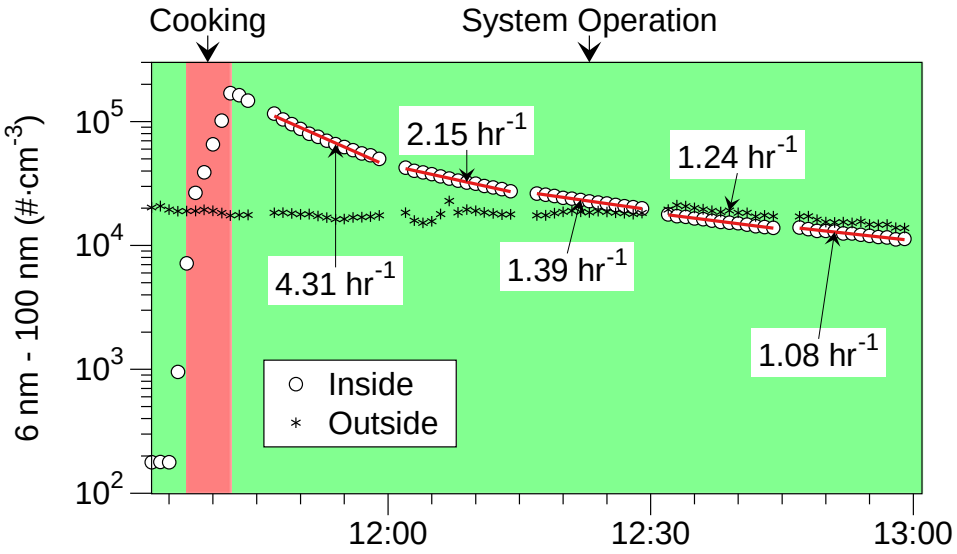

Figure IN-8-C-4. Number concentrations of 6–100 nm diameter particles during cooking experiment with System C on Jul 30, 2014. Data obtained by subtracting counts in range of 100 nm – 2.5 µm from counts in range of 6 nm – 2.5 µm. Fitted decay rates during each period reflect sum of all particle transformation and removal mechanisms including growth, ventilation, deposition and filtration.

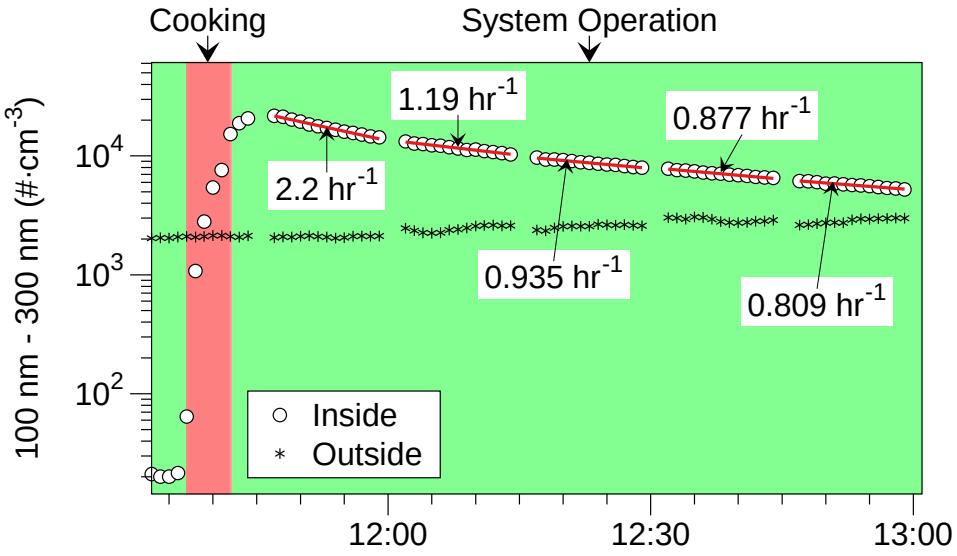

Figure IN-8-C-5. Number concentrations of 100-300 nm diameter particles during cooking experiment with System C on Jul 30, 2014. Data obtained by subtracting counts in range of 0.3–2.5 μm particles (MetOne 637) from the counts measured in the range of 100 nm–2.5 μm by the CPC3781 with size selective inlet. Fitted decay rates during each period reflect sum of all particle transformation and removal mechanisms including growth, ventilation, deposition and filtration.

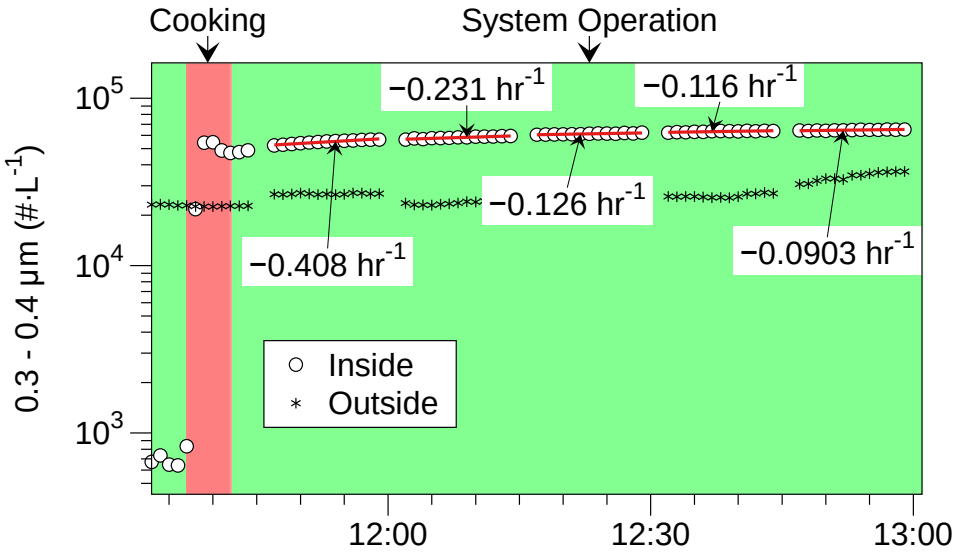

Figure IN-8-C-6. Number concentration of 0.3–0.4 μm diameter particles during cooking experiment with System C on Jul 30, 2014. Fitted decay rates during each period reflect sum of all particle transformation and removal mechanisms including growth, ventilation, deposition and filtration. Disconnected data during period just after cooking are from the two instruments switching between indoors and outdoors and may reflect small differences in the sampling efficiency at the lower cut point that is particularly sensitive to rapidly changing particle size distributions from the indoor source. Negative decay during this period indicates that the number of particles in this size bin is increasing.

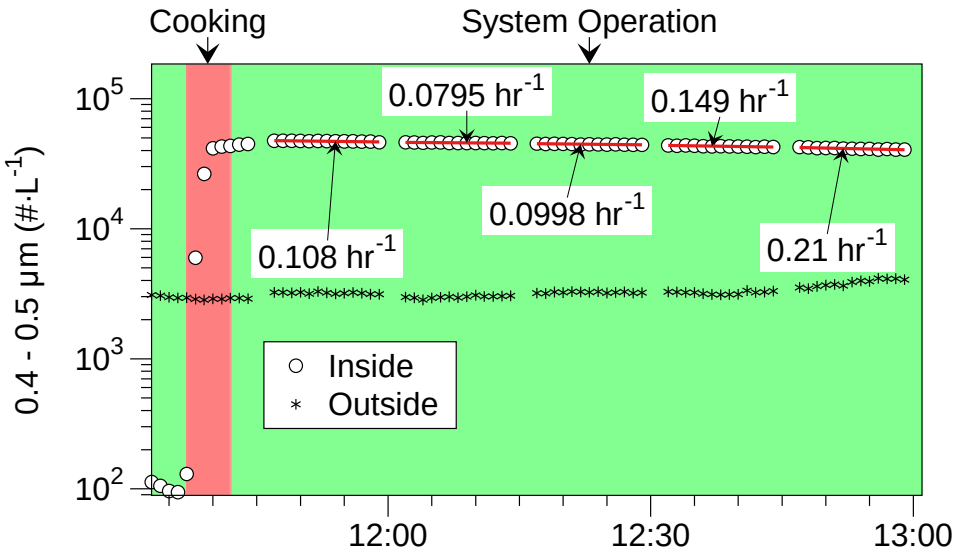

Figure IN-8-C-7. Number concentration of 0.4–0.5 µm diameter particles during cooking experiment with System C on Jul 30, 2014. Fitted decay rates during each period reflect sum of all particle transformation and removal mechanisms including growth, ventilation, deposition and filtration.

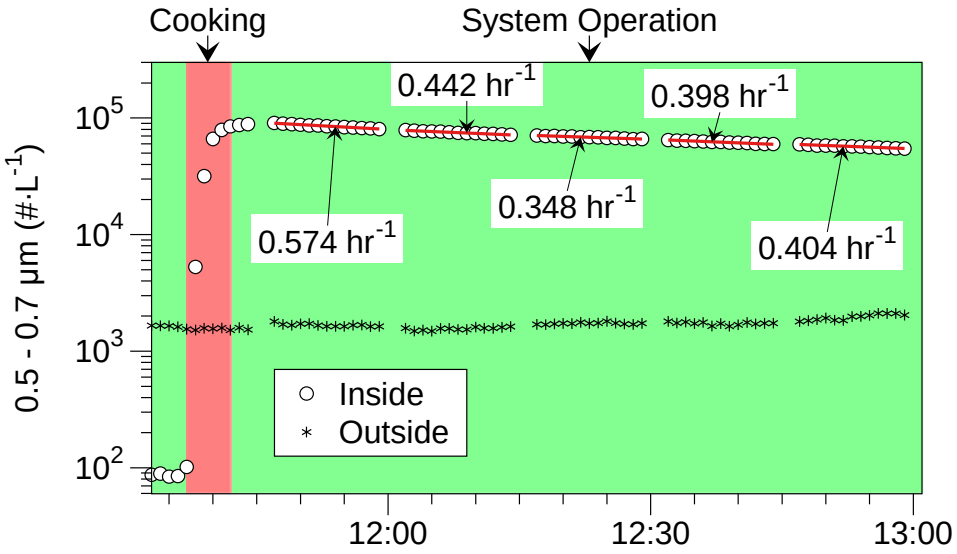

Figure IN-8-C-8. Number concentration of 0.5–0.7 µm diameter particles during cooking experiment with System C on Jul 30, 2014. Fitted decay rates during each period reflect sum of all particle transformation and removal mechanisms including growth, ventilation, deposition and filtration.

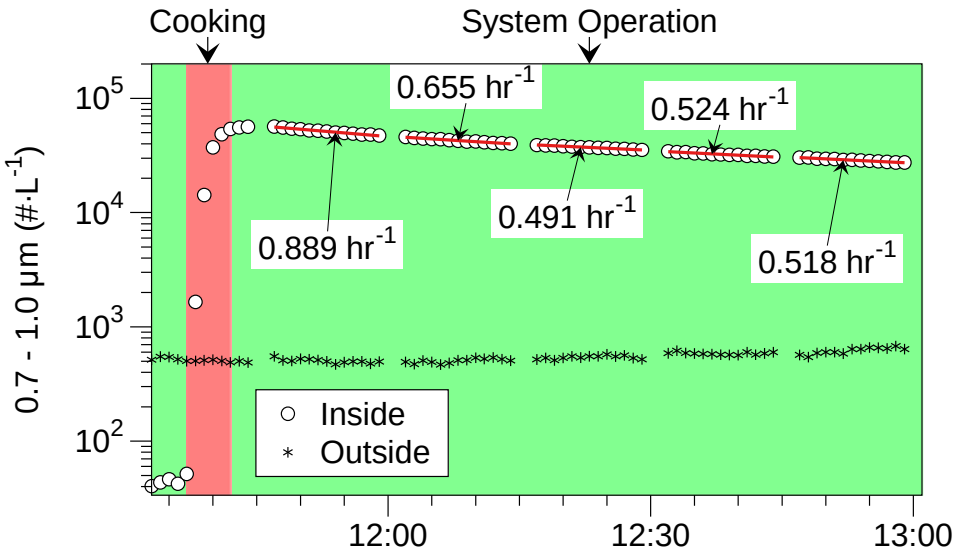

Figure IN-8-C-9. Number concentration of 0.7-1.0 µm diameter particles during cooking experiment with System C on Jul 30, 2014. Fitted decay rates during each period reflect sum of all particle transformation and removal mechanisms including growth, ventilation, deposition and filtration.

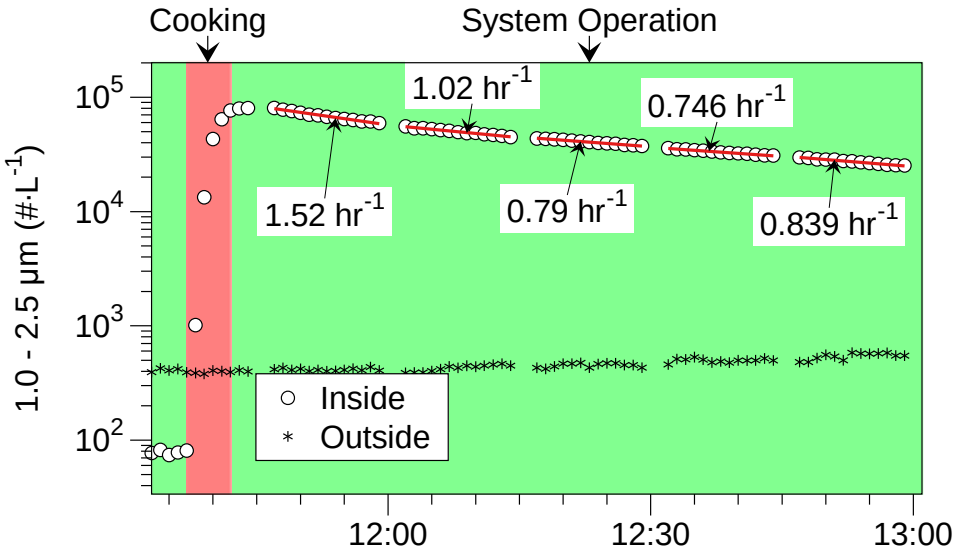

Figure IN-8-C-10. Number concentration of 1.0–2.5 µm diameter particles during cooking experiment with System C on Jul 30, 2014. Fitted decay rates during each period reflect sum of all particle transformation and removal mechanisms including growth, ventilation, deposition and filtration.

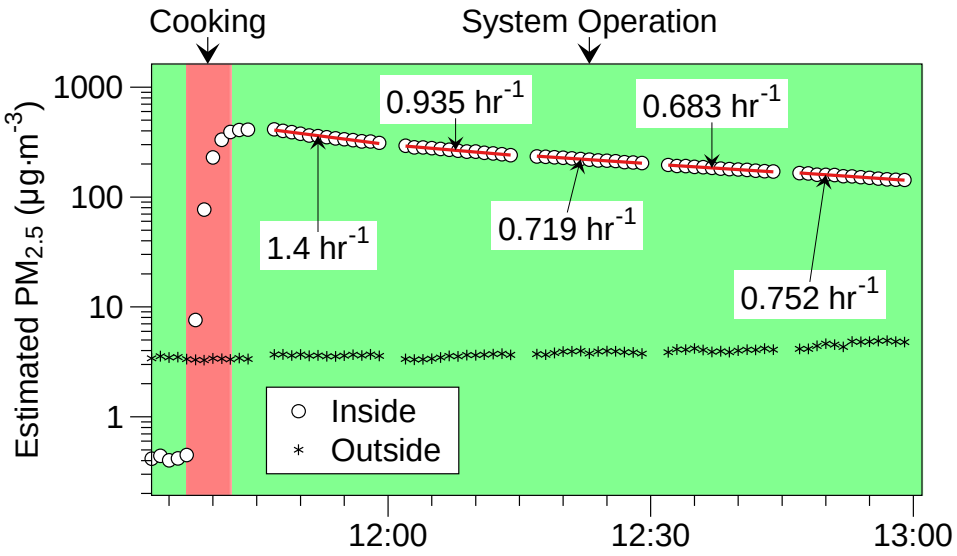

Figure IN-8-C-11. Estimated $PM_{2.5}$ concentration calculated from size-resolved particle number concentrations during cooking experiment with System C on Jul 30, 2014. Refer to Methods section of main report for details on this calculation. Fitted decay rates during each period reflect sum of all particle transformation and removal mechanisms including growth, ventilation, deposition and filtration.

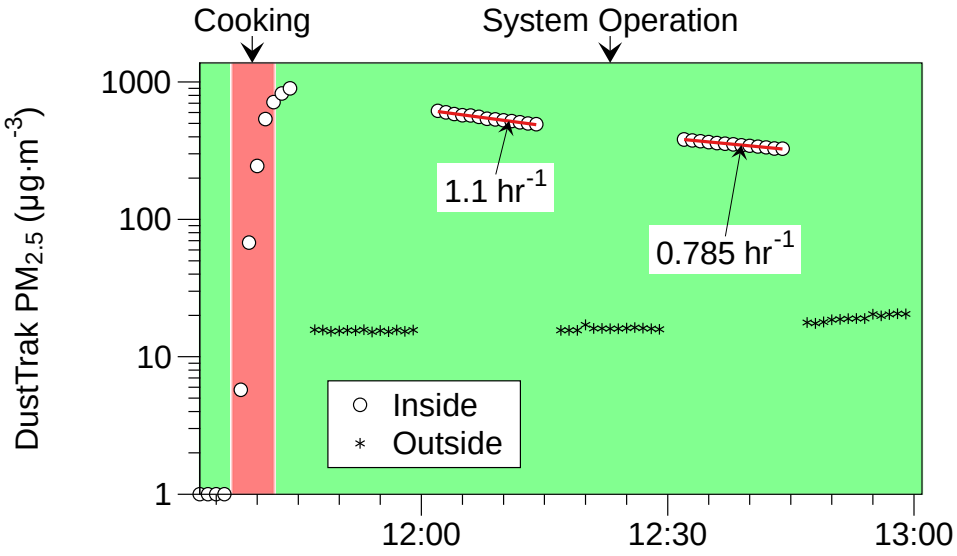

Figure IN-8-C-12. $PM_{2.5}$ concentrations measured by TSI DustTrak II 8530 during cooking experiment with System C on Jul 30, 2014. Data shown for a single instrument only, the other had communication problems. Fitted decay rates during each period reflect sum of all particle transformation and removal mechanisms including growth, ventilation, deposition and filtration.

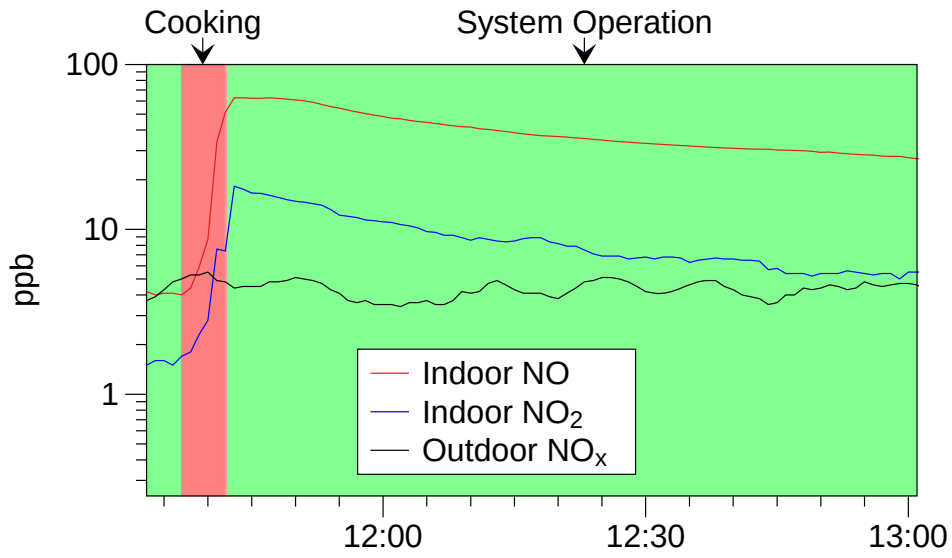

Figure IN-8-C-13. Concentration of NO and NO_2 during cooking experiment with System C on Jul 30, 2014.

Appendix IN-9-B. System B Performance for Cooking-Related Pollutants, August 6, 2014

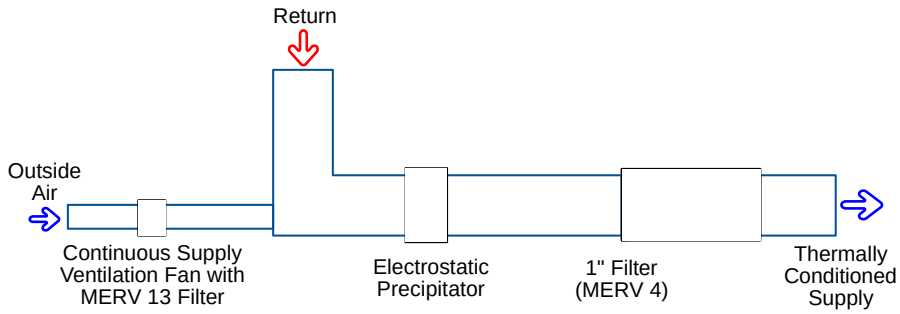

Notes about this monitoring period

2014/08/06 08:43:42.6,3, Walked into the house
2014/08/06 09:58:32.0,5, Turned off the SF_6 injectors and did a spiked release
2014/08/06 10:14:28.4,4,On burner
2014/08/06 11:19:20.6,7, Forced the FAU on
2014/08/06 11:50:08.9,1,Turned the FAU off

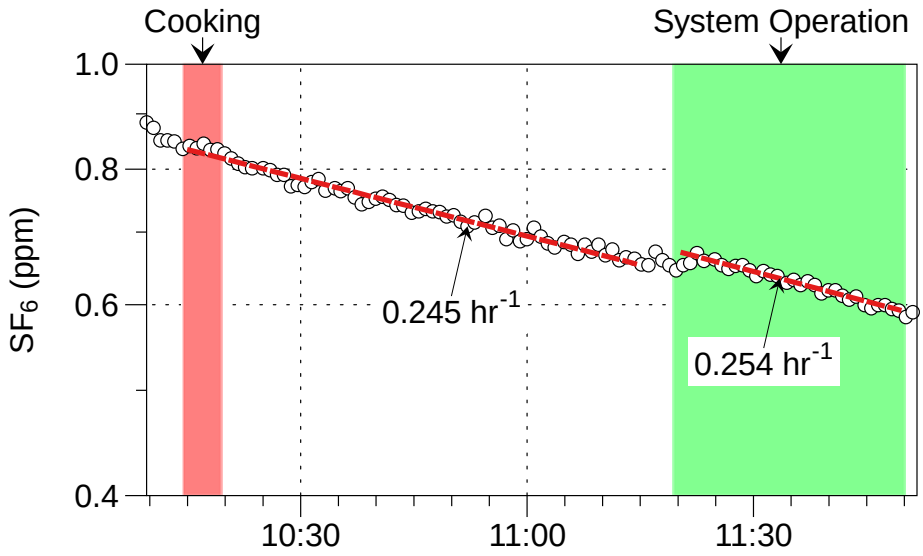

Figure IN-9-B-1. SF_6 during cooking experiment with System B on Aug 6, 2014. Injection occurred prior to the display interval. During each interval, a red line shows a best-fit, first-order decay rate that indicates the air exchange rate. Stir-frying of green beans occurred during the first shaded interval. This system was not on a fan controller, but the FAU fan was manually turned on ~11:19. Ventilation decay rates determined for SF_6 are used to calculate first order removal rates of particle deposition and filtration.

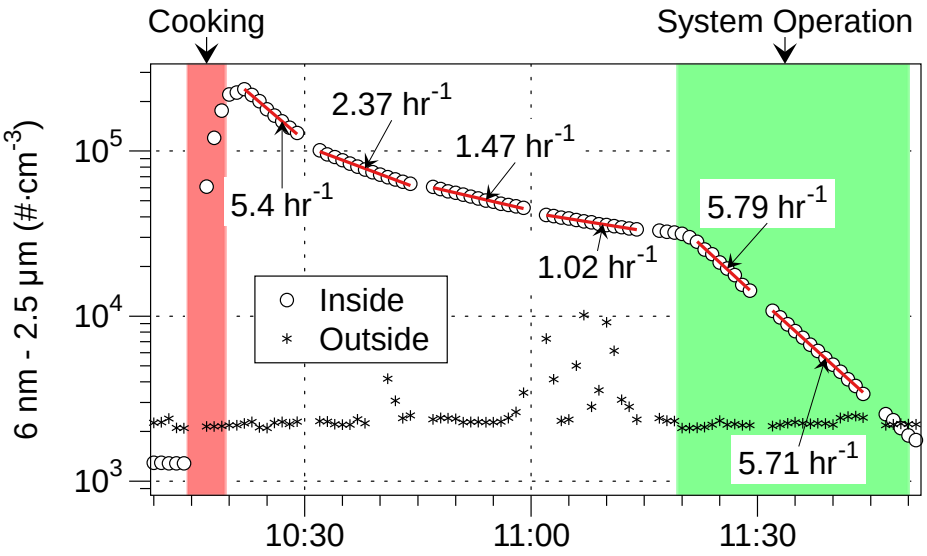

Figure IN-9-B-2. Number concentration of 6 nm to 2.5 µm diameter particles during cooking experiment with System B on Aug 6, 2014. Fitted decay rates during each period reflect sum of all particle transformation and removal mechanisms including growth, ventilation, deposition and filtration.

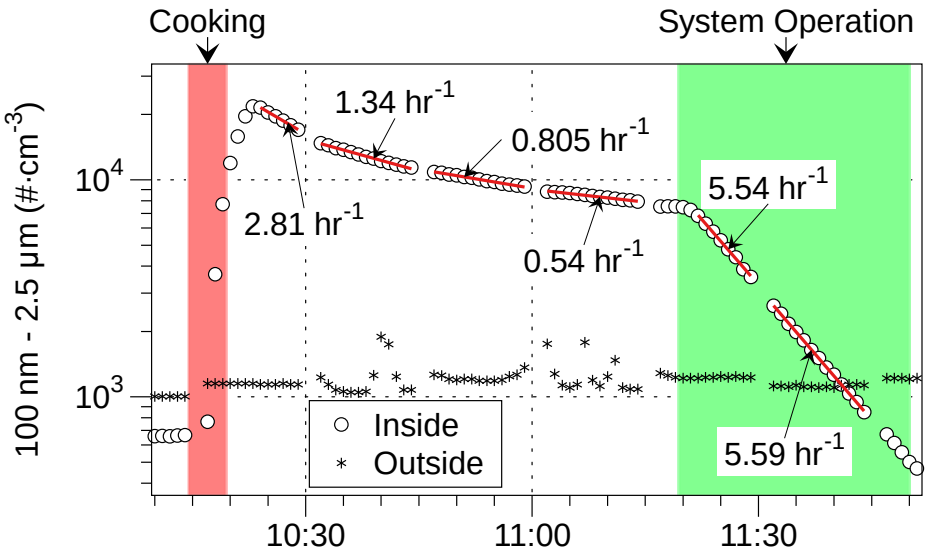

Figure IN-9-B-3. Number concentrations of 100 nm to 2.5 µm diameter particles during cooking experiment with System B on Aug 6, 2014. Fitted decay rates during each period reflect sum of all particle transformation and removal mechanisms including growth, ventilation, deposition and filtration.

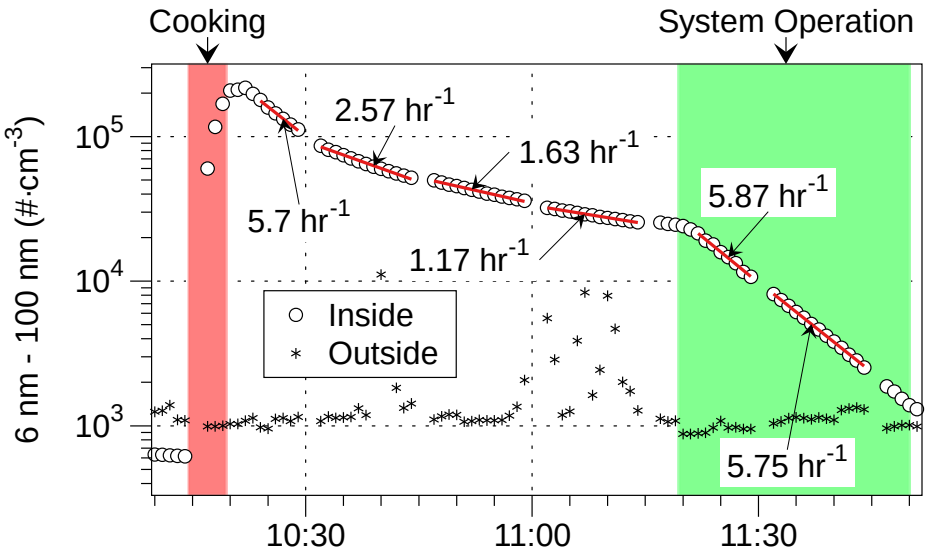

Figure IN-9-B-4. Number concentrations of 6–100 nm diameter particles during cooking experiment with System B on Aug 6, 2014. Data obtained by subtracting counts in range of 100 nm – 2.5 µm from counts in range of 6 nm – 2.5 µm. Fitted decay rates during each period reflect sum of all particle transformation and removal mechanisms including growth, ventilation, deposition and filtration.

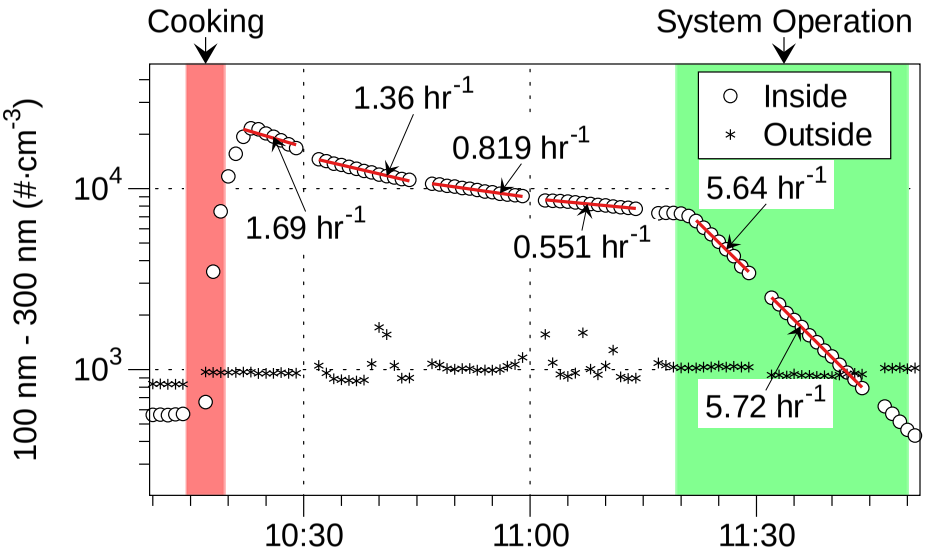

Figure IN-9-B-5. Number concentrations of 100-300 nm diameter particles during cooking experiment with System B on Aug 6, 2014. Data obtained by subtracting counts in range of 0.3–2.5 µm particles (MetOne 637) from the counts measured in the range of 100 nm–2.5 µm by the CPC3781 with size selective inlet. Fitted decay rates during each period reflect sum of all particle transformation and removal mechanisms including growth, ventilation, deposition and filtration.

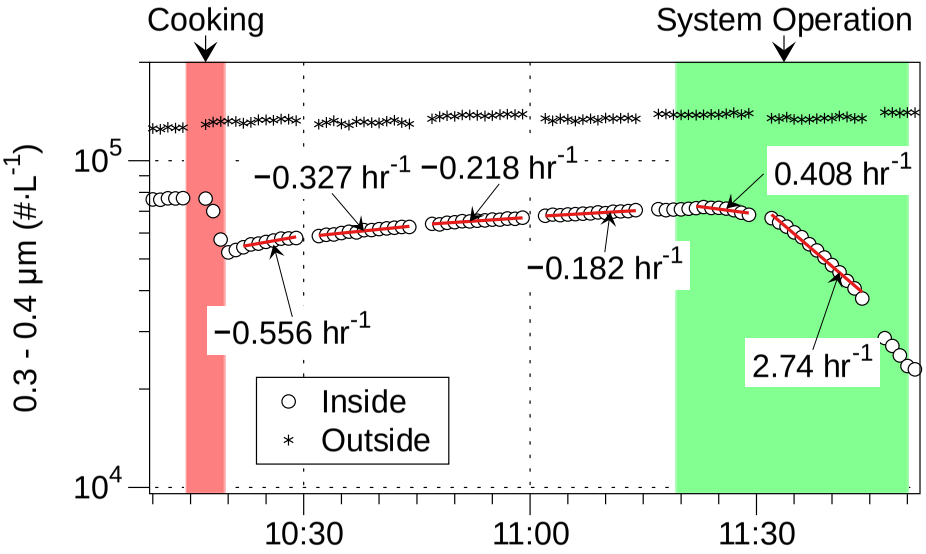

Figure IN-9-B-6. Number concentration of 0.3–0.4 µm diameter particles during cooking experiment with System B on Aug 6, 2014. Fitted decay rates during each period reflect sum of all particle transformation and removal mechanisms including growth, ventilation, deposition and filtration. Disconnected data during period just after cooking are from the two instruments switching between indoors and outdoors and may reflect small differences in the sampling efficiency at the lower cut point that is particularly sensitive to rapidly changing particle size distributions from the indoor source. Negative decay during this period indicates that the number of particles in this size bin is increasing.

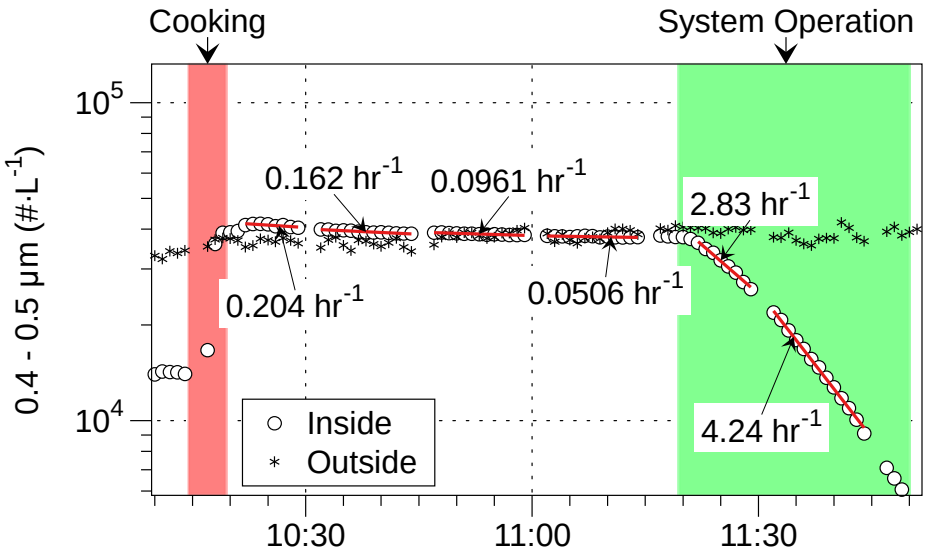

Figure IN-9-B-7. Number concentration of 0.4–0.5 µm diameter particles during cooking experiment with System B on Aug 6, 2014. Fitted decay rates during each period reflect sum of all particle transformation and removal mechanisms including growth, ventilation, deposition and filtration.

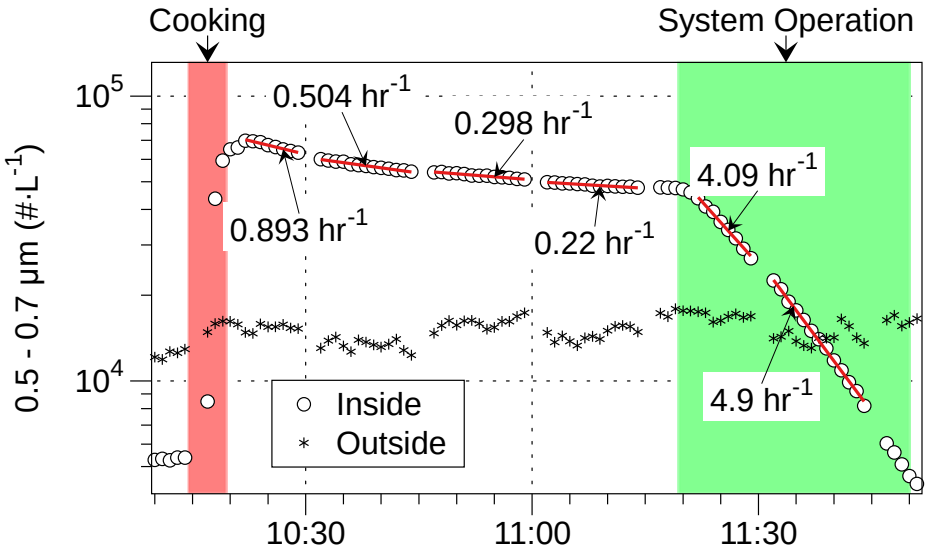

Figure IN-9-B-8. Number concentration of 0.5–0.7 µm diameter particles during cooking experiment with System B on Aug 6, 2014. Fitted decay rates during each period reflect sum of all particle transformation and removal mechanisms including growth, ventilation, deposition and filtration.

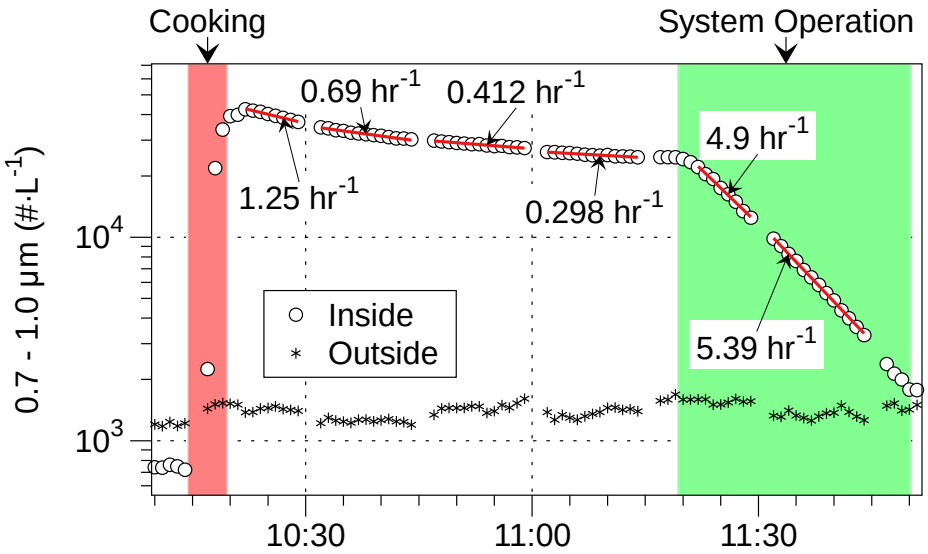

Figure IN-9-B-9. Number concentration of 0.7-1.0 µm diameter particles during cooking experiment with System B on Aug 6, 2014. Fitted decay rates during each period reflect sum of all particle transformation and removal mechanisms including growth, ventilation, deposition and filtration.

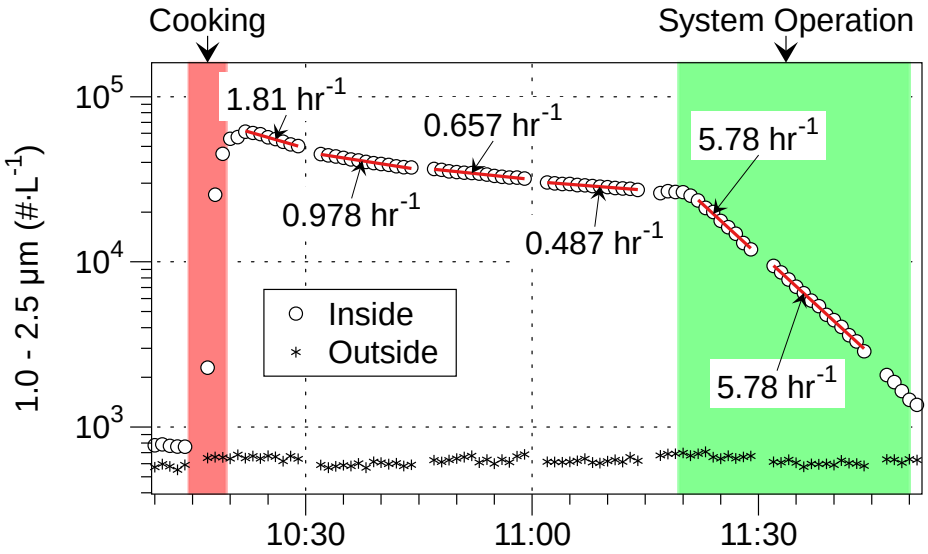

Figure IN-9-B-10. Number concentration of 1.0–2.5 µm diameter particles during cooking experiment with System B on Aug 6, 2014. Fitted decay rates during each period reflect sum of all particle transformation and removal mechanisms including growth, ventilation, deposition and filtration.

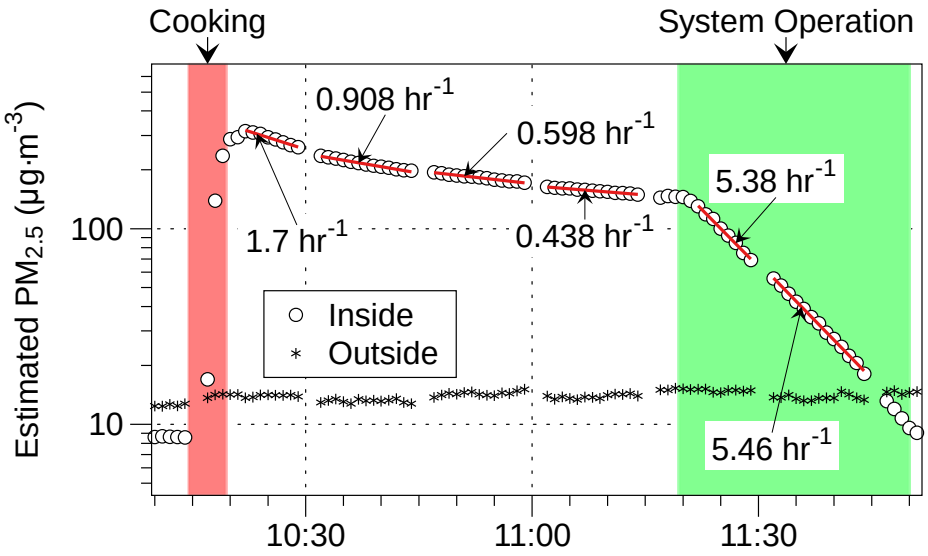

Figure IN-9-B-11. Estimated $PM_{2.5}$ concentration calculated from size-resolved particle number concentrations during cooking experiment with System B on Aug 6, 2014. Refer to Methods section of main report for details on this calculation. Fitted decay rates during each period reflect sum of all particle transformation and removal mechanisms including growth, ventilation, deposition and filtration.

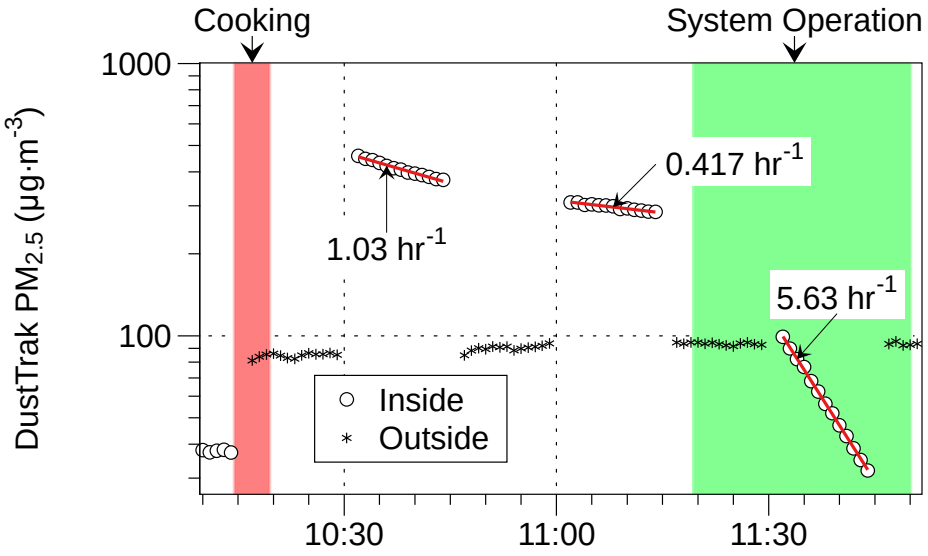

Figure IN-9-B-12. $PM_{2.5}$ concentrations measured by TSI DustTrak II 8530 during cooking experiment with System B on Aug 6, 2014. Data shown for a single instrument only, the other had communication problems. Fitted decay rates during each period reflect sum of all particle transformation and removal mechanisms including growth, ventilation, deposition and filtration.

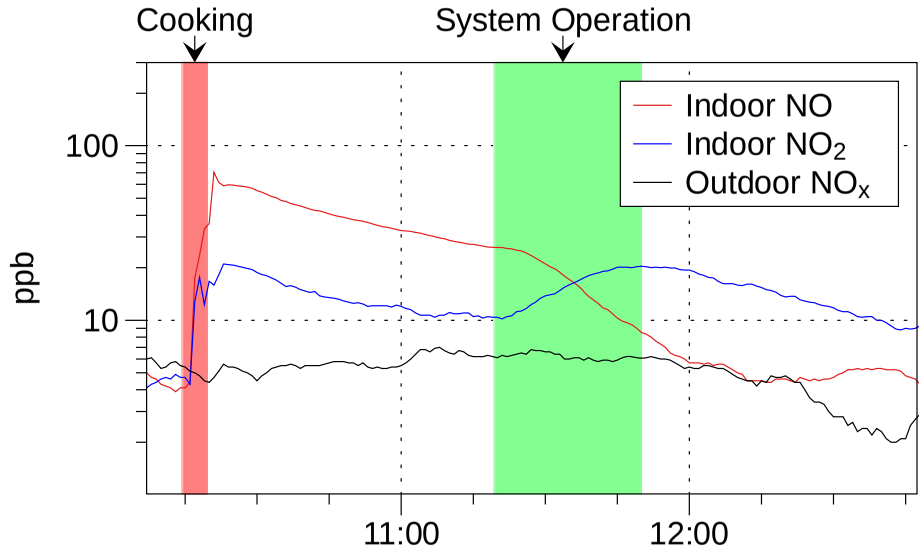

Figure IN-9-B-13. Concentration of NO and NO_2 during cooking experiment with System B on Aug 6, 2014.

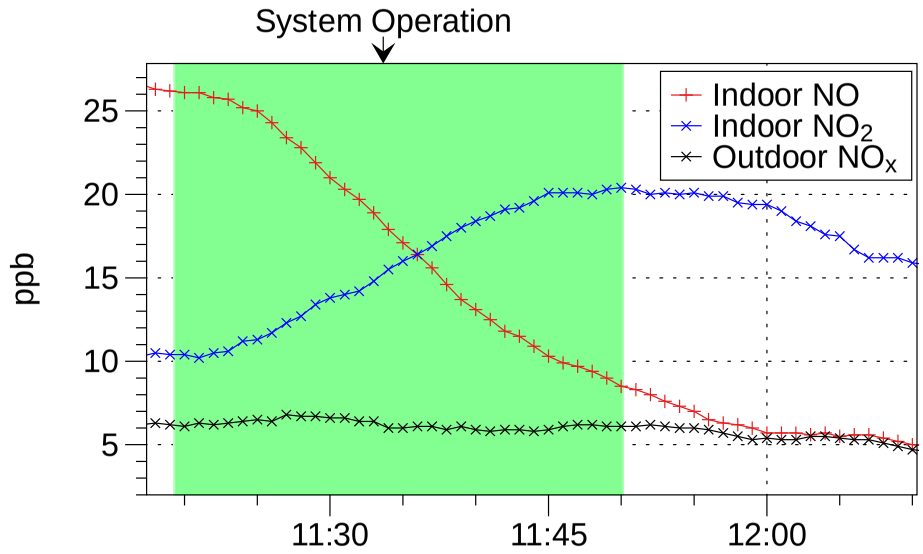

Figure IN-9-B-14. Zoomed in Concentration of NO and NO_2 during cooking experiment with System B on Aug 6, 2014, during ESP operation. (Note the linear scale.) The NO is, presumably, being converted to NO_2 by the ozone generated by the ESP operation.